PNG-1, A PEPTIDE: N-GLYCANASE LIMITS AXON OUTGROWTH AND BRANCHING IN *Caenorhabditis elegans*

Nasrin Habibi-Babadi

Thesis submitted to the
Faculty of Graduate and Postdoctoral Studies
in partial fulfillment of the requirements
for the Doctorate in Philosophy degree in Neuroscience

Department of Cellular and Molecular Medicine
Faculty of Medicine
University of Ottawa

ABSTRACT

Assembly of neuronal networks with distinct patterns of connectivity during nervous system development involves the growth, extension and branching of axons and dendrites. Over the years genetic and biochemical studies in model organisms have contributed significantly in identifying mechanisms regulating axon growth and extension. However the molecular mechanisms underlying axon branching remain unclear.

The egg-laying neuronal circuitry in *C. elegans* has proven to be a robust system for identifying and characterizing novel genes involved in neuronal morphology. This circuitry which mediates egg-laying behavior in nematodes is composed of two families of motorneurons, HSNs and VCs, which are among the most branched neurons in *C. elegans*. A genetic screen for axon branch defects in the egg-laying neurons identified *png-1* to disrupt neuronal morphology including axon branching. *png-1* encodes a Peptide: N-glycanase (PNGase), a conserved cytosolic enzyme that removes N-linked sugar moieties from glycoproteins. In this thesis I present my work characterizing and examining *png-1* and its role in mediating axon branching. Mutations in *png-1* resulted in excessive ectopic axon branching in the VC4 and VC5 egg-laying neurons as well as branching in the normally unbranched AVL and DVB neurons. Behavioral analysis in these mutants revealed defects in egg-laying behavior and mild *in-utero* egg retention phenotypes. Cellular characterization shows ubiquitous expression of *png-1* in many

tissues including vulva cells, muscles, gonads, and neurons. My analysis also shows that *png-1* acts both cell-autonomously and cell non-autonomously from neurons and epithelial cells to restrict axon branching around the vulva. Using a candidate gene approach I identified a deletion allele of the DNA repair gene, *rad-23*, to display axon branching defects and interact with *png-1* within a common pathway to regulate axon branching. Additionally, through a genetic modifier screen for enhancers and suppressors of VC4-5 branching defects in *png-1*, I identified a new allele of *sax-2* as an enhancer mutation. *sax-2* encodes a scaffolding protein that regulates the activity and localization of *sax-1*, an NDR kinase. Examination of neuronal phenotypes in *sax-1* and *sax-2* mutants revealed similar *png-1* like defects in VC4-5. Genetic analysis of the double mutants *png-1;sax-1* and *png-1;sax-2* revealed strong synergistic phenotypes suggesting that *png-1* and *sax-1*/*sax-2* function in parallel pathways to regulate axon branching. In summary, this thesis reveals novel components and pathways in the regulation of neuronal branching.

DEDICATION

To My Father and Mother

All I Am, All I Have

Is From You

ACKNOWLEDGEMENTS

I would like to take this opportunity to express my gratitude to everyone who has contributed to this thesis. First and foremost, I would like to thank my supervisor, Dr. Antonio Colavita for believing in me and giving me the opportunity to become a member of his laboratory. Antonio's guidance and support allowed me to overcome many challenges and obstacles. I will always be grateful for all he had taught me. I would like to extend my appreciation to all members of my advisory committee: Drs. Luc Sabourin, David Park, Balwant Tuana, and Margaret Sonnenfeld, for the time and effort they put forth to guide me during my studies.

I would like thank past and present members of Antonio Colavita's laboratory, Jiravat "David" Visanuvimol, Claudia Arauz, David Carr, Raymond "Mathew" Tanner, Janice Imai, and Leticia Sanchez-Alvarez. I also like to thank Anna Su who assisted me through the majority of my studies. Anna's wide experience in molecular biology and biochemistry contributed significantly to my knowledge and progress in the initial years of my graduate studies. Additionally, I like to thank Cristina Slatculescu for the all the coffee breaks and also for enduring my endless complaints about failed experiments over the last years.

There have been numerous people at the Departments of Neuroscience and Cellular and Molecular Medicine who assisted me during my graduate studies and I am deeply grateful for their assistance. I would like to thank members of the Hakim,

Schlossmacher, Park, and Tuana labs for technical support over the years. I also like to thank Dr. Charlie Thompson for his help with the confocal microscope. I will miss our daily chats about politics, science, dogs, and the art of photography.

Last but not least, I would like to express my deepest gratitude to my family. My pillars of strength, my father and mother, whose unconditional love and countless support have allowed me to become the person I am today. All I have and will accomplish are due to your understanding, generosity, and encouragement. I am so blessed to have you in my life and will work hard to spread what you taught me through the years. Thanks are also due to my older brother, Afshin, whose sense of humor helped me overcome my fears and realize that life is not built on success only. Also I would like to thank my ever humble brother, Farshad, for his continuous support. I cannot think of a word or figure value that I can use to demonstrate your role in the past ten years of my life. I am forever indebted to you. Lastly, Ahmad, whom I had the opportunity to witness his birth and metamorphosis into a wise young man. Thank you for being there for me whenever I needed support.

STATEMENT OF ORIGINAL CONTRIBUTION

The work in this thesis has been performed by the candidate, Nasrin Habibi-Babadi, unless stated otherwise.

Nasrin Habibi-Babadi

March, 2014

TABLE OF CONTENTS

LIST OF ABBREVIATIONS

(-/-)	Knockout	cAMP	Cyclic Adenosine Monophosphate
ADF	Actin Depolymerising Factors	Cdc	Cell Division Cycle protein
ADS	Actin Depolymerization/ Severing	cGMP	Cyclic Guanosine Monophosphate
Akt	Protein Kinase B	CNX	Calnexin
ALM	Anterior Lateral Microtubule cell	CP	Core particle
		CRT	Calreticulin
APN	Actin Polymerization/Nucleation	DIC	Differential Interference Contrast
Arp2/3	Actin-Related Protein 2/3	DRG	Dorsal root ganglion
PI3K	Phosphatidulinositol -3-Kinase	DTC	Distal Tip Cell
		E1	Ubiquitin activating
ATF4	Activating Transcription Factor	E2	Ubiquitin conjating e
		E3	Ubiquitin-ligase
ATF6	Activating Transcription Factor 6	eIF	Translation initiation factor
		Eph	Ephrin
ATP	Adenosine Triphosphate	ER	Endoplasmic Reticulum
BDNF	Brain-Derived Neurotrophic Factor	ERAD	Endoplasmic Reticulum-Associated Degradation
C	Central	ERQC	ER Protein Quality Control
C2	Protein Kinase c (PKC) Conserved 2	F-actin	Actin Filament
		FAK	Focal Adhesion Kinase
Ca^{2+}	Calcium Ion	GAP	GTPase Activating Protein

GDP	Guanosine Diphosphate	PTEN	Phosphatase Tensin Homologue
GEF	Guanine Nucleotide Exchange Factor	PUB	Peptide Ubiquitin-Associated
GK3	Glycogen Synthase Kinase 3	Rab	Ras-related in brain
GTP	Guanosine Triphosphate	Rad23	Radiation Safety 23
Hiw	Highwire	Ras	Rat Sarcoma
HSN	Hermaphrodite Specific Neuron	RING	Really Interesting New Gene
HSP	Heat Shock Protein	Robo	Roundabout receptor
IGF	Insulin-like Growth Factor	ROCK	Rho associated Kinase
Ire1	Inositol Requiring Kinase 1	Rp	Regulator particle
LAT	Large Tumor Suppressor	*sax*	Sensory Axon guidance gene
MT	Microtubule	Sema3A	Semaphorin 3 A
NDR	Nuclear Dbf2-related	*seu*	Suppressor of Ectopic UNC-5 gene
NER	Nucleotide Excision Repair	*slt*	SLIT (Robo ligand) homologue gene
NGF	Nerve Growth Factor	T	Transitional
P	Peripheral	TGFβ	Transforming Growth F actor Beta
PAK	p21-Activated Kinase	*Trc*	Tricornered gene
PDE	Postdeirid Sensory Neuron	*Trk*	Tropomyosin related kinase
PDI	Protein Disulfide Isomerases	Ub	Ubiquitin
PI3K	Phosphatidylinositol 3-Kinase	UBA	Ubiquitin-Associated
PIP2	Phosphatidylinositol 4,5-bisphosphate		
PKC	Protein Kinase C		

UBD	Ubiquitin Domain	WASP	Wiskott-Aldrich Syndrome Protein
UBL	Ubiquitin-Like		
UPR	Unfolded Protein Response	XBP1	X-Box Binding Protein 1
UPS	Ubiquitin-Proteasome system		
VNC	Ventral Nerve Cord		

LIST OF TABLES

Chapter 1

Chapter 2

Chapter 3

LIST OF FIGURES

Chapter 1

Chapter 2

Chapter 3

CHAPTER 1: WIRING THE NERVOUS SYSTEM

1.1 INTRODUCTION

The nervous system is a complex network of millions of neuronal processes and synapses. A single cubic centimetre of the human brain contains a few million neurons, each connecting with thousands of other cells and neurons. The intricate pattern of neuronal connectivity is achieved through well orchestrated developmental processes to ensure high level of function. A key issue during nervous system development is centered about the establishment of functional neuronal networks that are able to process sensory information and generate proper output signals. Failure of proper network formation can have profound effects on development, function, and viability. Neuro-developmental disorders such as Down syndrome, autism, mental retardation, as well epilepsy have been linked to abnormalities during human nervous system development.

To wire up the nervous system, neurons extend long processes (axons) traveling long trajectories to reach their final targets and form synapses. Over a decade ago, the founder of neuroscience Ramón y Cajal proposed that club-shaped structures at the tips of processes sprouting from the nerve cells, which he named "growth cones", were responsible for navigation decision in the embryo, thus enabling nerves to connect with their targets. Indeed, growth cones are the sensory and motile organelles of neurons that enable neuronal polarization, outgrowth, target recognition, branching, and synapse formation for the precise wiring of the neuronal networks. Genetic and

biochemical studies identified a host of attractive, repulsive, and bifunctional guidance cues as well as signaling mechanisms that play evolutionarily conserved roles in directing axons toward appropriate targets (Shilton, 2006; Tessier-Lavigne and Klodkin, 2010).

While axon guidance plays an important role in the establishment of neuronal networks, the refinement of these networks depends on the dynamic process of axon branching. In vivo and in vitro studies have shown that guidance cues and intracellular signaling components can also promote axon branching. However, unlike the well characterized neuronal guidance mechanisms, the cellular and molecular mechanisms regulating branching are not well defined. Therefore, uncovering new genes and pathways that mediate axon branching can further expand our understanding of neuronal network assembly during development. They can also provide further insights into different pathological conditions and has implication for developing therapeutic in neurodevelopmental disorders (Kalil and Hutchines, 2011; Hagg, 2006; O'Leary et al., 2005, 1990; Batsmyer and O'Leary, 1996). In the next section, I will review key aspect of axon branching, and describe conserved molecular mechanism that control branching.

1.1.1 Growth cone structure, function, and dynamics

The neuronal growth cone is a unique polarized structure with a pivotal role in wiring of the nervous system during development. This structure is involved in the

processing of information from external cues and producing coordinated changes in the cytoskeletal dynamics (Dickson, 2001, Schaefer et al., 2008). The axon shaft is a long cylindrical compartment composed of three different filaments: neurofilaments, microtubules (MT), and actin microfilament (F-actin); however, the role of neurofilaments in growth cone guidance and branching is not clear (Letourneau P, 2009**).** The growth cone can be divided into three domains based on their cytoskeletal composition: the central (C) domain, the peripheral (P) domain, and the transitional (T) domain (Okabe and Hirokawa, 1990; Gallo and Letourneau, 2004; Kalil and Dent, 2005). The C domain is located near the neuronal cell body and is rich in MTs, as well as membrane-associated vesicles and organelles such as endoplasmic reticulum and ribosomes (Gallo and Letourneau, 2004). These organelles are important for mRNA translation and expression of cytoskeletal associated proteins and growth cone associated receptors.

The P domain is located at the most distal end of the growth cone and it is composed of actin filaments. This domain is associated with lamellipodia, flat veil-like protrusion composed of a highly branched network of short actin filaments. Filopodia, are thin-finger like structures that extend from lamellipodia, and actin filaments that are packed into actin bundles. The T domain is located between the actin rich P domain and MT rich C domain, where it contains the molecular motor myosin that serves to translocate F actin assembled bundles from the P domain to the C domain in a process

known as F actin retrograde flow (Schaefer et al, 2008). In this processes actin filaments are rapidly polymerized into F-actin bundles in the P domain, while in the C domain actin is depolymerised into actin monomers (G-actin). Retrograde flow acts to limit the diffusion of MT into the peripheral domain (Dent and Gertler, 2003).

Filopodia are the main sensory structures within the P domain that can mediate growth cone behavior in response to external factors (Bentley and Toroian-Raymond, 1986; Chien et al., 1993). Removal of filopodia does not alter axon growth, but it can affect its navigation toward its final target (Bentley and Toroian-Raymond, 1986; Chien et al., 1993). Numerous signalling cascades have been identified that control growth cone behavior during nervous system development. The majority of these pathways converge on controlling the activity and organization of actin and microtubule cytoskeletons (Scheafer et al., 2008; Dent and Gertler, 2003; Zhou and Cohan, 2004).

Actin is a globular protein that can exist as ATP-bound monomer (G-actin) or as polymerized ADP-bound double stranded actin filament (F-actin). Actin filaments are polarized with two distinct ends: a fast growing barbed end that is oriented toward the distal plasma membrane and a slow growing pointed end. G-actin monomers assemble rapidly at the barbed end, promoting actin polymerization, while actin depolymerization occurs mainly at the pointed end in a process known as treadmilling (Neukirchen and Bradke, 2011; Lowery and Van Vactor, 2009; Bernstein and Bamburg, 2003). This rapid actin turnover occurs in the T domain, and plays a crucial role in

growth cone motility and path finding. Assembly of F-actin at the barbed end drives the filopodia forward, while retrograde flow of actin filament mediated by myosin motors, causes it to retract (Neukirchen and Bradke, 2011; Lowery and Van Vactor, 2009, Schaefer et al., 2008). Several actin cytoskeleton binding proteins have been identified that can bind directly to F- and G-actin where they modulate growth cone dynamics and growth. These proteins can be divided into two groups: actin polymerization/nucleation (APN) and actin depolymerization/severing (ADS). Actin-related protein 2, and 3 (Arp2, Arp3) and formins are well known members of the APN group that have been reported to increase actin polymerization and nucleation (Chen and Janetopoulos, 2003; Dent and Gertler, 2003; Korobova and Svitkina, 2008). Arp2/3 forms a complex with several other molecules that binds and nucleates actin filaments, leading to an increase in the number of free barbed ends. Actin depolymerizing factors (ADFs) are activated by dephosphorylation, where they bind to actin and increase the dissociation of and severing of actin filaments (Samiere and Bamburg, 2003).

Microtubules also play an important role in growth cone motility and guidance (Samiere and Bamburg, 2003). Microtubule protofilaments are composed of polymerized α and β tubulin heterodimers assembled in a head to tail fashion. Tubulin is a nucleotide triphosphatase where both α and β tubulin bind to GTP. Interestingly, only GTP- bound β tubulin is able to hydrolyze to GTP. GTP bound to α tubulin remains unhydrolyzed. A single microtubule (MT) tube is composed of approximately

13 parallel protofilaments with distinct plus and minus ends (Jordan and Wilson, 2004; Desai and Mitchison, 1997). The plus end which is usually oriented toward the F-actin meshwork in the P domain is more dynamic than the minus end because it contains β tublin subunits (Neukirchen and Bradke, 2011).

MT polymerization, like actin polymerization, is dynamic and involves the rapid addition of tubulin dimers to the fast growing plus end, and the dissociation of tubulin dimers from the minus end (Howard and Hyman, 2003; Baas PW, 2002). In vitro studies report MT undergoing slow continuous growth at the plus end, punctuated by specific phases named catastrophe and rescue. Dissociation of tubulin dimers during MT depolymerization cause MT shrinkage, which is rescued by addition of new dimers in the plus end. The rapid transition between growth and shrinkage is called dynamic instability and it is the underlying mechanism for MT dynamics. As MT bundles enter the growth cone, their dynamic plus end fans out (defasciculate) and invade the actin rich P domain, where they continue to grow and elongate along with F-actin in the P-domain (Howard and Hyman, 2003; Schaefer et al., 2002).

1.1.2 Formation of axon branches

As the nervous system develops, axons travel long trajectories to reach final targets aided by a variety of guidance cues. Axons that are not able to extend directly onto their final targets must extend axon branches to establish appropriate connections. Axonal branches have been found throughout the vertebrate nervous system.

Visualization of fluorescently labelled callosal axons in early postnatal cortical slices showed primary cortical axons developing complex branching morphologies (Dent et al., 2003). Time-lapse observation of neuronal branching show that branch formation consists of rapid expansion-retraction cycles at specific regions of the projecting axon, which results in axonal arborization at the site (Wang and Macagno, 1998).

Several forms of axonal branching have been described in the nervous system (Figure 1.1). Growth cone bifurcation generates the simplest form of branching, giving rise to two similar daughter branches with growth cones nearly half the size of the original grow cone. This type of branching is mostly associated with dendrites. Branching by bifurcation allows multiple targets to be innervated by terminal axon branches. Interstitial branching refers to the *de novo* formation of collateral branches from the axon shaft away from the nerve terminals (Acebes and Ferrus, 2000). These branches allow a single neuron to project and innervate multiple target cells independent of the growth cone and its targets (O'Leary et al., 1990; Gianluca Gallo, 2010). The dorsal root ganglion (DRG) sensory neurons are a simple model that demonstrates different branching phenotypes. DRG neurons bifurcate upon entry in the spinal cord, extending branches that project rostrally and caudally in the spinal cord. After a waiting period, interstitial branches extend from these two stem axons and terminate in the dorsal and ventral layers of the spinal cord where they further branch and arborise (Shemidt et al., 2007, 2012; Ozaki and Snyder, 1997).

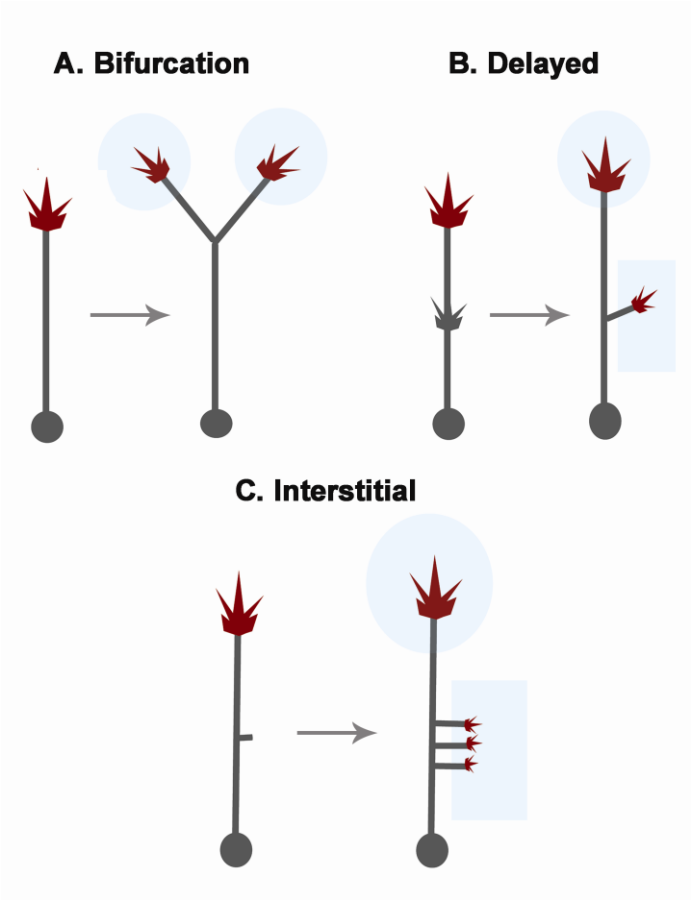

Figure 1.1 Modes of branching in the nervous system

Axons generate branches to connect with multiple synaptic targets. **A)** Bifurcation occurs at axon terminals, producing two branches with active growth cones. **B)** In the delayed mode, a single branch protrude from an unstable region on the axon shaft occupied be a previous growth cone. **C)** In collateral formation, daughter branch(s) form de novo from the axon shaft through protrusion of filopodia and/or lamellipodia. Adapted and modified from Gibson and Ma (2011) with permission.

The delayed form of branching happens along the axon shaft at sites distal to the growth cone. As the growth cone extends, it leaves behind a region with unstable cytoskeletal activity and frequent filopodial expansion. Subsequently this region develops a branch that protrudes from the axon shaft and extends toward its final target (Kalil et al., 2000; Kalil and Dent, 2005. Sensorimotor cortical neurons display delayed type branching morphologies (Kalil et al., 2000; Acebes and Ferrús, 2000). Even though axonal branches form through different modes, the mechanism underlying their formation is largely due to dynamic cytoskeletal remodelling.

One of the best models for studying cytoskeletal remodelling is the growth cone, which undergoes rapid cytoskeletal reorganization during axon outgrowth and guidance. In the last decade numerous signalling and molecular mechanisms were identified regulating growth cone outgrowth and guidance (Kalil and Hutchines, 2011; Hagg, 2006; O'Leary et al., 2005, 1990; Ma and Tessier-Lavigne, 2007). It is not surprising that some of these mechanisms were also implicated in governing branching also.

1.1.3 Intracellular Signal Transduction Modulating Axon Branching

Changes in cytoskeletal organization and dynamics are regulated by conserved intracellular signalling pathways. Two major conserved intracellular signalling pathways have been widely characterized for their role in regulating actin and microtubule dynamics in the growth cones: (1) the Rho GTPases and (2) the

serine/threonine kinases: the lipid kinase phosphatidylinositol 3-kinase (PI3K), protein kinase B (also known as Akt), as well as glycogen synthase kinase 3 (GSK3). In fact most axon guidance and branching signals are transduced through these two pathways which results in the appropriate modulation of growth cone motility, outgrowth, direction, as well as the extent of the outgrowth (Table 1.1).

Rho GTPases

The Ras-related super family of small guanosine triphosphatse (GTPases) includes more than 200 conserved proteins that have been implicated in signal transduction during axon guidance and branching. This class of proteins is further divided into six groups: Rho, Ras, Rab, Arf, Sar, and Ran (Colicelli, 2004; Hall and Lalli, 2010) and of these the Rho group of small GTPases have emerged as key regulators of cytoskeleton dynamics through a variety of guidance and branching receptors systems. Rho GTPases act as "molecular switches", where they cycle between an active, GTP-bound and an inactive, GDP-bound state. Only activated Rho GTPases are able to propagate downstream signalling events that control diverse biological activities such as actin cytoskeleton reorganization, microtubule dynamics, cell adhesion, as well as gene transcription (Harden et al., 2002; Hesasman and Ridley 2008). In response to various extracellular cues, guanine nucleotide exchange factors (GEFs) turn "ON" Rho GTPases by catalyzing the GDP exchange for GTP. In contrast, GTPase-activating proteins (GAPs) facilitate intrinsic GTPase activity by catalyzing hydrolysis of GTP and

subsequently turning Rho GTPases "OFF" (Jaffe and Hall, 2005). Additionally, guanine nucleotide dissociation inhibitors modulate Rho GTPases by inhibiting GDP dissociation, which leaves Rho GTPases in an inactive state.

Three members of the Rho GTPases subfamily are known for their role in modulating cellular morphology in both neuronal and non-neuronal cells and they are: Ras homologous member (Rho) A, Ras related C3 botulinum toxin substrate (Rac) 1-3 , as well as cell division cycle 24 (Cdc42) (Bishop et al., 2000; Ridley, 2006; Nobes and Hall, 1995). Several studies strongly support a key role of Rho GTPases in axon branching and guidance. In Drosophila, RhoA mutants display excessive dendritic branching, while loss of Rac1 causes strong branching defects, but no guidance defects. Interestingly, loss of all three Rac genes (Rac1-3) results in axon outgrowth, guidance, as well as terminal arborization defects (Ng et al., 2002). Furthermore, in vivo studies in *C. elegans* revealed that expression of constitutively active Rac mutant resulted in extensive ectopic branching defects (Struckhoff and Lundquist. 2003). Similarly, expression of RhoA in cortical neurons, in vitro, promoted branching defects (Ohnami et al., 2008).

Other than GAPs and GEFs, activation of Rho GTPases are also regulated by several proteins acting downstream of extracellular cues. Once activated by the latter, Rho GTPases bind to downstream effectors, controlling cytoskeleton reorganization, primarily through actin polymerization/depolymerization, microtubule reorganization, and gene regulation (Bustelo et al., 2007; Gibon and Ma, 2010). Rho-associated kinase

(ROCK) is the main downstream effector of Rho (Da Silva et al., 2003; Amano et al., 1997). ROCK activation induces phosphorylation of myosin II resulting in increased actomyosin contraction and actin depolymerization (Hirose M et al., 1998; Amano et al., 1996). Another downstream effector of Rho is the formin mDia, whose activation modulates actin polymerisation as well as promotes microtubule stabilization (Wen et al., 2004). One of the Rac effectors is the p21-activated kinase (Pak), a conserved serine/threonine kinase, whose activation signals multiple pathways leading to actin and microtubule stabilization (Wittmann, et al, 2003).

Kinases

In addition to Rho GTPases, PI3K, Akt, and GSK3 kinases work closely to regulate numerous signalling pathways to modulate cytoskeleton dynamics. The lipid kinase phosphatidylinositol 3-kinase (PI3K) plays a significant role in initiating a series of signalling pathways that are involved in multiple cellular and neuronal functions such as differentiation, survival, neuronal polarity, and outgrowth (Krasilnikov 2000; Rodgers and Theibert, 2002; Menager et al., 2004; Ditlevesen et al., 2003). PI3K is usually activated by upstream factors such as Ras (Yoshimura et al., 2006), and insulin receptor substrate-1 after stimulation by neurotrophins (Oinuma et al., 2007; Yoshimura et al., 2006; Yamada et al., 1997). Translocation of activated PI3K is necessary for the phosphorylation of membrane phosphatidylinositol 4, 5-bisphosphate (PIP2), thereby producing phosphatidylinositol 3, 4, 5-bisphosphate (PIP3).

Table 1. 1 Summary of molecules regulating axon branching

Molecule	Effect on Branching	References
Extrinsic Cues		
NGF	Promote	Zhou et al., 2004; Sanchez et al., 2006
BDNF	Promote	Gallo and Letourneau, 2004
Sema3A	Inhibit	Bagri et al., 2003; Dent et al., 2004
Slits	Promote/Inhibit	Ma and Tessier-Lvigne, 2007; Yang and Bashaw, 2006; Ozdinler and Erzurumlu 2002
Rho GTPases		
RhoA	Promote	Bishop et al, 2000; Ng et al., 2002
Rac	Promote	Ng et al., 2002
GEFs	Inhibit	Jaffe and Hall, 2005; Bos et al., 2007
Kinases		
PI3K	Promote	Menager et al., 2004; Gallo and Letourneau 1998
Akt	Promote	Ketscheck and Gallo, 2010; Markus et. al, 2002
GSK3	Inhibit	Bilimoria et al.,2010
Sax1/NDR kinase	Promote/Inhibit	Emoto et al., 2004; Zallen et al., 2000
Ubiquitin Ligases		
Highwire/RPM-1	Promote/Inhibit	D'Souza et al.; 2005; Schaefer et al., 2002
Nedd-4	Promote	Drinjakovic et al., 2010

PIP3 is an important mediator in various downstream signalling pathways and it acts by recruiting multiple cytoskeleton and signalling proteins to the membrane. PIP3 activates Rho GTPase signalling as well as Ras and Cdc-42 signalling through GEFs, which are direct downstream effectors of PI3K (Rodgers and Theibert, 2002; Krasilnikov 2000; Bondeva et al., 1998).

Another downstream effector of PIP3 is Akt, which is also translocated to the membrane upon PI3K activation. A serine/threonine specific kinase, Akt, contains a Pleckstrin Homology domain that binds with high affinity to PIP3 (Ketscheck and Gallo, 2010). Akt signals several signalling pathways after its activation by PDK1 (phosphoinositol-dependent protein kinase-1), and subsequently phosphorylates and inhibits GSK3, a downstream target of Akt (Ketschek and Gallo, 2010).

GSK3 acts a negative regulator of microtubule dynamics; usually constitutively active, GSK3 is inhibited following phosphorylation by Akt. Inhibition of GSK3, through PI3K/Akt, is involved in neuronal differentiation/polarity through Wnt/Frizzled signalling, while PI3K and Akt activity is required for nerve growth factor (NGF) and neurotrophin mediated signalling to regulate neuronal polarity and promote axonal outgrowth and branching (Ketscheck and Gallo, 2010; Markus et al., 2002). Pharmacological inhibition of PI3K blocked branching in cultured DRG neurons and sensory neurons (Gallo and Letoumeau 1998; Ketschek and Gallo,2010) as well as neuronal differentiation (Menager et al., 2004); overexpression of a constitutively active

PI3K promoted multi axon formation (Read and Gorman, 2009; Yoshimura et al., 2006).

PTEN (tensin homology deleted on chromosome ten) regulates PI3K activity through dephosphorylating PIP3 to PIP2 (Leslie and Downes, 2002). PTEN activity is required to maintain basal PIP3 levels. PTEN deletion studies in mice showed an increase in PIP3 levels that translated to a significant increase in sensory axon branching in these mutant mice (Kwon et al., 2006), while overexpression of PTEN disrupted axon formation and polarization (Shi et al., 2003). Even though the activity of each of these kinases varies, their interconnected function comprises an effective branch promoting signalling pathway.

Other kinases have also been implicated in modulating axon morphology, guidance and branching. The NDR (nuclear Dbf2-related) family of kinases is classified as subgroup of the conserved AGC group of serine/threonine protein kinases based on the sequence of the conserved catalytic domain (Hergovich et al., 2006). These include NDR1, NDR2, LATS1 (large tumor suppressor-1) and LATS2 in mammals, *trc* (tricornered), and Lats/Warts in Drosophila, SAX-1and LATS in *C. elegans*, Dbf2, Dbf20, and Cbk1 in *S.cerevisiae*, and Cot1 *in N. crassa* (Hergovich et al., 2006). NDR kinases are characterized for having a central kinase catalytic domain and two phosphorylation sites (ser281 and Thr444 of human NDR1) (Hergovich et al., 2006). In vitro and in vivo studies established multiple roles for NDR kinases in regulating cellular and neuronal development and growth. In Drosophila, mutations in *trc* causes branching and

splitting of epidermal hairs, and bristles as well as dendritic branching and arborization defects (Emoto et al., 2004; He et al., 2005a).

Second messengers

Intracellular signalling transduction cascades can also be triggered by second messengers such as calcium (Ca^{2+}) and cyclic nucleotides cAMP and cGMP. Cytoplasmic calcium levels in growth cones are tightly regulated through membrane ion channels and internal stores (Hong et al., 2000; Nishiyama et al., 2003). Asymmetric influx of Ca^{2+} can trigger signalling cascades that ultimately mediate growth cone outgrowth and branching. Changes in Ca^{2+} can alter the activity of GAPs, GEFs, Rho GTPases, kinases such as Calmodulin kinases (CamKs), as well numerous phosphatase. The effect of these signalling cascade on growth cone behavior is mediated by changes in cytoskeleton dynamics (Wang and Poo, 2005; Henley and Poo, 2004; Kalil and Hutchines, 2011). Guidance molecules such as Netrins and NGFs induce growth cone steering through calcium signalling. In fact changes in calcium levels can convert Netrin mediated attraction in growth cones to repulsion (Hong et al., 2000).

Cyclic nucleotide levels are enzymatically controlled through the conversion of ATP and GTP into cyclic AMP (cAMP) and cyclic GMP (cGMP). Changes in the cAMP and cGMP levels, similar to Ca^{2+} levels, can trigger signalling pathways. Protein kinase A (PKA), one of cAMP targets, is involved in cAMP-induced growth cone turning (LeBrasseur, 2007). Inhibition of PKA through low cGMP levels alters growth cone

behavior from attraction to repulsion (Song and Poo, 1999). Thus the ratio of cAMP to CGMP is critical for maintaining proper growth cone behavior; growth cone attraction is favored by high ratio, whereas repulsion is caused by low ratios (LeBrasseur, 2007, Nishiyama et al., 2003).

Ubiquitin ligases

The ubiquitin proteasome system (UPS) is widely known for its role in cellular degradation. Interest in the role of UPS in nervous system development started with the discovery multiple genes involved in UPS dependent axon growth and guidance. In Drosophila, *highwire (hiw*) mutants displayed abnormal axon arborization and branching (Wan et al., 2000). *Highwire* encodes a protein with a RING-H2 domain that is conserved among ubiquitin ligase (E3) proteins. Disruption of this domain underlies growth cone morphological defects in Drosophila. Mutations in *rpm-1*, *highwire* homologue in *C. elegans* also displayed similar defects in synapse organization as well as branch arborization (Schaefer et al., 2000; Zhen et al. 2000). Highwire, RPM-1 and the mammalian homologues Pam and Phr1 are all members of the PHR (Pam/Highwire/RPM-1) family of conserved proteins that share the conserved RING-H2 domains. These mutants all display defects in terminal axon arborization and synapse development (Gue et al., 1998; Schafer et al., 2000; Wan et al., 2000; Burgess et al., 2004). The mouse PHR homologue was further characterized to control growth cone morphology as well as arborization through modulating microtubule dynamics in the

growth cone (Lewcock et al., 2007). Recently another ubiquitin ligase, Nedd4 , has been identified to promote branching through modulation of PTEN activity (Drinjakovic et al., 2010).

1.1.4 Extracellular Molecular Signals Regulating Axon Branching

Modulation of cytoskeletal dynamics is mediated by a variety of extracellular cues. Work in the last decades has identified four major families of guidance cues playing a significant role in nervous system formation. The Netrins, Semaphorins, Ephrins, Slits, as well as their associated receptors have been shown to stimulate neuronal guidance and outgrowth through attractive or repulsive behavior (Shilton, 2006). Furthermore, their role in cytoskeletal reorganization and interaction (as well other biological processes) has been reported to be mediated through Rho GTPase and kinase signal transduction pathways (Gallo and Letournau, 1998; Kim et al., 2006; Bilimoria et al., 2006; Ohnami et al., 2008; Ng et al., 2002).

Additional factors have also been identified to play a vital role in neuronal network assembly. Neurotrophins do not share any similarities with the four guidance cue families, but none the less are involved in guidance and branching (Gallo and Letourneau, 2004; Goodwin and Yap, 2004; Sanchez et al., 2009; Schafer et al., 2000).

Ephrins

Ephrins are a family of transmembrane proteins recognized by Ephrin (Eph) receptors that can act as either repulsive or attractive cues in directing axonal branching

and outgrowth (Yates et al., 2001). These proteins are divided into two classes A and B. EphrinAs (A1-A6) are anchored to the plasma membrane through glycolsulphosphatidylinositol-linkages while EphrinBs (B1-B3), have a single-pass hydrophobic transmembrane domain and lack a catalytic intracellular domain. These cues are recognized by 16 -18 different receptor tyrosine kinases known as Eph (erythropoietin-producing hepatocellular) receptors. While these receptors are divided into EphA and EphB groups, unlike their ligands, they are all structurally similar (Meier et al., 2011).

Ehprin interactions have been shown to be important for topographic mapping of the RGC in the superior colliculus (Yates et al., 2001). Additionally ephrinA/EphA signalling is also necessary for guidance axons branches to their final targets in Drosophila (Boyle et al., 2006). EphA acts as repulsive cues through activation of Rho GTPases and Rock or Rac/Pac signalling pathways (Mann et al., 2002; Reber et al., 2004).

Semaphorins

Semaphorins are a large family of membrane-bound and secreted proteins, exhibiting both attractive and repulsive activities through their interaction with the plexin/neuropilin receptor family (Kruger et al., 2005; Lui and Strittmatter, 2001). Semaphorin 3A (Sema3A), one of the best studied semaphorins, is widely characterized for its repulsive activity in mediating growth cone extension, branching, and collapse. Studies about semaphorins and specifically Sema3A provided strong evidence that axon

outgrowth is regulated independently from axon branching. In vivo and in situ studies report Sema3A inhibiting axonal branching, while not affecting axonal outgrowth (Dent et al., 2004; Bagri et al., 2002). Furthermore, application of Sema3A in cortical neuron cultures reduced axonal branching (by approximately 50%), without inhibiting or reducing axonal outgrowth (Bagri et al., 2002; Dent et al., 2004; Bagnard et al., 1998). Sema3A regulates cytoskeleton dynamics, where it can cause actin depolymerization and microtubule collapse resulting in growth cone collapse.

Sema3A functions through a receptor complex consisting of neuropilin, a ligand binding co-receptor, and plexin, a signal-transducing element; these two ligands are downstream effectors of Rho GTPases. In hippocampal cultured neurons, GEFs were found in complex with plexin/neuropilin receptors (Toyofuku et al., 2005). The growth cone collapse and repulsive response to Sema3A are mediated through Rac1 and RhoA activation (Jin and Strittmatter, 1997; Turner et al., 2004; Hall and Lalli, 2010).

Neurotrophins

Neurotrophins belongs to large family of secreted growth factors that promote axon guidance and branching such as nerve growth factor (NGF) and brain-derived neurotrophic factor (BDNF). NGF and BDNF signal predominantly through two classes of receptors: the Tropomyosin related kinase (Trk) and the p75 neurotrophin receptors (Gallo and Letourneau, 2004). NGF is involved specifically in regulating cytoskeletal

dynamics. Activation of Trk receptors in sensory neurons triggers signalling pathways that involve PI3K and Ras (Zhou et al., 2004b; Markus et al., 2002).

Slits

Slit proteins are a large family of secreted proteins that were among the first extracellular signals shown to regulate axonal branching(Brose and Tessier-Lavigne, 2000). Slit's repulsive activity is mediated through its interaction with members of the Robo (Roundabout) receptor family. These receptors are highly conserved single-pass transmembrane proteins that contain up to four conserved cytoplasmic domains necessary for binding to Slits (Spitztweck B, et al., 2010; Evan and Bashaw, 2010).

Slit stimulation leads to binding of GAP proteins to the Robo intracellular domain, which activates Rac signaling cascades but not Cdc42 or RhoA (Wong et al., 2001; Yang and Bashaw, 2006). In vitro studies have shown that Slit2 regulates sensory axon collateral branching as well as DRG arborization (Wang et al., 1999; Ozdinler and Erzurumlu, 2002). Knockout mice lacking Slit repulsive activity displayed an increase in branching of sensory neurons, similar to the phenotype seen in knockout mice lacking Robo activity (Ma and Tessier-Lavigne, 2007).

1.2 *C. elegans*: AN IDEAL MODEL ORGANISM

C. elegans are free living soil nematodes that exist primarily as self-fertilizing hermaphrodites (959 somatic cells), but males (1013 somatic cells) can arise by spontaneous non-disjunction and usually compromise 0.05% of the total population (Corsi, 2006). A single hermaphrodite can produce a large progeny pool (>300) which can be greatly enhanced (>1000) if hermaphrodites mate with male worms (Hodgkin et al., 1991). The genetics of *C. elegans* is well characterized and follow Mendelian principles. An adult worm is approximately 1 mm in length and has a generation time of 3 days at 20°C.

The life cycle *C. elegans* consists of three stages, 14 hours of embryogenesis, 36 hours of postembryonic development that occurs through four larval stages (L1-L4), and finally adulthood lasting approximately 15-20 days. Multiple differentiated tissues such as muscles, hypodermis, gastrointestinal tract, and nervous system develop during the four larval stages (Ambros, 2000). More than 35% of *C. elegans* genes are highly conserved and have human homologs (Hiller et al., 2005). Additionally, the cell-lineage of each somatic cell has been traced (Sulston et al., 1983), providing a complete fate map for each cell.

A complete map of the wiring and synaptic connectivity of the nematode's nervous system has been established by electron microscopy (Hall and Altun, 2008). These maps are powerful tools for analysis of cell-cell interaction during development,

and provide a strong reference for assessing genetic mutation effects on developmental processes. Moreover, the worm's transparent body facilitates the study of cellular differentiation during development using various microscopy techniques.

The popularity of *C. elegans* as a model organism for understanding nervous system development and function is largely due to the power of forward genetic screens, which allows for the dissection of genetic pathways (and their components) involved in nervous system development. In a classic forward genetic screen, geneticists expose the germ-line of the hermaphrodites to DNA- damaging mutagens such as ethyl methylsulfonate (EMS) or trimethyl phosphate (TMP) to generate mutations with desired phenotype that are later characterized and traced to mutations in relevant genes (Jorgensen and Mango, 2002). Several forward genetic screens and modifier variations such as enhancer and suppressor screen in *C. elegans* contributed significantly to our understanding of axonal outgrowth and guidance (Zallen et al., 1999; Colavita and Culotti, 1998; Mehta et al., 2004).

In post-genomic era faster and more direct genetic methods were developed to modify a candidate gene and characterize the phenotypic consequences of the modification. Known as reverse genetics, stable mutants of candidate genes are generated by random mutagenesis (DNA insertion, deletion, or point mutation). Additionally, target genes can by potentially silenced in *C. elegans* by double stranded RNA (dsRNA) either by direct injection of dsRNA into the gonad, feeding bacteria

expressing dsRNA, or in dsRNA containing media (Fire et al., 1998; Timmons and Fire, 1998; Tabara et al., 1998; Kamath et al., 2003). The Worm Knockout Consortium was established with the goal of generating libraries of deletion mutants for every single gene in the *C.elegans* genome.

Over the years, research on *C. elegans* contributed significantly to our understanding of numerous biological processes such as the apoptotic pathways in addition to the discovery of RNA interference (Horvitz et al., 1999; Fire et al., 1998).

1.2.1 Wiring up the C. elegans nervous system

Many molecular and signalling pathways that regulate nervous system development are highly conserved in *C. elegans*. The *C. elegans* nervous system is a well characterized and extremely simple system composed of 302 neurons, divided into sensory neurons, interneurons, and motor neurons, which control the worm's normal behaviors such as locomotion, feeding, defecation, and egg-laying (White et al., 1986). The majority of these neurons exhibit simple morphology where they extend unipolar or bipolar unbranched processes along the anterior-posterior axis (AP) or the dorsal-ventral (DV) axis, with the exception of few neurons that display distinct branching patterns such as the HSN and VC motorneurons (Altun and Hall, 2011).

The simple neuronal circuits that control the nematodes behaviors provide an attractive model for studying the molecular and cellular basis of nervous system development and function.

1.2.2 C. elegans egg-laying model

The egg-laying system in nematodes is comprised of the gonads, vulva, uterine and vulval muscles, and a simple egg-laying neuronal circuitry consisting of two HSNs and six VC motorneurons (Figure 1.2)(Schafer, 2006). Egg-laying happens when muscle contractions open up the vulva to expel eggs from the uterus, and occurs in a distinct temporal pattern (Schafer, 2006; Waggoner et al., 1998): clusters of eggs are laid in short bursts (also called active phase, 1-2 minute duration), separated by longer inactive periods where individual eggs are laid (inactive phase, 20 minutes duration).

Vulva, the egg-laying organ

The vulva is a hermaphrodite-specific organ that functions as a passageway connecting the gonads to the external environment. This organ is derived post-embryonically from six vulval precursor cells (VPCs) that are born during the first larval stage (Schindler and Sherwood, 2012). The three ventral VPCs, P5.p-P7.p, undergo a series of inductive interactions that induces the P6.p to adapt a 1° vulva lineage, producing the outer vulva cells, while P5.p and P7.p are induced to adapt the 2° vulval lineage, producing the outer cells of the vulva. The remaining VPCs express a non-vulval fate and fuse with the hypodermal syncytium (Sternberg and Horvitz, 1986). After undergoing multiple cell division cycles, each of the VPCs generate 22 differentiated vulval cells at early L4. The latter cells undergo morphogenetic changes

to from the adult vulva consisting of a stack of 7 toroids at the midline (Sharma-Kishore et al., 1999).

Egg-laying muscles

A total of 16 muscles comprise the egg-laying musculature including the eight uterine muscle cells attached to the uterus, whose contraction promotes egg expulsion from the gonads. The remaining eight muscles are vulval muscles (Vms) which attach to and contract the vulva (Schafer, 2006; Garriga et al., 1993). Of all vulva muscles, four Vm2 muscles play an important role in egg-laying since they receive extensive synaptic input from the egg-laying motor neurons (White et al., 1986; Schafer, 2006). In fact ablation of the M cell, vulva muscle progenitor cell, eliminates egg-laying completely (Li and Chalfie, 1990; Schafer, 2006).

Egg-laying neurons

The Vm2 vulva muscles receive considerable synaptic input from a pair of hermaphrodite specific motorneuron (HSN), and six ventral cord type C(VC) motor neurons (VC1-6), which together make up the egg-laying neuronal circuit (Figure 1.2) (Schafer, 2006). The HSNs are two bilateral motor neurons with cell bodies located subventrally posterior to the vulva with a long axon that extends ventrally into the ipsilateral ventral nerve cord (VNC) and then anteriorly to the nerve ring (White et al., 1986). At specific locations near the vulva HSNs form short branches and synapse with Vm2 muscles and VCs (specifically VC5).

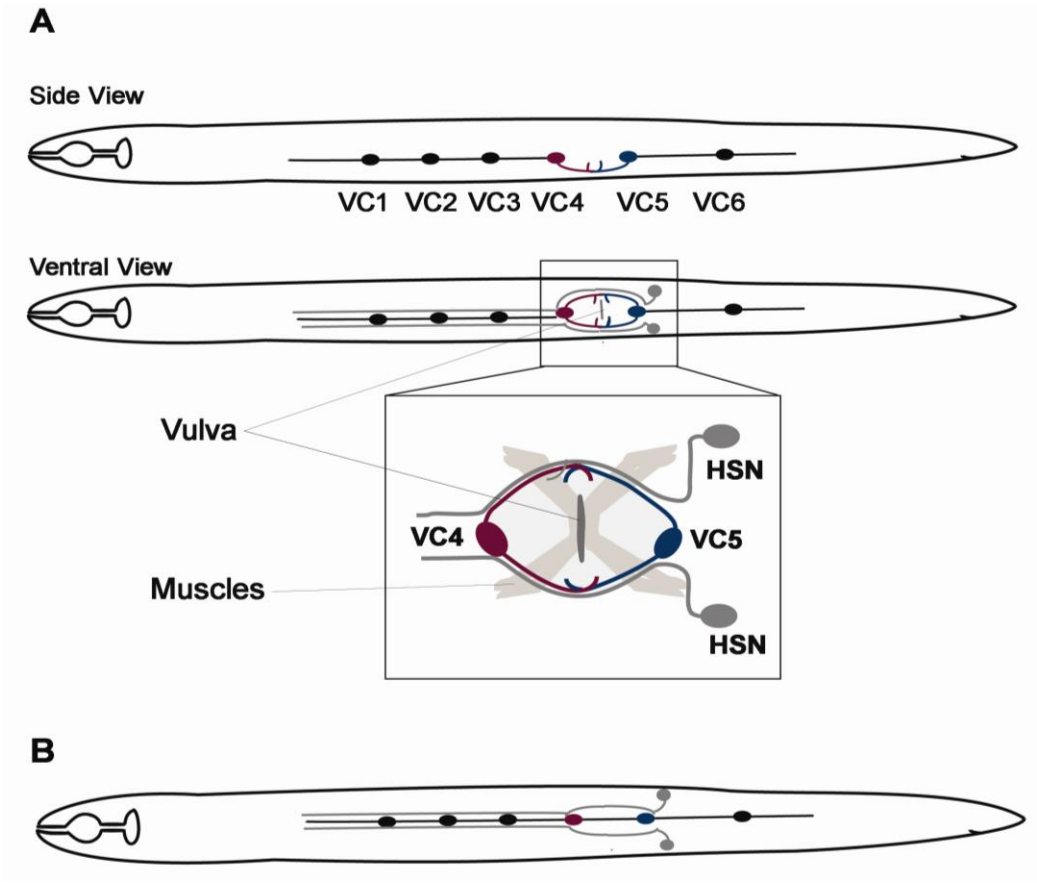

Figure 1.2 Egg-laying system in *C. elegans*

A) The egg-laying system is composed of 16 vulva and uterine muscles and two classes of motorneurons, VC4-5, and HSNs. At L4, VC4-5 axons project laterally around the vulva forming a circular tract. Overlapping branches form branches or arborizations at distinct sites on the left and right side of vulva. VC4-5 and HSN axon morphology is dictated by branching cues secreted from the vulva. **B)** VC4-5 display bipolar axon morphology (similar to VC1-4 and VC6) in vulvaless mutants.

The six hermaphrodite specific VCs are bipolar neurons with cell bodies positioned along the VNC (Figure 1.2). Based on their morphology they are divided into two classes. The vulva-proximal VC4 and VC5 flank the egg-laying organ and extend their axons mediolaterally, forming a circular tract around the vulva. VC4-5 axons form distinct stereotypical branches that innervate Vm2 vulval muscles (Colavita and Tessier-Lavigne, 2003). Vulva-distal neurons, VC1-3 and VC6, in contrast to VC4-5, are oriented anteroposteriorly, with axons growing along the ventral nerve cord (Schafer, 2006; Duerr et al., 1999).

The egg-laying neurons express more than one neurotransmitter: the HSNs contain serotonin, acetylcholine, and FMRFamid related neuropeptide (Waggoner et al., 1998, Schafer, 2006). The cholinergic VCs also contain FMRFamid related neuropeptide, and possibly serotonin (Schafer, 2006). VCs also contain the vesicular monoamine transporter CAT-1, even though they do not express the serotonin biosynthetic enzyme tryptophane hydroxylase (Duerr et al., 1999, 2001; Waggoner et al, 1998; Schafer, 2006).

Laser ablation studies and analysis of egg-laying defective (*egl*) mutants with HSN defects revealed a vital role for HSNs in regulating egg-laying in nematodes (Desai and Horvitz, 1998). HSN activity is particularly important in inducing the active-phase of egg-laying; loss of HSN in worms results in a significant reduction in the occurrence of clusters of egg-laying events (Waggoner et al., 1998). HSNs induce egg-laying

primarily through serotonin, however studies suggest additional roles for other neurotransmitters expressed by HSNs in egg-laying stimulation also (Kim et al., 2001).

Laser ablation of VC neurons in worms suggests a less significant role for these neurons on their own, but they can significantly enhance egg-laying defects in *egl* mutants (Schafer 2006, Waggoner et al., 1998). Over the years numerous models have been generated describing the effect of this neuronal circuitry on egg-laying behavior. A current model proposes a central commanding role for HSNs in inducing egg-laying directly through excitation of Vm2 muscles and indirectly throughVC4-5. In this model, VC4 and VC5 have dual function exciting Vm2 vulva muscles and inhibiting HSNs through a negative feed-back loop (Zhang et al., 2008; Waggoner et al., 1998).

1.2.3 Development of egg-laying neuronal circuitry

Growth and branching of the egg-laying neurons is closely coordinated with morphogenesis of the egg-laying organ (Li and Chalfie, 1990). Vulva epithelia act as guidepost cells during the vulva morphogenesis providing inductive signals promoting branching and arborization of the HSN and VC4-5 neurons (Shen and Bargman 2003, Chao et al., 2009).

The HSNs are born during embryogenesis in the tail and migrate to the midbody before hatching (Sulston and Horvitz, 1977). Initial axon outgrowth starts at L2 and L3 guided by primary vulva precursor cells (P6.p) and other ventral nerve cord neurons. At early L4, each HSN extends a long axon ventrally into the VNC and extend anteriorly

to the nerve ring from there. At the fourth larval stage, HSNs defasciculate dorsally from the VNC and branches form off the HSN axons that ultimately innervate the Vm2 vulva muscles and synapse with VC5 (Garriga, et al., 1993). The same epithelial cells are also responsible for mediating axonal growth and branching of the VC neurons (Li and Chalfie, 1990).

VCs are born at first larval stage but delay axon outgrowth till late L3 in synchrony with vulva development. Studies in vulva-less mutants and vulva-ablated animals show VC4-5 extending axons along the anterior-posterior axis, similar to vulva-distal VC neurons. Additionally, in these worms the HSNs and VC4-5 do not display any branching at vulva (Figure 1.2) (Li and Chalfie, 1990; Garriga et al., 1993).

The egg-laying neurons are an excellent model to study the mechanisms underlying neuronal development. A forward genetic screen for VC4-5 axon morphology defects using the *Pcat-1::GFP* reporter transgene (used to visualize VC4 and VC5) identified mutations in *png-1* to cause excessive ectopic branching at the vulva (Habibi-Babadi et al., 2010). This gene was found to encode a highly conserved cytosolic enzyme belonging to the transglutaminase super family of enzymes that are involved in the processing of misfolded proteins prior to degradation by the proteasome(Suzuki, 2007). In the following section I will briefly describe the role of *png-1* homologues in processing of misfolded proteins.

1.3 THE ENDOPLASMIC RETICULUM QUALITY CONTROL SYSTEM

The endoplasmic reticulum (ER) is a multifunctional specialized compartment with a central role in many specialized cellular functions including calcium storage, synthesis, modification, processing, and folding of transmembrane and secretory proteins, as well as synthesis and assembly of the lipid bilayer. The ER uses an elaborate surveillance system called the ER protein quality control (ERQC) to ensure that only properly modified and folded proteins are transported into the Golgi compartment. In general, only accurately folded proteins can pass the ERQC checkpoints. Misfolded proteins are prevented from entering the secretory pathway and are retrotranslocated from the ER to the cytosol for degradation in a ubiquitin-proteasome manner in a process called ER-associated degradation (ERAD) (Rock et al., 2004; Murray AW, 2004). ERAD occures in three primary steps: 1), selective substrate recognition , 2) retrotranslocation and ubiquitylation, and 3) degradation by the 26S proteasome (Hedge and Ploegh, 2010; Araki and Nagata, 2011). The mechanisms by which ERAD substrates are recognized from properly formed protein remains largely unknown, however, studies in yeast, drosophila, nematodes, and mice have proposed a model of substrate recognition and targeting that combines multiple factors (Figure 1.2)(Araki and Nagata, 2011; Malhotra and Kaufman, 2007).

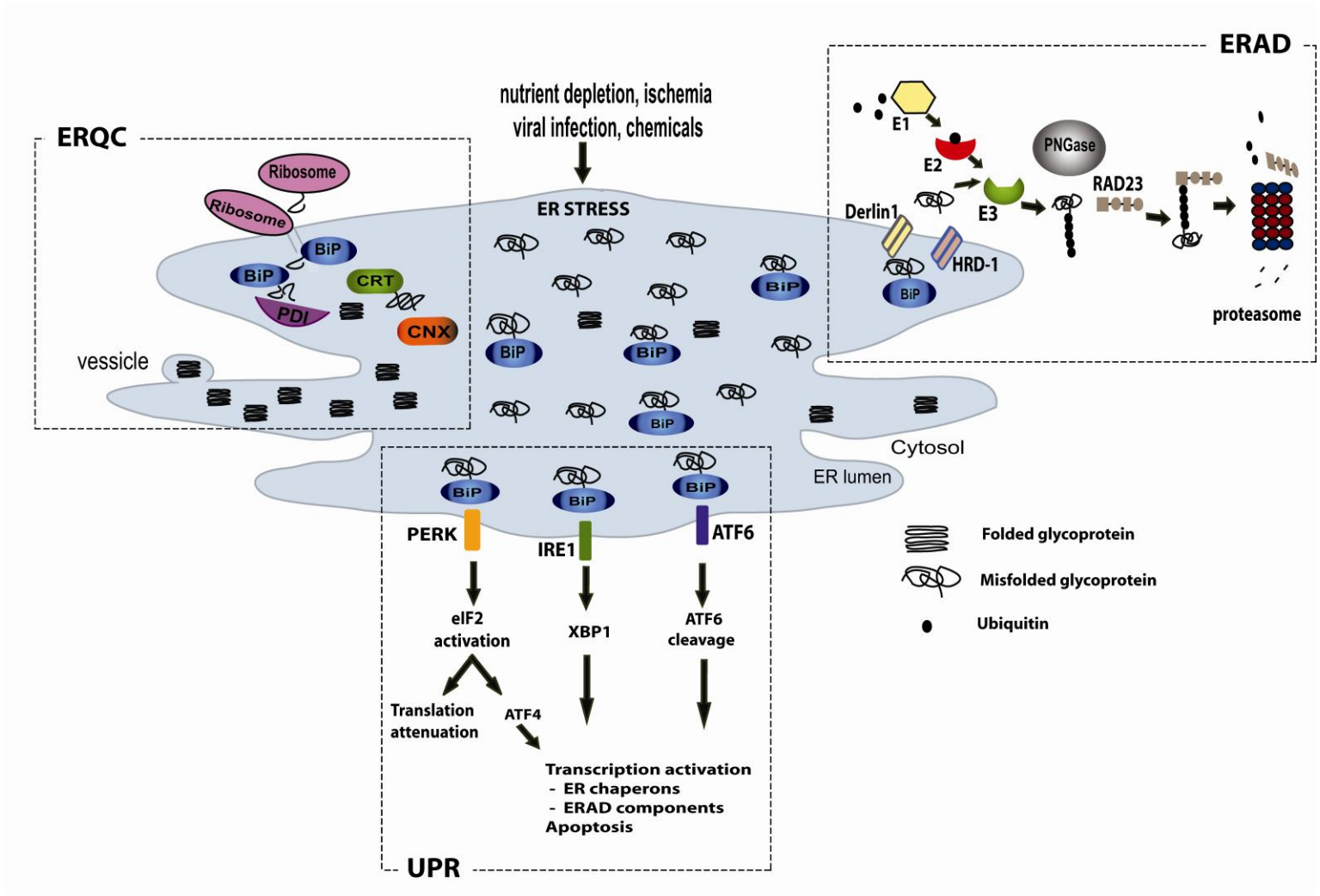
ERAD
nutrient depletion, ischemia
viral infection, chemicals
ERQC
Ribosome
Ribosome
BiP
BiP
CRT
PDI
CNX
vessicle
ER STRESS
BiP
BiP
BiP
BiP
E1
E2
E3
PNGase
RAD23
Derlin1
HRD-1
BiP
proteasome
Cytosol
ER lumen
BiP
BiP
BiP
PERK
IRE1
ATF6
eIF2
activation
XBP1
ATF6
cleavage
Translation
attenuation
ATF4
Transcription activation
- ER chaperons
- ERAD components
Apoptosis
UPR
Folded glycoprotein
Misfolded glycoprotein
Ubiquitin

Figure 1.3 Endoplasmic reticulum quality control

Secreted or transmembrane proteins enter the endoplasmic reticulum(ER) where they interact with a variety of chaperon molecules and undergo series of modification processes to fold accurately. Only properly folded proteins pass the ER quality control machinery (ERQC), after which they are secreted to their final targets. In ERAD, misfolded proteins that do not pass the quality control machinery are retrotranslocated to the cytoplasm for proteasomal degradation. Following ubiquitination substrates are transferred to the proteasome for degradation by Rad23, a shuttle protein that can bind directly to the proteasome. ER homeostasis can be disrupted upon exposure to various factors, which can cause misfolded proteins to accumulate in the ER. ER stress activates the unfolded protein response (UPR) consisting of three signalling cascades to restore ER homeostasis. IRE1 activation splices an intron from XBP1, facilitating its translation of this transcription factor. Activation of Xbp1 upregulates chaperons and ERAD genes. Activation of PERK is followed by eIF2 phosphorylation, and subsequently stops protein translation. Activated ATF6 is translocated to the Golgi apparatus where it along with Xbp1 functions to upregulates ER resident chaperons. The figure was inspired from the following reviews: Malhotra and Kaufman, 2007; Scheuner and Kaufman, 2008; Ma and Hendershot, 2001; Araki and Nagata, 2011.

1.3.1 Selective substrate recognition

The ER houses three families of molecular chaperones and folding enzymes: chaperones of the heat shock proteins (Hsp) family including Hsp70, Hsp40, and BiP, lectins-like chaperons such as calnexin (CNX) and calreticulin (CRT), and members of the thiol disulphide oxidoreductases such as the protein disulfide isomerases (PDIs). Following translocation into the ER lumen, newly synthesized polypeptides interact with a variety of resident chaperones and enzymes and undergo multiple posttranslational modifications including glycosylation and disulfide bond formation (Ellgaard and Heleneius, 2003; Araki and Nagata, 2011). Once proteins attain their correct tertiary structures they are released from ER chaperones and enter the ER exit sites. Proteins that fail to fold are retained (in the ER lumen) and must be degraded to prevent formation and accumulation of toxic protein aggregates (Mehnert et al., 2010; Schroder and Kaufman, 2006).

1.3.2 Ubiquitylation and retrotranslocation of ERAD substrates

The Ubiquitylation of ERAD substrates is a well established process that is important for substrate recognition for proteasome-dependent degradation, as well as for the retrotranslocation of these substrates to the cytosol (Jarosch et al., 2002). Ubiquitin (Ub) is a 76 amino acid protein that is conserved from yeast to mammals. Ubiquitylation, an ATP-dependent process, occurs in the cytosol and the ER membrane by the concerted action of three sets of enzymes. First, a ubiquitin activating enzyme

(E1), uses a single ATP molecule to form a thioester bond between E1 and a Ub protein (Hershko and Ciechanover, 1998). Following activation the ubiquitin moiety dissociates from E1 and is transferred to a ubiquitin conjugating enzyme (E2). Finally, E2 transports Ub directly to target protein substrates in a process catalyzed by a ubiquitin ligase (E3). Additional Ub molecules are added in successive reactions, mediated by E2 and E3, to form a polyubiquitin chain on the target protein (Hershko and Ciechanover, 1998).

As ERAD occurs in the cytosol, misfolded proteins must be translocated from the ER lumen back to the cytoplasm. Retrotranslocation is a substrate-specific complex process that is mediated by multiple ERAD components acting as channels or carriers for transport across the ER membrane. The retrograde transfer of several ERAD substrates is carried by p97 AAA-ATPase, a member of the magnesium dependent type II AAA-ATPases, in complex with UFd1 and Npl4 cofactors. This complex contains ubiquitin binding domains, where it interacts directly with ubiquitinated substrates and subsequently extracts them from the ER lumen (Ye et al., 2001, 2004).

The translocation channel, Sec61, a multiprotein doughnut shaped pore on the ER membrane, is a conserved protein involved in the retrograde transport of Ub. Studies in yeast have shown that the degradation of ubiquitinated substrates is either delayed or reduced in sec61 mutant strains (Pilone et al., 1997; Plemper et al., 1997). Studies in T-cells infected with the human cytomegalovirus implicated Sec61 in the

transfer of MHC class I heavy chains across the ER membrane (Shatz C, 2009; Huh et al., 2000; Wiertz et al, 1996).

Alternatively, the ER utilizes other channels to transfer different substrates across its membrane. Members of the conserved Derlin family (Derlin1-3) participate in the retrograde transfer of substrates in complex with other ER resident components and Ub ligases. Derlin-1 is a membrane protein that interacts directly with the cytosolic p97 AAA-ATPase to extract Ub tagged substrates from the cytosol through the retrotranslocation channel (Ye et al., 2004). Inactivation of Derlin-1 homologues in *C. elegans* and yeast induces ER stress by preventing the elimination of misfolded glycoproteins from the ER lumen (Knop et al., 2006; Ye et al., 2004; Schaheen et al., 2009). The complexity of the nature of retrotranslocation channels is further enhanced by studies showing Derlin proteins complexes with components of the ERAD such as Hrd1 and p97 AAA-ATPases (Guerriero and Brodsky, 2012; Lilley and Pleogh 2005; Kny et al, 2011). There remain many unanswered questions regarding how these complexes work in the recognition and transfer of misfolded proteins prior to proteasomal degradation.

1.3.3 Proteasomal degradation

Post-translational modification by ubiquitin signals protein degradation and serves to target Ub- tagged proteins to the 26S proteasome. Even though the general pathway of the ERAD is chartered, the processes of detection, transport and the subsequent processing of ubiquitylated substrates by the proteasome are still not fully

known. However, most of the components associated with ERAD share a common affinity for recognition and binding of ubiquitin (and polyubiquitin chains on glycopeptides); these receptor proteins have either ubiquitin binding domains (UBDs), or ubiquitin interacting motifs (UIMs) that regulates their association with ubiquitin. Several subunits of the regulatory particle (RP) subcomplex of the 26 proteasome utilize multiple UIM motifs to recognize and recruit selective ubiquitylated substrates to the proteasome. These include Rpn1 (S2/PSMD2 in mammals), Rpn10 (S5a in human), and Rpn13 (Hartmann-Petersen and Gordon, 2004a; Raasi et al., 2005; Finley, 2009). Yeast Rpn10 was reported to act as a multi-ubiquitin receptor in vitro, binding to only ubiquitin chains containing four or more Ub moieties. However, deletion of this gene did not show any alteration in the yeast's development or viability, a sharp contrast to the importance of a functional proteasome for numerous cellular functions (van Nocker et al., 1996; Szlanka et al., 2002).

Genetic and biochemical studies in *S. cerevisiae* proposed the role of adaptor proteins bridging the transfer of ubiquitylated proteins to the 26S proteasome such as members of the radiation sensitive23 (Rad23), dominant suppressor of kar2 (Dsk2), and DNA damage-inducible1 (Ddi1)(Deveraux et al., 1999; Thrower et al., 2000; Wilkinson et al., 2001; Buchberger, 2001; Hartmann-Petersen et al., 2004b). These adaptor proteins are characterized by having distinct UBD domains including a ubiquitin-like (UBL) domain and one or more ubiquitin-associated (UBA) domain(s). UBA domains facilitate binding

to polyubiquitin chains on substrate proteins, while UBL domain mediates interaction with receptors on the proteasome.

1.3.4 Unfolded protein response

Impairment of ER functions due to accumulation of unfolded proteins trigger the activation of UPR, a complex intracellular signalling pathway, to enhance protein folding and re-establish homeostasis. In response to ER stress, three ER transmembrane signal transducers are activated to mediate three phases of regulation at transcriptional and translational levels in a process that is highly conserved in eukaryotes (Figure 1.2) (Shen et al., 2004; Kaufman et al., 2002).

The first response to ER stress is mediated by PERK, a double stranded RNA-activated protein kinase-like kinase. Activation of PERK leads to attenuation of mRNA translation, thereby preventing protein synthesis and reduce folding in the stressed ER lumen. PERK inhibits protein synthesis through phosphorylation of translation initiation factor 2 (eIF2); paradoxically, phosphorylation of eIF2 mediates the selective translation of activating transcription factor 4 (ATF4) mRNA (Shen et al., 2004;Harding et al., 1999, 2000).

The second mechanism that is activated by ER stress is mediated by the inositol requiring kinase 1 (IRE1). Initially discovered in *S. cerevisiae*, IRE1 is a kinase with a site-specific endoribonuclease (RNase) activity (Nikawa and Yamashita, 1992; Mori et al., 1993; Cox and Walter, 1996). IRE1 is localized at the ER membrane and bound to BiP

(under non-stressed conditions). Upon accumulation of unfolded proteins IRE1 is released from BiP and undergoes phosphorylation to activate its RNase and kinase activity. IRE1's RNase activity initiates the splicing of the X-box binding protein 1 (XBP1), a transcription factor that initiates the transcription of a variety of UPR target genes (chaperones, folding factors). The increase in chaperons and modifying factors assists in correcting protein folding defects in the stressed ER (Urano et al., 2000a, 2000b; Shen et al., 2004).

The last mechanism triggered by ER stress involves the activation of activating transcription factor 6 (ATF6), an ER-transmembrane protein, that is generally found bound to BiP chaperon (in unstressed cells)((Yoshida et al., 2001). Similar to IRE1, in response to ER stress, ATF6 is released from its complex with BiP, and translocated to the Golgi complex where it is involved in transcription of new proteins that are responsible for targeting and degrading accumulated misfolded protein in the ER (Kaufman and Malhotra, 2007; Shen et al., 2004; Yoshida et al., 2003).

1.3.5 Radiation sensitive 23 (Rad23)

Rad23 protein from *S. cerevisiae* belongs to a large family of proteins that are involved in nucleotide excision repair (NER) in addition to functioning as a shuttle protein, linking the ubiquitylated substrates to the proteasome (Suzuki et al., 2001). Rad23 is a highly conserved protein with orthologues in *C. elegans* (*rad-23*), fruit fly (dRad23), mouse (mHR23), and humans (hHR23A and B) (Figure 1.3). Numerous

characterization studies of Rad23 proteins in plants, yeast, and mammals report similar biochemical and physiological function in NER and UPS (Husnjak and Dikic, 2012; Suzuki et al., 2001, 2003).

Primary structure of Rad23

Rad23 is a member of a family of UBD-containing proteins that interact with both poly-ubiquitin and the proteasome, where it acts as a shuttle protein in the ubiquitin-proteasome pathway. It contains four domains: two ubiquitin-associated domains, central UBA (UBA1), and a C-terminal UBA (UBA2), an N-terminal ubiquitin-like domain, as well as a xeroderma pigmentosum complementation group C binding (XPCB) domain (Kamionka and Feigon, 2004; Mastuani et al., 1997). Through the two UBA domains Rad23 is able to recognize and bind to Ub and poly-ubiquitin moieties on substrate glycopeptides. The UBA motif has been reported to bind to Ub-poly chains in vitro and in vivo with specific preference to certain structural features in the Ub-poly chains; UBA2 in hHR23A prefers 48-lysine linked chains, while UBA1 preferentially binds to 63-lysine linked chains (Madura et al., 2004; Wilkinson et al., 2001; Ortolan et al., 2000).

The UBL domain plays an important role in mediating Rad23 interaction with receptors on the proteasome, mainly RPN1, and RPN10 (S5A in human). These receptors have unique ubiquitin-interacting motif, which enables them to mediate the transfer of Ub-tagged substrates into the proteasome catalytic core.

Crystallographic studies of RAD23/Rad4 and hHRad23/XPC complexes showed that Rad23 binds to Rad4/XPC through a motif distinct from the UBL and UBA domains (Min and Pavletich, 2007; Kamionka and Feigon, 2004). The conserved XPCB domain is the only domain that is not associated with binding to Ub or ubiquitylated substrates. In fact, binding of Rad23 to Rad4/XPC during NER, is mediated through the XPCB domain specifically. This conserved domain also binds Peptide: N-glycanase (PNGases), deglycosylating proteins involved in processing of ubiquitylated substrates targeted for proteasomal degradation (Biswas et al., 2004; Lee et al., 2005).

Primary function of Rad23

Nucleotide excision repair (NER) is a conserved process responsible for removal of large variety of helix-distorting DNA lesions with varying efficiency. Nucleotide excision repair of DNA lesions caused by multiple factors such as ultraviolet (UV) light, DNA intrastrand and interstrand crosslinks is found in all living organism ranging from simple bacteria to mammals. It was found that this process involved 20-30 genes, acting in a several ordered steps involving: (I) recognition and demarcation of DNA lesion, (II) strand excision, (III)displacement of lesion, followed by filling of gap with newly synthesized oligonucleotide (IV). The mechanism of NER is not well understood, however, *in vivo* genetics and in vitro biochemical studies in model organisms contributed significantly in identifying the major components of this mechanism.

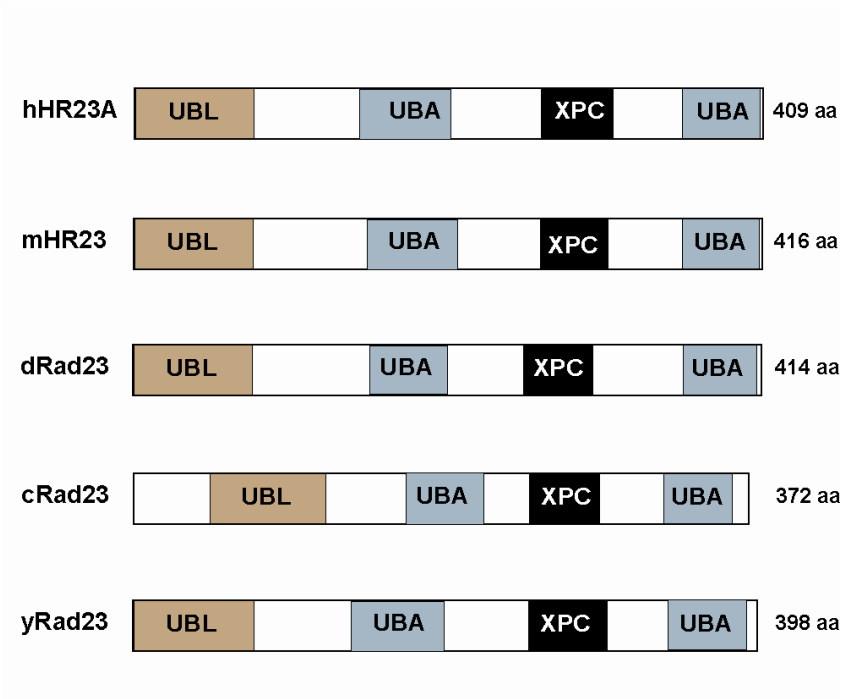

Figure 1.4 Domain architecture of Rad23 orthologs

Rad23 is highly conserved in eukaryotes where orthologs display similar domain structure. r*ad23* interaction with the proteasome is mediated through the UBL domain, while the UBA domain(s) are involved in interaction with ubiquitinated substrates. Rad4, a key component of the NER pathways interacts directly with Rad23 through the XPC domain (Human, hHR23A; mouse Rad23, mHR23; *C.elegans* Rad-23; cRad-23; *S. cerevisiae* Rad23, yRad23).

NER in *S. cerevisiae* was found to be recognized by several members of the Radiation sensitive genes, such as Rad1, Rad2, Rad3, Rad4, Rad7, Rad10, Rad14, Rad23, and Rad25 (Prakash and Prakash, 2000). The majority of these NER proteins are indispensable for repair; most specifically the repair transcription factor RFIIIH, Rad4/(XPC in human), and Rad14(XPA in human). Rad23 is a highly conserved protein with well characterized orthologues in all eukaryotes (Figure 1.3). Yeast and human Rad23 form a complex with Rad4/XPC (xeroderma pigmentosum complementation group C, the human ortholog of Rad4 in human) that is involved in initial DNA damage recognition and excision (Volker et al., 2001). Defects in NER has been linked to UV-hypersensitivity in yeast, sever developmental defects and male sterility in mice, in addition the hereditary Xeroderma pigmentosum syndrome in humans that lead to skin cancer (Lambertson et al., 1999; Ng et al., 2003; Rivera-Bergman et al., 2007). In *C. elegans*, several Rad mutants as well as other NER deficient genes (*xpa-1, xpe-1*) were identified with distinct hypersensitivity to UV radiation (Park et al, 2004, 2002; Kamath et al., 2003; Harman and Herman 1982). The precise role of Rad23 in NER is not well known, however it was shown to be necessary for maintenance of Rad4/XPC and preventing its degradation by the proteasome (Ng et al., 2003; Rassi and Pickart, 2003; Zhao et al., 2006).

In addition to its function in NER, Rad23 plays an essential role as an adaptor protein, shuttling ubiquitylated substrates to the proteasome. Similar to the two other

Ub-receptors (Dsk2 and Ddi1), Rad23 utilizes its UBL and UBA domains to target Ub-tagged substrates and transfers them to the proteasome through its association with Ub-receptors in the 19S regulatory particle. In vitro and in vivo analysis of Rad23 function established the role of UBA domain in recognition and binding to ubiquitin moieties on misfolded proteins (Madura et al., 2001; Ortolan et al., 2000; Lambertson et al., 1999). Interestingly, UBL domain interaction with the proteasome is required for optimal NER function. Deletion of the UBL domain in yRad23 led to UV-sensitivity. Genetic and biochemical studies in *S. cerevisiae* identified a gene encoding cytoplasmic PNGase (Png1) to interact directly with yRad23 (Suzuki et al., 2000, 2001). The core transglutaminase domain of mouse PNGase (mPng1) has been shown to form a complex with mHR23 through its XPC domain, also (Zhao et al., 2007).

1.3.6 Peptide: N-glycanase (PNG1)

In addition to ubiquitin, some ERAD substrates carry a glycan residue after their translocation to the cytosol. These bulky N-glycan residues can sterically hinder insertion of proteins inside the barrel shaped proteasome (Hirsch et al., 2003), thus blocking substrate processing by the proteasome. These residues are removed in a deglycosylation process catalyzed by the protein Peptide: N-glycanase (PNG, PNGase, N-glycanase, Peptide:N4-(N-acetyl-b-D-glycosaminyl). PNGase is responsible for the de-N-glycosylation of asparagine-linked (N-linked) sugar chains on glycoproteins and glycopeptides (Figure 1.4) in a reaction that releases an intact oligosaccharide and

converts the hydrolyzed asparagine residue to aspartate (Berger et al., 1995; Suzuki et al., 2007). PNGases are ubiquitously present in prokaryotes and various eukaryotes.

PNGases were first discovered in almond seeds (Takashi, 1977). PNGaseF, identified from the bacteria Flavobacterium meningosepticum (Plummer et al., 1984), was shown to be involved in the de-glycosylation of high mannose and complex native glycoproteins (Gosain et al., 2012). PNGase activity in animals was first reported in the Medaka fish embryo. PNGaseM is reported to be active at acidic pH, of lysosomal origin, and was involved in the deglycosylation of glycophosphoprotein, a major egg yolk glycoprotein, leading to accumulation of N-glycans (Seko et al., 1991; Gosain et al., 2012). Cytoplasmic PNGase activity was first reported in the budding yeast *S. cerevisiae* (Suzuki et al., 1998) and subsequently in various mammalian cells (Suzuki et al., 1993, 1994; Kitajima et al., 1995; Harding and Ron, 2002), and the fruit fly *Drosophila melanogaster* (Funakoshi et al., 2010).

Cytoplasmic PNGases differ from lysosomal PNGases in that they require a thiol reactive group, a neutral pH, and a reducing environment for optimal activity, in addition to possessing unique carbohydrate binding properties. Additionally, cytoplasmic PNGases are only involved in deglycosylation of non-native glycoproteins only (Seko et al., 1997, 1999; Suzuki et al., 1994; Hirsch et al., 2003, 2004).

Primary structure of PNG1

Comparison of cytoplasmic PNGases among various species ranging from plants, worms, insect, mammals as well as budding yeast revealed that PNGases are highly conserved enzymes, implying that deglycosylation is crucial for various biological processes (FIGURE 1.6). PNGase orthologues contain a conserved transglutaminase (TGase) core that shares high homology with the enzymatic core of other members of the transglutaminase-like super family that includes papin-like thiol proteases, N-acetyl transferases, deubiquitinases, and factor XIII transglutaminase (Murzin et al., 1995; Diepold et al., 2007). The catalytic mechanism of TGase-like enzyme employs a putative catalytic triad consisting of cysteine, histidine and aspartate residues. TGases catalyze the formation of peptide bonds, in addition to disulfide isomerases and isopeptide hydrolysis reactions. Transglutaminases have been reported to play a significant role in neuronal growth and regeneration, cellular differentiation, apoptosis, and angiogenesis (Lorand and Graham, 2003; Shane et al., 2003; Esposito and Caputo, 2005, Diepold et al., 2007). Amino acid substitution in the catalytic histidine residue in yeast PNGase, yPng1, alters the yeast's deglycosylation activity. *In vitro* and *in vivo* studies report a sharp decrease in the degradation of misfolded secretory proteins in the mutant yPng1 (Suzuki et al., 1998, 2000, 2002). Deletion of conserved TGase domain in the Drosophila PNGase orthologue (dPng1) led to severe developmental defects and reduced viability in addition to sterility among adult flies (Funakoshi et al.,

2011). Similarly, mutation in the conserved core domain of PNGase orthologue in *Neurospora crassa*, abolished PNGase catalytic activity and led to hyphae malformation (Maerz et al., 2010). In contrast to yeast and plants, PNGase orthologues in higher eukaryotes have extended domains at both the amino-and carboxy-terminal (FIGURE 1.6). Mammalian orthologues of PNGase (mNGLy1, hNGLY1) in addition to insect PNGase (dPNGase/dPNG1) contain a PNGase ubiquitin-associated (UBA) or ubiquitin-regulatory (UBX) motif, known as the PUB domain. UBA and UBX sequence motif is found on numerous proteins and interact with UBDs in addition to proteasome subunits (Park et al., 2001). These include ubiquitin hydrolases, ubiquitin conjugating enzymes, and ubiquitin ligases (Buchberge et al., 2001; Park et al., 2001). The UBA motif plays an important role in recognition and binding of components of the ubiquitin-proteasome pathway. In fact, interaction between yeast Rad23 and Ddi1p is mediated through the UBA domain (of yRad23). Similarly, UBX is also an evolutionary conserved sequence that shares similar three- dimensional structure as ubiquitin. The UBX domain have been reported to facilitate binding to the AAA-ATPase Cdc48 (p97/valosin-containing proteins in mammals) during ERAD. The PUB domain has been shown to mediate binding of the mouse PNG1 to various components of the ubiquitin-proteasome system (Suzuki et al., 2001; Suzuki and Lennarz, 2003; Li et al., 2005).

Unlike other PNGases, the *C.elegans* PNGase orthologue, PNG-1, contains a conserved N-terminal thioredoxin domain. Thioredoxin (Trx) belongs to a large family

proteins characterized by the highly conserved Cys-X-X-Cys catalytic motif, as well as the thioredoxin fold. The two cysteines in the active site catalyze the reduction of disulfide bonds in proteins. These proteins are expressed in all living organisms from bacteria to humans (Vlamis-Gardikas and Holmgren, 2002). They function as electron donors, antioxidants, as well as redox regulators ; they are involved in multiple cellular functions such as regulation of oxidative stress, protein folding, cell proliferation, DNA repair, signal transduction, transcription regulation, aging, etc. (Meyer et al. 2008). The thioredoxin domain in PNG-1 is an active enzyme, and the dual enzymatic activity of PNG-1 has been reported to operate independently of each other. Expression of full length PNG-1 as well as only the thioredoxin domain in yeast strains lacking functional cytosolic thioredoxin (trx1D) and mitochondrial thioredoxin (trx2D), was reported to rescue the severe cell growth defects associated with these strains. Additionally, the same study reported an active PNGase activity, independent of the Trx activity, utilizing a highly sensitive in vivo assay measuring radiolabeled glycopeptides (Suzuki et al., 2005) in yPng1 null mutants expressing PNG-1(Suzuki et al., 2007).

The C-terminal domain of Drosophila, mouse, human, and *C.elegans* PNGase is also highly conserved, but a clear role for this domain has not yet been specified. Biochemical, biophysical and crystallographic studies in yPng1 and mPng1 suggests that PNGases have an affinity to free glycan chains derived from its own glycoprotein substrates (Zhao et al., 2006; Hirsch et al., 2004). Studies involving mouse Png1

identified a novel mannose-binding features of mPng1, mapping to the C-terminal domain that contributes to substrate recognition and specificity of this protein. Base substitution in the mannose binding sites of mPng1 (c-terminal) abolished the recognition and binding of oligomannose, as well as causing a significant reduction in the core (PNGase) catalytic activity (Zhao et al., 2006). The diversity in amino- and carboxy- terminals in various PNGases is a clear indication of acquired complex physiological function and properties during evolution.

Primary function of cytoplasmic PNGases

A role for PNGase in N-glycoprotein catabolism was revealed with the elucidation of the ERAD pathway. The ER surveillance system actively sorts unfolded or aberrant proteins and retrotranslocates them from the ER to the cytosol. ERAD-targeted glycoproteins are catabolized in the cytosol by a combination of PNGase mediated deglycosylation and degradation by the proteasome (Hirsch et al., 2003; Blom et al., 2004; Kim et al., 2006). In mammalian cells, PNGases have also been implicated in the cytoplasmic processing of N-glycosylated peptide fragments into epitopes that maximize MHC class I cell-surface antigenicity (Selby et al., 1999; Altrich-VanLith et al., 2006; Kario et al., 2008). MHC class I molecules are a member of the major histocompatibility complex (MHC) molecules and they are expressed in all nucleated cells. They are heterotrimeric complexes that present a wide range of antigens derived from endogenous proteins for recognition by $CD8^+$ T lymphocytes, and natural killer

(NK) cells, expressed on a variety of cells of the immune system (Zinkernagel and Doherty, 1997). The heterotrimeric complex is formed in the ER, consisting of MHC class I heavy chains, which contains a single N-linked glycan, light chain β_2 microglobulin, and an 8-10 amino acid residues long antigenic peptide. The Human Cytomegalovirus (HCMV) encoded gene product US2 and US11 are able to inhibit MCH class I antigen presentation through the activation ERAD pathway. US2 and US11 bind to class I MHC heavy chains in the cytosol, and initiate their translocation from the ER lumen to the cytosol through the ER Sec61 or Derlin-1 channels. Class I heavy chains are further processed in the cytosol by an N-glycanase that removes the single N-linked glycan heavy chains prior to their degradation by the proteasome (Huppa and Ploegh, 1997; Suzuki et al, 2000). Inhibition of the proteasome results in the accumulation of deglycosylate the heavy chains in the cytosol. In addition to MHC class I molecules, several other substrates undergo similar mode of degradation, such as α-chain of the T-cell receptor (TCRα), and the cystic fibrosis conductance regulator (Johnston et al., 1998; Huppa and Ploegh, 1997; Wiertz et al., 1996).

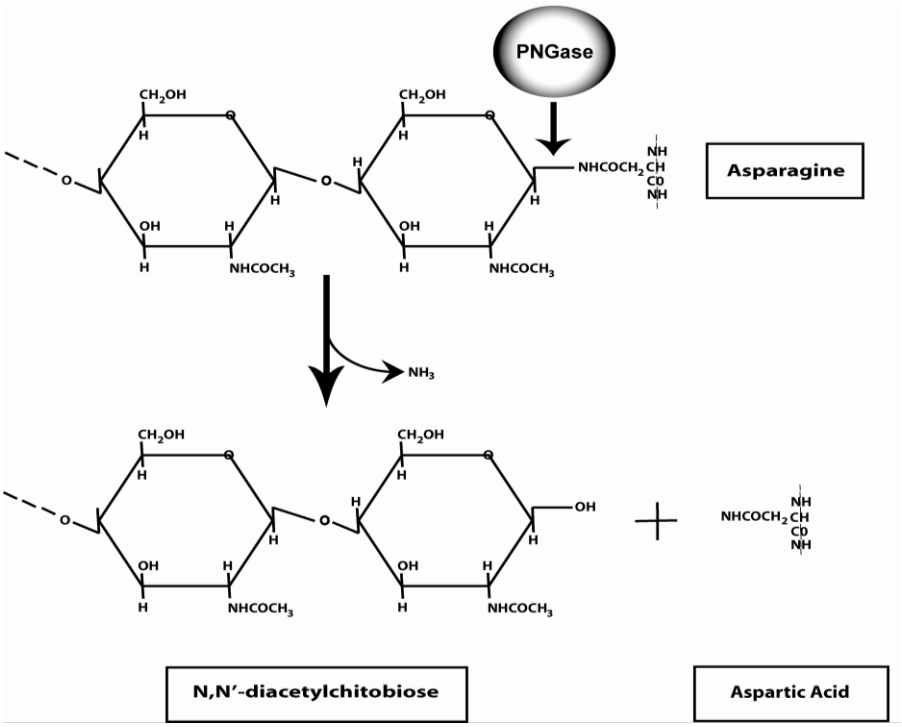

Figure 1.5 PNGase hydrolyzes N-linked glycans from proteins

PNGase hydrolysis of the β-aspartylglycosylamine bond of asparagine linked glycopeptides and glycoprotein releases an intact oligosaccharide and an aspartic acid residue on the protein or peptide. Adapted and modified with permission from Suzuki et al., 2002.

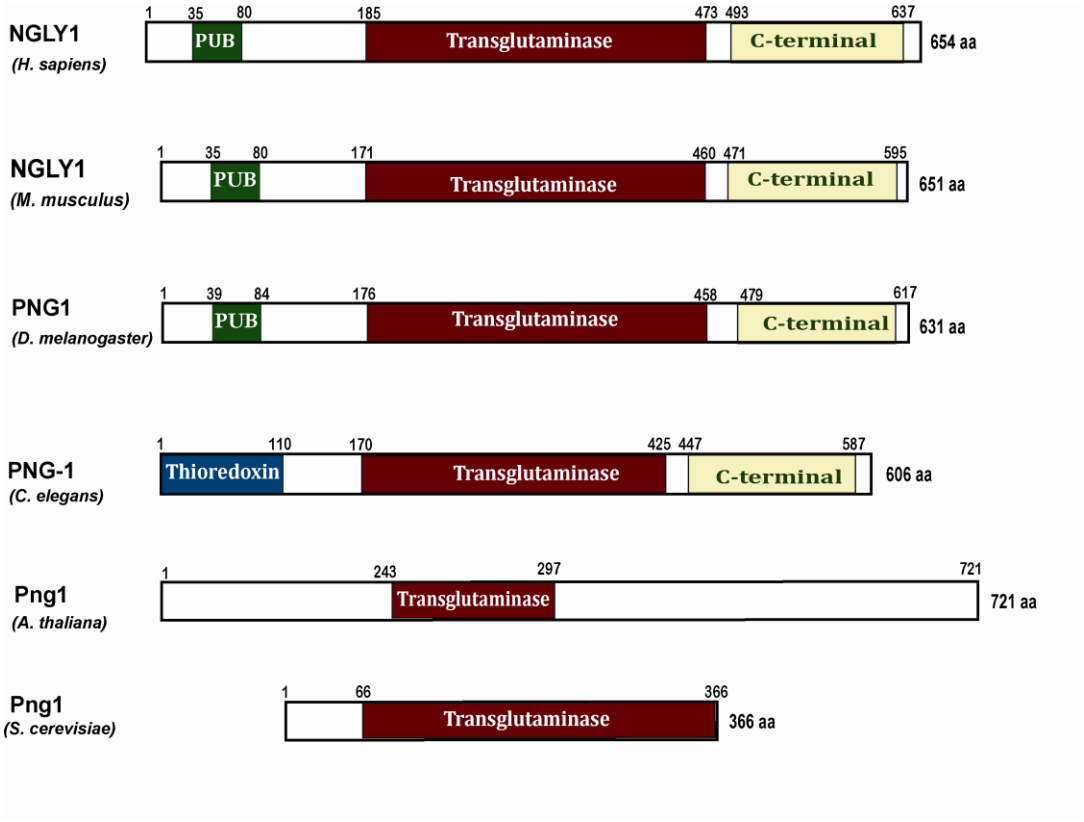

Figure 1.6 Domain architecture of PNGase orthologs

PNGases are highly conserved proteins that share a common transglutaminase core domain. With the exception of *S. cerevisiae*, PNGases carry additional domains that can mediates PNGase recognition and biding to ubiquitin and proteins with ubiquitin binding domains such as Rad23. *C. elegans* homologue, PNG-1, contains a thioredoxin domain necessary for protein-protein interaction (Homo sapiens, NGLY1; Mus Musculus, NGLY1; Drosophila melanogaster, PNG1; Arabdidopsis thalaina, Png1, *S. cerevisiae*, Png1).

1.4 THESIS PRELUDE AND OBJECTIVE

The establishment of neuronal networks involves the guided extension and branching of axons and dendrites under the orchestration of guidance and branching cues. Although a variety of cues and signalling pathways have been identified, the molecular mechanisms controlling axon branching remain poorly defined. The goal of my graduate research was to identify neuronal pathways underlying axon branching using the egg-laying system in *C. elegans* as a model. A forward genetic screen identified two alleles of *branching abnormal* gene, *bam-1 (cy8)* and *(cy9)* that displayed excessive ectopic branching at VC4 and VC5 egg-laying neurons. Initial mapping and rescue analysis identified *bam-1(cy8)* and *bam-2(cy9)* to be the *C. elegans* homolog of Peptide: N-glycanase, a highly conserved cytosolic enzyme with conserved housekeeping roles in cellular homeostasis. I used *bam-1*, which was appropriately renamed *png-1* as the first homologue of conserved PNGase in nematodes, to uncover potential new pathways mediating neuronal branching. The objectives of this thesis are:

Chapter 2: Characterization of *png-1* in *C. elegans*

1. To characterize the role of *png-1* in regulating neuronal growth and branching
2. To Analyze the role *png-1* on regulating egg-laying behavior
3. To identify the subcellular localization of PNG-1

Chapter 3: Identification and characterization of potential *png-1* genetic interactors

1. To isolate and characterize new genes involved in regulating axon branching in VC4-5 via a candidate gene approach
2. To identify genetic interactions between *png-1* and other genes involved protein degradation
3. To identify components of PNG-1 mediated pathways in regulating axon branching

This thesis will reveal novel pathways involved in regulating axon growth and branching during the development of the nervous system in *C. elegans*.

CHAPTER 2: CHARACTERIZATION OF PNG-1 IN *C. ELEGANS*

The following chapter has been reproduced with modification from:

The N-glycanase *png-1* act to limit axon branching during organ formation in *C. elegans*

Nasrin Habibi-Babadi, Anna Su, Carlos E. De Carvalho, Antonio Colavita

J of Neurosci, Feb 3; 30(5): 1766-1776 (2010)

Contribution to this chapter:

Antonio Colavita and Anna Su mapped *png-1(cy9)* mutant

Ann Su provided technical support in biochemical experiments

Carlos E. de Carvalho characterized *in utero* egg counts in *png-1(cy9)* mutants

ABSTRACT

Peptide: N-glycanase (PNGases) are cytoplasmic de-N-glycosylation enzymes that have been shown in vitro to facilitate the degradation of misfolded glycoproteins during endoplasmic reticulum-associated degradation (ERAD) and in the processing of MHC Class I antigens for proper cell surface presentation. The gene encoding PNGase activity was initially described in almond seeds, and subsequently in mammalian cells and budding yeast (Png1p), and shown to be highly conserved from yeast to humans but physiological roles in higher organisms have not been elucidated. Here we describe the peripheral nervous system defects associated with the first loss-of-function mutations in an animal PNGase. Mutation in *png-1*, the *C. elegans* PNGase orthologue, results in increase in axon branching during morphogenesis of the vulval egg-laying organ and egg-laying behavior changes. Neuronal defects include an increase in the branched morphology of the VC4 and VC5 egg-laying neurons as well as inappropriate branches from axons that run adjacent to the vulva but would not normally remain branched. We show that *png-1* is widely expressed and can act from both neurons and epithelia cells to restrict axon branching. In summary, our analysis reveals a novel developmental role for a PNGase in the regulation of neuronal branching and outgrowth during organ innervation.

2.1 INTRODUCTION

The innervation of peripheral targets involves the remarkable ability of innervating neurons to precisely interpret path finding cues along intermediate targets and then respond to specific organ-derived factors that regulate branching patterns in order to achieve optimal innervation density (Glebova and Ginty, 2005). Morphogenesis of the *C. elegans* egg-laying system provides an attractive invertebrate model to simplify the task of identifying genes and mechanisms involved in organ formation and innervation.

The nematode egg-laying organ is an anatomically simple structure, consisting of a vulval epithelial channel linking the uterus to the external environment, eight vulval muscles attached to the channel, and the HSN and VC motor neurons that innervate the vulval muscles and coordinate muscle excitations responsible for egg-laying (Figure 2.1 A) (Li and Chalfie, 1990). Innervation of the vulval muscles occurs in tandem with vulval organogenesis during the 4th larval (L4) stage long after the generation and wiring of sensory and motor circuits and therefore notable as the final neural circuit to form in *C. elegans* (Li and Chalfie, 1990; Garriga et al., 1993). Cell ablation and genetic studies have shown that vulval epithelial cells play an essential role in the innervation and shaping of the egg-laying circuit by providing a source of axon guidance, axon branching, and synapse formation cues (Li and Chalfie, 1990; Garriga et al., 1993; Colavita and Tessier-Lavigne, 2003; Shen et al., 2004; Adler et al., 2006).

Peptide:N-glycanse (PNGase, N-glycanase) is an enzyme that is responsible for the de-N-glycosylation of asparagine-linked (N-linked) sugar chains on glycopeptides or glycoproteins. This enzyme cleaves the β-asparatylglucosaminyl bond in a reaction that releases an intact oligosaccharide and a converts the hydrolyzed asparagine residue to aspartate (Berger et al., 1995; Suzuki et al., 2007). PNGases are highly conserved and ubiquitously present in prokaryotes and eukaryotes. This enzyme was initially discovered in almond seeds (PNGaseA) (Takashi, 1977). Cytosolic PNGases activity was subsequently reported in various mammalian cells (Suzuki et al., 1993, 1994; Kitajima et al., 1995), S. cerevisiae (Suzuki et al., 1998) and Drosophila (Funakoshi et al., 2010). Cytoplasmic PNGase differ from other PNGase (found in plants, fish and bacterium) in that they can modify misfolded aberrant glycoproteins only (Seko et al., 1997; Suzuki et al., 1994; Hirsch et al., 2004).

A role for PNGase in N-glycoprotein catabolism was revealed with the elucidation of the endoplasmic reticulum (ER)-associated degradation (ERAD) pathway. The ER surveillance system actively sorts unfolded or aberrant proteins and retrotranslocates them from the ER to the cytosol. ERAD-targeted glycoproteins are catabolized in the cytosol by a combination of PNGase mediated deglycosylation and degradation by the proteasome (Hirsch et al., 2003; Blom et al., 2004; Kim et al., 2006). In mammalian cells, PNGases have also been implicated in the cytoplasmic processing of N-glycosylated peptide fragments into epitopes that maximize MHC class I cell-surface

antigenicity (Selby et al., 1999; Altrich-VanLith et al., 2006; Kario et al., 2008). Despite these recent findings the physiological roles for cytosolic N-glycanases remain unknown. Phenotypic analysis of PNGase mutants in the budding yeast *S. cerevisiae* (Suzuki et al., 2000) and the plant *A. thaliana* (Diepold et al., 2007) which could have shed light on *in vivo* roles were not overly informative as mutants lacked obvious abnormalities. A PNGase mutant in *N. crassa*, a filamentous fungus, displays a noticeable hyphal growth defect, the underlying cause of which is not known (Seiler and Plamann, 2003).

The nematode PNGase orthologue, PNG-1 was identified in a genetic screen for VC4 and VC5 branching abnormal mutants using a *cyIs4 [Pcat-1::GFP]* reporter to visualize the VC4-5 egg laying neurons (Antonio Colavita, unpublished data). These mutants displayed a highly penetrant increase in the complexity of the VC4-5 branching morphology compared to wild-type. In this chapter, I will report my phenotypic analysis of the first loss-of-function mutations in an animal PNGase. This analysis reveals a novel developmental role for this highly conserved enzyme in neuronal branching during organ innervation.

2.2 MATERIALS AND METHODS

2.2.1 Nematode strains and genetic methods

C. elegans strains were grown on nematode growth medium (NGM) plates inoculated with *Escherichia coli* strain OP50 (Brenner, 1974). Strains were maintained at at 15°C, 20°C or 25°C, depending on the experimental requirements.

The wild-type N2 (Bristol) strain was used as standard reference, and the following mutant alleles were used: LG I: *unc-75(e950)*, *png-1 (ok1654)*, LG IV: *unc-30(e191)*, LG *V: egl-1(n986)*. The following green fluorescent protein (GFP) reporter transgenes were used to visualize and score neuroanatomy: *cyIs4[Pcat-1::GFP, rol-6(su1006]* to label VC4,VC5, and PDE, *cyIs3[Punc-4::GFP]* to label VC1-6, *kyIs179[Punc-86::GFP]* to label HSN, *unc-30(e191); juIs76[Punc-25::GFP]* to label AVL and DVB, o*tIs92[Pflp-10::GFP]* to label DVB, *evIs79 [unc-129::GFP]* to label DA, and DB, *oyIs14 [sra-6::GFP]* to label ASH, PVQ, *zdIs5[mec-4::GFP]* to label ALM,PLM,AVM, AVM, *akIs3 [nmr-1::GFP]* to label AVA,AVD, AVE, AVG, and PVC neurons. All strains were backcrossed at least three times. Neuron specific GFP reporter strains were crossed into *png-1* alleles using standard genetic methods (Brenner, 1974). Homozygous animals were verified using polymerase chain reaction (PCR) and restriction fragment length polymorphism (RFLP) genotyping (Table 2.2).

2.2.2 *Mapping, sequencing and genotyping*

png-1 (cy9) was previously mapped using standard N2/CB4856 SNP mapping methods within the *bli-4 unc-75* interval on LGI by isolating 51 *Bli* non-*Unc* progeny from a *bli-4(e937) cy9 unc-75(e950)*/ Hawaiian (N2/CB4856) parent in which 43 recombinants were *cy9*/+ and 8 were *cy9*/*cy9*. *cy9* was then mapped more precisely to a small interval between cosmids W02B9 and ZK1025 using SNP markers within the *bli-4 unc-75* interval (A. Colavita, unpublished data).

Mutations in *cy8* and *cy9* were identified by sequencing PCR amplified exons from genomic DNA using primers listed in Table 2.1. To genotype mutant alleles, genomic DNA from each mutant was PCR-amplified and examined by restriction enzyme digest or PCR fragment size (for deletion mutation). Table 2.2 list all primers required for *png-1* genotyping.

2.2.3 *Plasmid construction and molecular cloning*

Rescuing, translational and transcription plasmids were prepared using standard cloning procedures or fusion PCR. The transcriptional *Ppng-1::GFP* (pAC3) reporter was prepared by PCR amplifying 606bp upstream of the predicted F56G4.4-F56G4.5 operon start site and cloning it upstream of the GFP start codon in pPD95.77 (Fire lab vector kit). The translational *Ppng-1::PNG-1::GFP* (pAC7) plasmid was made by inserting the open reading frame from a PNG-1 cDNA (yk811b02, a gift from Y. Kohara) between the promoter and GFP in pAC3. pAC3 and pAC7 cloning accuracy were verified by

restriction enzyme digest and sequencing. Expression clones for cell-specific studies were made by replacing the *png-1* promoter in pAC7 using standard cloning techniques or by fusion PCR (Hobert, 2002). Briefly, the promoter regions were PCR amplified in one reaction and a PNG-1 cDNA tagged with GFP (from pAC7) containing an >20bp overlap sequence that corresponds to the promoter region (Expand long PCR, Roche), was amplified in a separate reaction. In a third step (fusion PCR), these two PCR fragments were fused together using a nested primer to produce the translational expression fusions. Table 2.3 list all primers used for preparing cell-specific plasmids and fusions and their site of expression. A PCR-based deletion strategy using pAC7 as a template was used to generate constructs containing in-frame deletions of the thioredoxin (residues 2-100) 5′-cgaaaaaattcggcaacactattcg-3′ and 3′-gccttgaacacctcatccttg atag-5′. Construct containing the deletion of the C-terminal (residues 426-600) domain was prepared using primers 5′-caaagttgctcgcggagcccataaaactg-3′ and 3′-atttttcatccaaatttt gaccgaaaagc-5′.

Site directed mutagenesis (QuickChange XL, Stratagene) was used to convert the two active site cysteines in the thioredoxin domain (pAC7) to two serines using primer 5′-gatttttcgctaattggtCtggCccgtCccgtatgatttctccg-3′.

2.2.4 Transgenic animals and germ line transformation

Extrachromosomal arrays were generated following standard microinjection techniques (Mello et al., 1991). A Zeiss Axiovert microscope equipped with 20X and 40X

lenses and an Eppendorf FemtoJet Microinjector were used to inject young adult hermaphrodites with various cosmid pools, plasmids, genomic PCR fragments or PCR fusion products. Cell specific rescue and structure-function analysis was performed by testing for rescue of VC branching defects in *png-1(cy9);cyIs4* animals after germline transformation. PNG-1 overexpression experiment were carried by injecting pAC7 at increasing concentrations (20, 25, 50, and 100 *ng/ul)* in *png-1 (cy9)* and wild type worms. pBluecript SK and pPD95.77 (Fire lab vector kit) were used as control constructs in rescue or overexpression experiments. Co-injection markers used for making transgenic lines were: *rol-6(at 20-25 ng/ul), Podr-1::dsRed*, expressed in the odorant sensory neurons in the head (at 20-30 *ng/ul)* or *Pmyo-2::mCherry:: unc-54 UTR*, expressed in the pharynx (at 5-10 *ng/ul).* Transgenic lines were confirmed in the F2 progeny by transmission of the co-injection marker.

2.2.5 Phenotypic analysis of neuronal morphologies

Worms expressing *cyIs4 [Pcat::GFP]* were scored for VC4 and VC5 neurite branching, axon outgrowth and branch termination defects. In late L4 and young adults, VC4 and VC5 neurons extend two axons that partially overlap to form a circular tract around the vulva with distinct left and right branching patterns. To simplify quantification, branching defects were binned into wild-type and excessively branched categories. VC neurons were scored as excessively branched at the young adult stage if more than 5 branches were observed on either the left or right side compared to the 1-5

branches normally observed in wild-type. Because VC4 and VC5 axons fasciculate at the site of branching, individual branches could not be unambiguously identified and therefore VC4 and VC5 axon branches were pooled for scoring purpose. Worms expressing *otIs92 [Pflp-10::GFP]* were scored *for* DVB motor neurons defects. DVB neurons terminate a short distance posterior to the vulva. A termination defect was scored as any DVB process that extends dorsally along the vulva epithelium or anteriorly past the vulva.

Animals expressing *unc-30(e191);juIs76[Punc-25::GFP]* were used to score for AVL and DVB defects. Axons were scored as displaying an axon branch if a distinct axonal protrusion at least 3-5μm in length (approximately one neuronal cell body diameter) was observed.

All worms were staged accordingly to vulval developmental milestones and verified accordingly using differential interference contrast (DIC) microscopy.

2.2.6 Egg-laying behavior analysis

Egg-laying behavior for *egl-1(n986)* and *png-1;egl-1(n986)* double mutants were performed as previously described (McGovern et al., 2007, Koelle et al., 2003). Egg-laying assays were performed by placing synchronized L4 larvae on plates with food and allowed to mature at 20°C for 24 hours. Ten Adult worms were transferred to new plates and allowed to lay eggs for 2 hours at 20°C, after which adult worms were

removed from plates and the numbers of eggs were counted. Additionally, the progeny of these plates were counted two days post egg-laying.

For the egg-retention assay, staged L4 larvae were placed on plates with food and allowed to mature for 24 hours as 20°C. The young adults were mounted on 2% agarose pads on a glass slide and immobilized with 10mM levamisole. The worms were viewed by a Zeiss AxioplanII microscope using under 40X objective lens, and the number of eggs in utero was counted.

2.2.7 Microscopy and imaging

Worms were mounted on 2% agarose pads in M9 buffer and immobilized with 10mM levamisole (Sigma). Neurons were visualized by epifluorescenc using a Zeiss AxioplanII microscope. Images were captured using a Zeiss LSM510 confocal microscope. Z-stack images of neurons were captured using 20X, 40X, and 63X objective lenses and were collapsed into a single image. Worms were staged with respect to developmental stages as described (Riddle et al, 1997).

2.2.8 Statistical analysis

All experiments were performed at least 3 times, unless specified otherwise. Data was analyzed using Prism V program (Graphpad). Data are reported as mean , or mean . Differences between strains were investigated by ANOVA followed by the Bonferroni post Hoc test. P values of < 0.05 were considered significant.

2.3 RESULTS

2.3.1 A PNGase (png-1) is disrupted in VC axon branching mutants

The *cy8* and *cy9* alleles were identified in a genetic screen for VC4 and VC5 (VC4-5) branching abnormal mutants using a *cyIs4 [Pcat-1::GFP]* reporter to visualize the VC4-5 egg-laying neurons (Antonio Colavita, unpublished). These mutants display a highly penetrant increase in the complexity of VC4-5 branching morphology compared to wild-type (Figure 2.1 *B-D*). A SNP-based mapping strategy was used to map *cy9* to a small interval on LGI between cosmids W02B9 and ZK1025. To identify the gene disrupted in our mutants we generated transgenic lines carrying PCR amplified genomic or cosmid DNA located within this interval and scored for rescue of the VC4-5 branching defects (Figure 2.2). A genomic fragment containing the co-transcribed genes F56G4.4 and F56G4.5 but not deletion derivatives that removed F56G4.5 rescued the branching phenotype. F56G4.5 was verified as the *cy9* locus by obtaining rescue with a full length cDNA driven by approximately 600bp of upstream sequence, identifying the DNA lesions in *cy8* and *cy9*, and showing that *ok1654*, an F56G4.5 deletion allele obtained from the *C. elegans* Gene Knockout Consortium, displays similar defects.

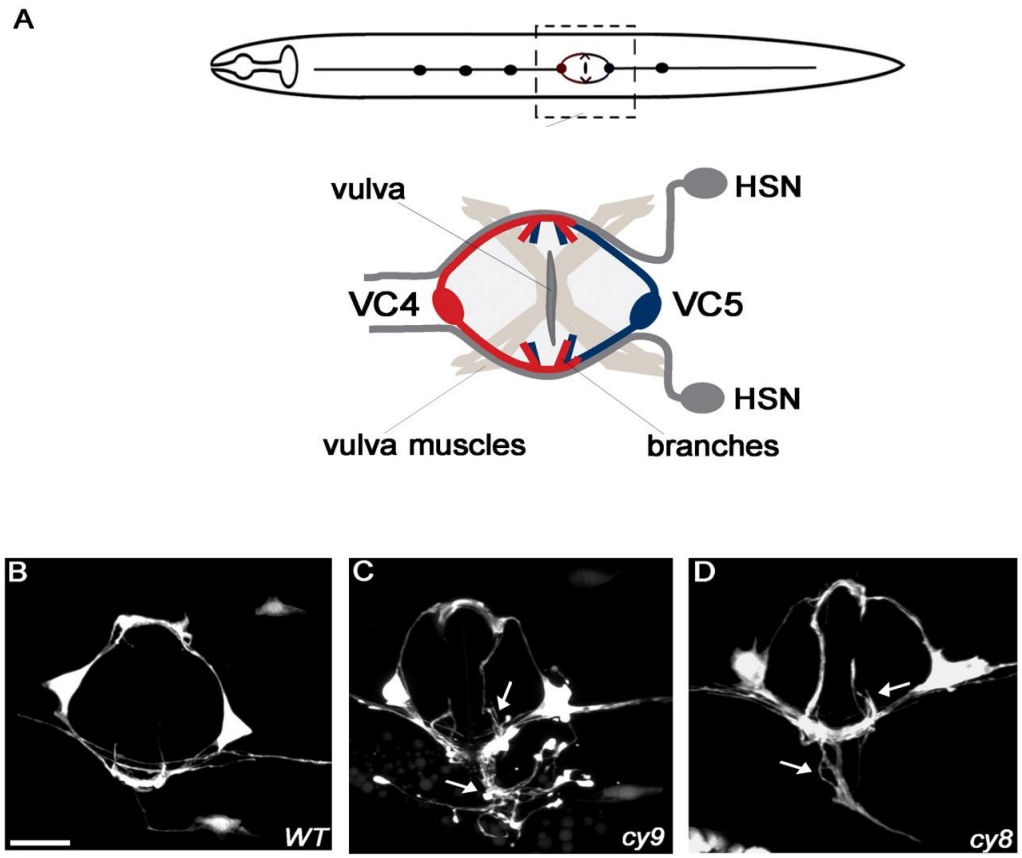

Figure 2.1 ***png-1*** **mutants display excessively branched VC4-5 axons**

A) Schematic of a worm (ventral view) showing the positions of VC4-5 and the vulval egg-laying organ innervated by the HSN and VC motor neurons. **B-D)** Ventral view of VC4 and VC5 neurons in adult wild type **(B)**, *cy9* and *cy8* (**C,D)** mutants visualized using *cyIs4 [Pcat-1::GFP*] neuronal reporter. Arrows indicate axon branching defects. Scale bar, 10μm.

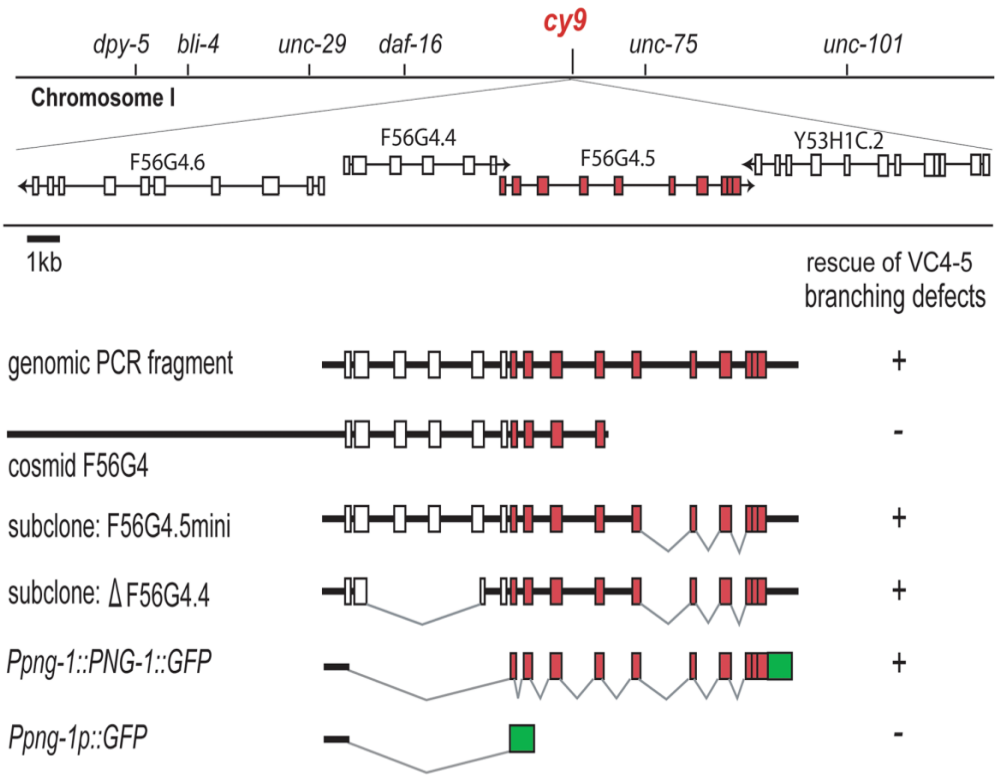

Figure 2.2 Positional cloning of PNG-1

The *cy9* mutant was mapped to a small genetic interval on chromosome I and identified as the F56G4.5/*png-1* gene (red) by complementation with genomic and cosmid fragments and a *png-1* translational fusion to GFP (green). PCR fragments containing *png-1* gene and *Ppng-1::PNG-1* cDNA rescued VC4-5 branching defects. Genomic structure indicated by lines and boxes (exons).

2.3.2 *Conserved PNGase catalytic triad disrupted in png-1 mutants*

F56G4.5 encodes the peptide: N-glycanase (PNGase) PNG-1 (Figure 2.3 A), a 606 amino acid protein consisting of an N-terminal thioredoxin domain, a central PNGase domain, and a predicted C-terminal mannose binding domain. PNGases belong to the transglutaminase (TGase) superfamily characterized by a highly conserved catalytic active site consisting of Cys, His, and Asp residues (Cys251, His278, and Asp295 in PNG-1) that are essential for N-glycanase activity.

Animal PNGases differ from those of lower eukaryotes in having extended N and C-terminal sequences (Figure 2.3 A). Mammalian and fly PNGases contain an N-terminal PUB domain known to interact directly with components of the ubiquitin-proteasome pathway and a C-terminal mannose binding domain (Suzuki, 2007). With the exception of a divergent N-terminal thioredoxin domain, which so far appears to be found only in some nematode PNGases, PNG-1 is a clear homologue of *S. cerevisiae* Png1p and human NGly1 displaying 30%-41% identity in the PNGase domain (Figure 2.3 A).

The molecular lesions in *png-1* alleles were identified (Figure 2.3 A, B). *cy9* is a candidate null allele as it introduces a stop at Q289 that should result in a premature termination within the PNGase domain and therefore abolish PNGase activity. *cy8* is a missense mutation that substitutes the invariant C251 catalytic residue in the PNGase active site with a tyrosine. This mutation in yeast Png1 abolishes PNGase activity

(Suzuki et al., 2007). *ok1654,* an allele obtained from the *C. elegans* Genetic Consortium (CGC), is a 1.1kbp deletion predicted to generate an in-frame deletion of residues 67-180.

2.3.3 png-1 mutants display abnormal axonal morphology in VC4-5

VC4-5 neurons are born during late L1 (1st larval stage) but delay axon outgrowth until the onset of vulval organogenesis at late L3. At the fourth larval stage, VC4-5 axons project laterally around the developing vulva forming a circular tract. The overlapping axons form branches or arborizations at distinct sites on the left and right sides of the vulva where connections are made with pre (HSN) and post-synaptic (vulval muscles) partners. *png-1* mutants displayed highly variable defects with super numery branches extending in multiple directions along the vulva or body wall epithelium, either in isolation or as loosely fasciculated bundles that often intersected.

As the first step in characterizing *png-1* mutants, I attempted to quantify VC4-5 branching defects. Since VC4-5 axons overlap and fasciculate, individual branches could not be unambiguously identified and counted. In wild type young adults, VC4-5 axons typically display 3-5 branches. Branching abnormalities in worms were reported if VC4-5 displayed an increase in branch number and/or branch length. To simplify VC4-5 branching characterization branching defects were binned into wild type and excessive categories. Animals were scored as wild type if they displayed less than 5 branches, and excessively branched if they displayed 6-20 branches (Figure 2.4 A and B). More than 65% of *png-1* mutants display excessive VC4-5 branching defects (Figure 2.4

C). The excessive VC4-5 branching phenotype is temperature sensitive and largely ameliorated when animals are grown at 15°C instead of 20°C or 25°C (Figure 2.4 C).

We did not observe any other morphological, locomotion, or viability defects in mutant animals. As all the molecular lesions appear to be null or strong loss-of-function mutations, temperature sensitivity does not appear to be the result of an allele specific effect on protein stability, but instead the result of a temperature sensitive process.

2.3.4 png-1 mutants display egg-laying behavior defects

The VC4-5 morphology defects suggested that *png-1* mutants may display changes in egg-laying behavior. In addition to VC4 and VC5, the HSN motor neurons also innervate the vulva muscles where they modulate the execution and regulation of egg-laying. The HSNs make extensive neuromuscular junctions with the vm2 vulva muscles, and also direct synaptic output to the VC5 motorneuron (Sulston and Horvitz,1977; Trent et al., 1983). An examination of HSN neurons using a *Punc-86::GFP* reporter did not reveal branching or morphology defects in mutant animals (Table 2.4).

To determine whether increased VC arborization correlates with changes in egg-laying behavior, we examined *png-1* mutants for egg-laying phenotypes. In a measure of the rate of egg laying in synchronized individual young adults carrying a single row of eggs *in utero,* we found that *png-1* mutants displayed a decrease in the number of eggs laid per 2 hour period (12.9 for *cy9* and 9.0 for *cy8*) compared with wild type controls (19.4) (Figure 2.5 B).

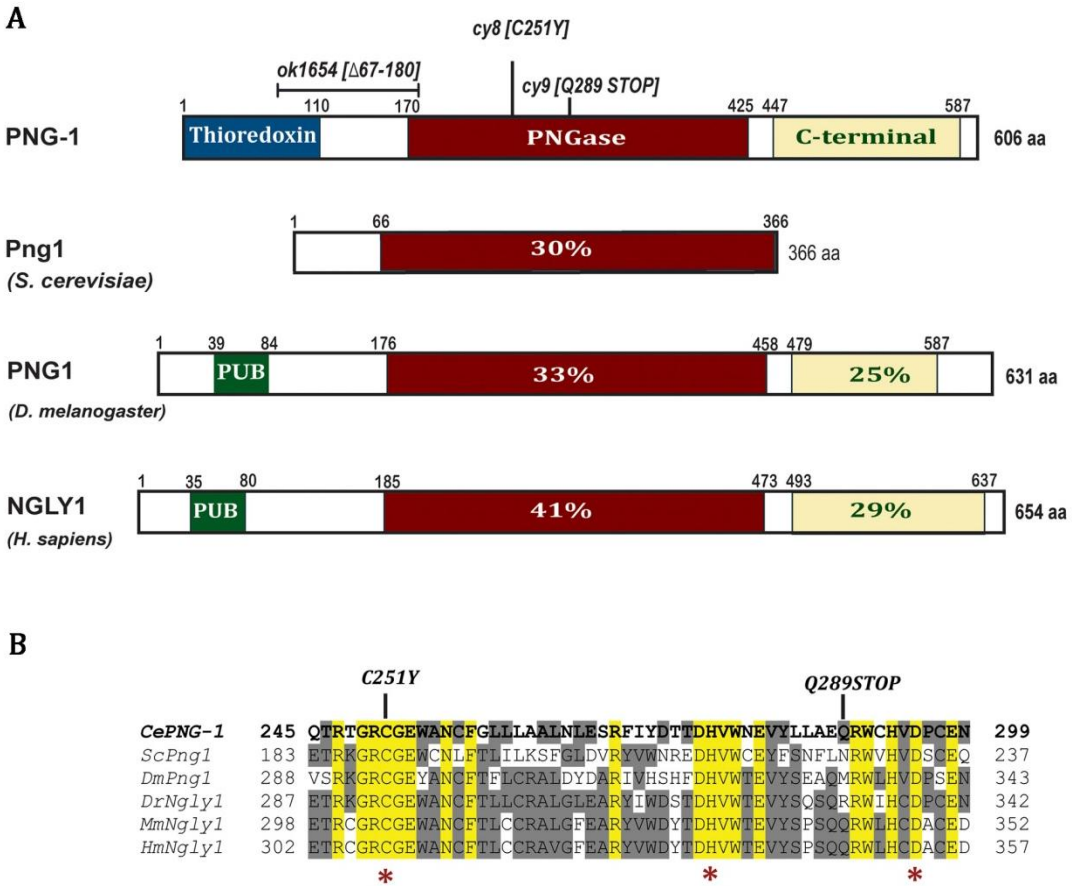

Figure 2.3 PNG-1 encodes a highly conserved PNGase

A) Domain organization of PNG-1 and orthologues showing percentage identity of conserved domains to PNG-1. Animal PNGase contain an extended N and C-termini. Nematode PNGase structure differs from fly and vertebrate PNGases in having N-terminal thioredoxin instead of a PUB domain. **B)** Alignment of core PNGase domains. Molecular lesions in *png-1* are indicated in (A) and asterisks mark the invariant Cys, His, Asp active site triad. *C. elegans* (Ce, GeneBank no. AAF74721), *S.cervisiae* (Sc, S61970), *Drosophila* (Dm, AAF74722), Zebrafish (Dr, AAH95313), mouse (m, AAF74723, human (h, AAF74720). ClustalW alignment (version 6.0)

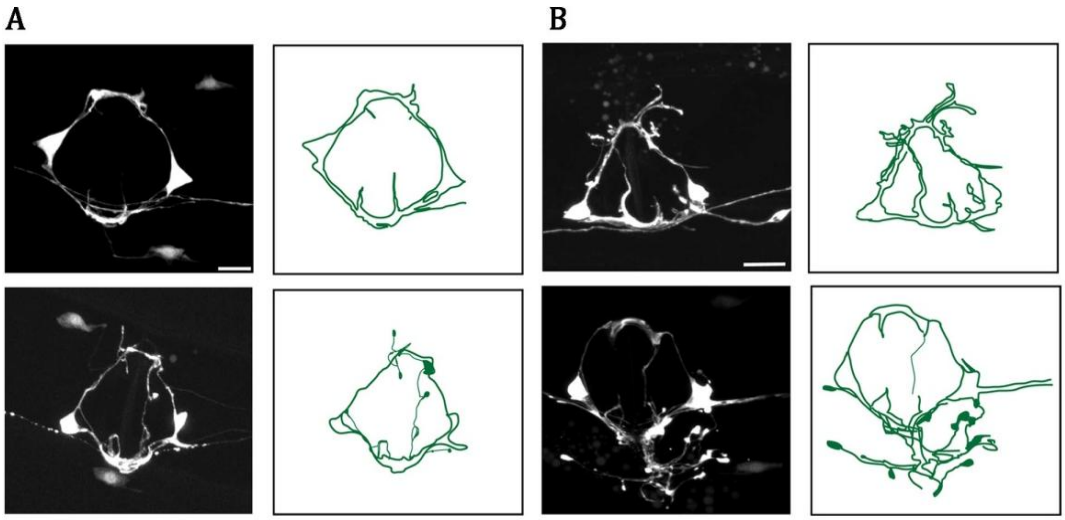
A
B
wild type: branching defects < 5
mutant: 6-20 branching defects

C

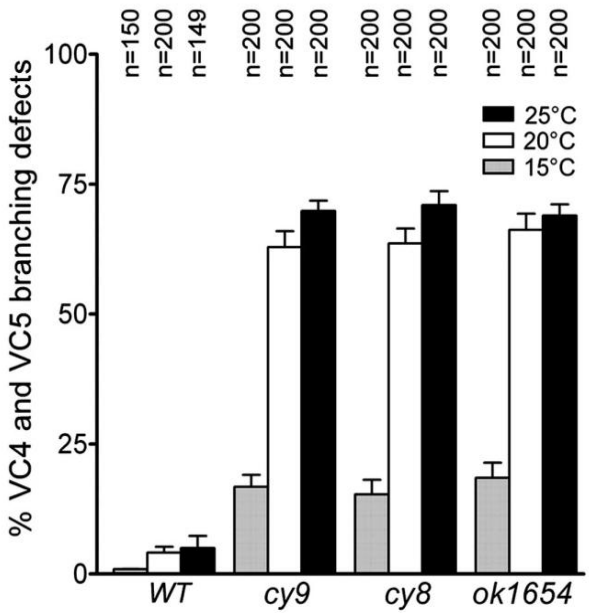
% VC4 and VC5 branching defects
100
75
50
25
0
n=150
n=200
n=149
n=200
n=200
n=200
n=200
n=200
n=200
n=200
n=200
n=200
25°C
20°C
15°C
WT
cy9
cy8
ok1654

Figure 2.4 Characterization of VC4-5 branching

Fluorescence images and diagrams of wild type and mutant axon morphologies. To simplify VC4-5 branching characterization, defects were binned based on the number of branching defects observed on the left and right sides of the vulva: wild type if VC4-5 displayed less than 5 branches defects **(A),** and excessive if 6-20 branching defects were counted in each worm**(B)**. **C)** Branching defect are temperature sensitive. Branching was enhanced at optimal growth temperature of 25°C and the defects were largely ameliorated at 15°C. Error bars represent denote standard error of mean (SEM) of three and/or independent counts (n=50, each). Ventral view of VC4-VC5, visualized by *cyIs4 [Pcat-1::GFP]* reporter transgene, anterior to the left. Scale bar, 10

We also found an egg retention phenotype in *png-1* mutants (22.2 for *cy9* and 21.3 for *cy8*) when counting the number of eggs in the uterus of synchronized young adults compared with wild type controls (13.8) (Figure 2.5 A). These findings suggest that VC morphology defects in *png-1* mutants may interfere with normal egg-laying behavior.

In a third assay, we took advantage of an *egl-1(n986)* gain-of function mutant in which HSN neurons undergo cell death to create a background in which egg laying is solely dependent on VC neuronal function (Waggoner et al., 1998). *egl-1(n986)* animals display a severe egg-laying retention phenotype. We found that *egl-1(n986)* animals (n= 300) displayed a severe egg laying defects where an average of 0.19 eggs were laid per 2 hour period (Figure 2.5 C). We hypothesized that, if our VC morphology defects interfered with VC neuronal activity or vulval muscle innervation, we would expect to see an enhancement of the egg-laying defects in an *egl-1(n986)* background. Instead, we found that *png-1(cy9); egl-1(n986)* and *png-1(cy8); egl-1(n986)* animals displayed a significant increase in the average number of eggs laid per 2 hour period (0.45 and 0.47 eggs respectively; *n*=300, 330) compared with *egl-1* single mutants. This is consistent with increased VC branching in *png-1* mutant animals causing increased stimulation of vulval muscles and partially compensating for the loss of the egg-laying stimulatory effect of HSN innervation.

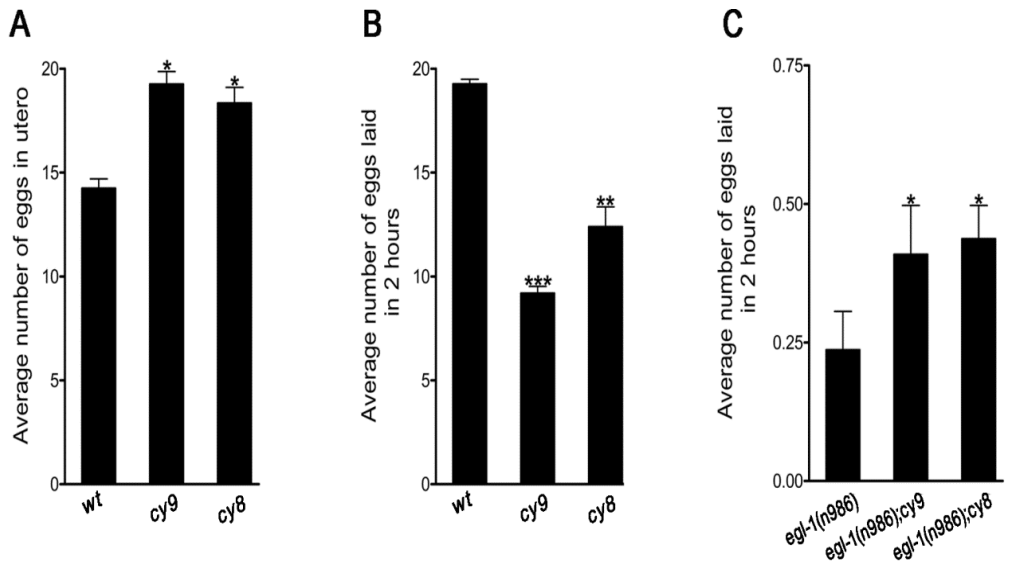

Figure 2.5 *png-1* mutants display abnormal egg-laying behavior

---

A,B) *png-1* mutants display a mild *egl* phenotype characterized by reduction in the rate of egg laying **(A)** and *in utero* retention of developing embryos **(B)**. **C)** *png-1* deficiency partially suppresses the egg-retention phenotype of *egl-1* gain-of-function mutants. HSN neurons undergo cell death in *egl-1(n986)* resulting in a genetic background where egg-laying behavior is dependent on VC innervation of the vulva muscles. Error bars denote standard error of mean (SEM) of 3-4 independent counts (n=50 each). *$P<0.05$, and ***$P<0.0001$, *t* test

2.3.5 png-1 is widely expressed in neurons and epithelium

To study *png-1* expression I made a *Ppng-1::GFP* transcriptional reporter using an approximately 600bp promoter that was shown to be sufficient in *png-1* rescue experiments (Figure 2.2 A). I obtained several transgenic lines with similar expression patterns. Transgenic animals carrying this reporter showed consistent *png-1* transcriptional activity in almost all cells in embryonic, larval, and adult stages, in most tissues including gonad, pharynx, intestine, body wall muscle and epithelial cells (Figure 2.6). In the egg laying system, promoter activity was detected consistently in all vulval cells from the late L3 stage to adulthood (Figure 2.6 B-D). To determine subcellular localization we generated *Ppng-1::PNG-1::GFP*, a translational GFP fusion. The expression and functionality of this construct was confirmed by transgenic rescue of the VC axon branching defects in *png-1* animals (Figure 2.2 A). However, we were unable to detect GFP fluorescence in animals carrying this transgene either directly or by indirect immunofluorescence using anti-GFP antibodies suggesting that PNG-1 may normally be expressed or maintained at low levels. At rescuing concentration of 40ng/μL, no GFP signal was detected, and at higher concentration (50 ng/μL, and 100 ng/μL), we still could not detect any GFP signal. Transgenic lines carrying higher concentrations of this rescuing plasmid did not display an increase in VC4-5 branching rescue levels, or enhance the defective branching morphology of these mutants. To address the possibility that broad overexpression of PNG-1 from its own promoter may

be detrimental, we drove PNG-1::GFP expression from pan-epithelial (*Pcol-10*) and pan-neuronal (*Prgef-1*) promoters to assess localization. Using these promoters we found that PNG-1 was consistently localized to the cytoplasm and excluded from the nucleus (Figure 2.6 J,K).

2.3.6 png-1 acts from neurons and epithelia to regulate axon branching

To determine if PNG-1 functions cell autonomously in VC neurons or cell non-autonomously in the surrounding epithelial cells to regulate VC neuronal morphology, we utilized cell-specific promoters to drive *png-1* expression exclusively in either neurons or epithelial cells in order to assess rescue of the axon branching and overgrowth defects in *png-1(cy9)* animals (Table 2.3). Cell specific expression was obtained by using the *rgef-1* promoter, which is expressed in post mitotic neurons (Altun-Gultekin et al., 2001), *unc-4* promoter, expressed in DA, VA, and the VC motor neurons (Likteig et al., 2001). Additionally we used the *cat-1* promoter, which is expressed in VC4-5, HSN motor neurons, and PDE neurons (Duerr et al. 1999). Expression in epithelia cells were achieved using the *col-10* and *ajm-1* promoters that are expressed exclusively in epithelial cells including vulval cells (Liu et al., 1995; Koppoen et al., 2001). We also used the vulva specific promoter *sqv-1*, (Herman et al., 1999), vulva specific promoter *egl-1 7*, and the *ocr-4* promoter, which is expressed in uterine cells (Tobin et al., 2002). We found that the penetrance of VC branching defects in *png-1(cy9)* animals (~64%) was reduced when *png-1* was expressed from all epithelial cells (29-

36%), neuronal cells (~40%), and vulval cells (32-37%), but not uterine cells. (~70%) or a subset of vulval cells (61-67%) (Figure 2.7).

2.3.7 The thioredoxin and PNGase domains are necessary for axon branching

To determine if the thioredoxin and the predicted C-terminal mannose binding domain are important for PNG-1 axon branching functions we generated PNG-1::GFP constructs with specific domain deletions or mutations and assessed their ability to rescue branching defects in *png-1* mutants (Figure 2.8). Constructs were designed based on the rescuing construct pAC7, consisting of *Ppng-1::PNG-1cDNA::GFP*, as this construct was able to rescue branching defects completely. We found that truncated PNG-1 protein missing the C-terminal mannose binding domain (residues 426-600) was capable of restoring normal VC axon branching when expressed in *png-1(cy9)* animals. Transgenic lines carrying the C-terminal deletions displayed 32-39% excess VC branching defects compared to control animals (65-68%) and similar to the rescue obtained with full-length PNG-1 (21-25%). Conversely, expression of PNG-1 lacking the thioredoxin domain (residues 2-100) (65-67%) or carrying a site-specific disruption of the CGPC (mutated to SGPS) redox active site (66-69%) did not rescue *png-1(cy9)* branching defects. These results indicate that the predicted C-terminal mannose-binding domain is dispensable for PNG-1 branching functions.

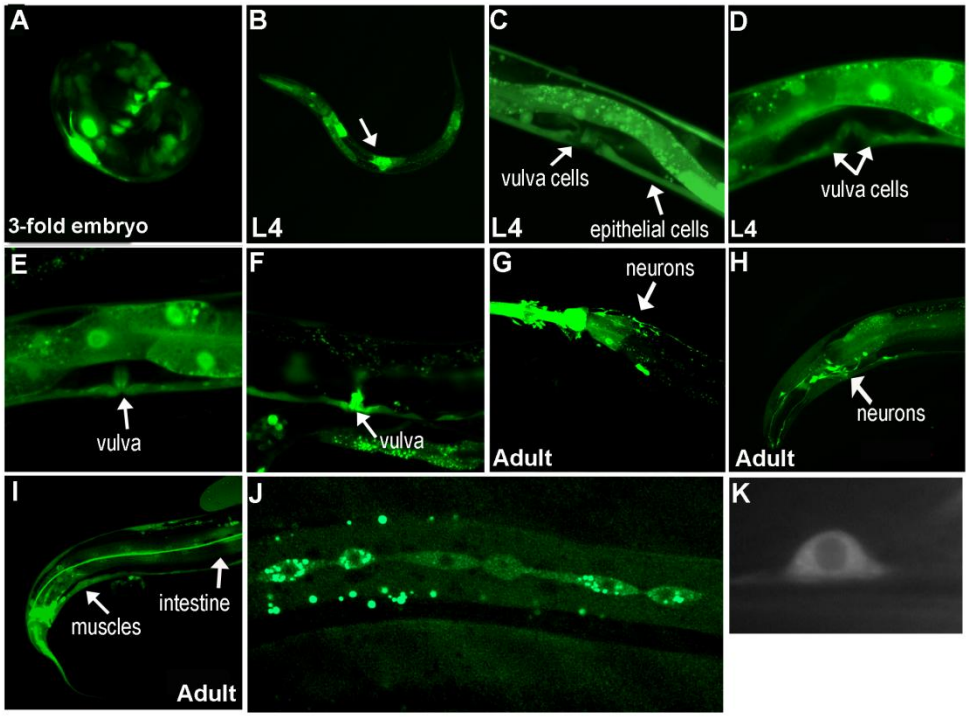

Figure 2.6 PNG-1 is widely expressed

(A–I) *png-1* promoter activity at various developmental stages visualized using a *Ppng-1::GFP* transcriptional reporter. The 600 bp promoter region was shown to be sufficient to rescue VC branching defects in *png-1* mutants. Promoter activity was found in multiple tissues, including epithelium, neurons, muscle, intestine, and vulval epithelial cells. **(J-K)** promoter shows cytoplasmic localization. Epithelial seam cells (**J**) are shown. Scale bars, 10μm.

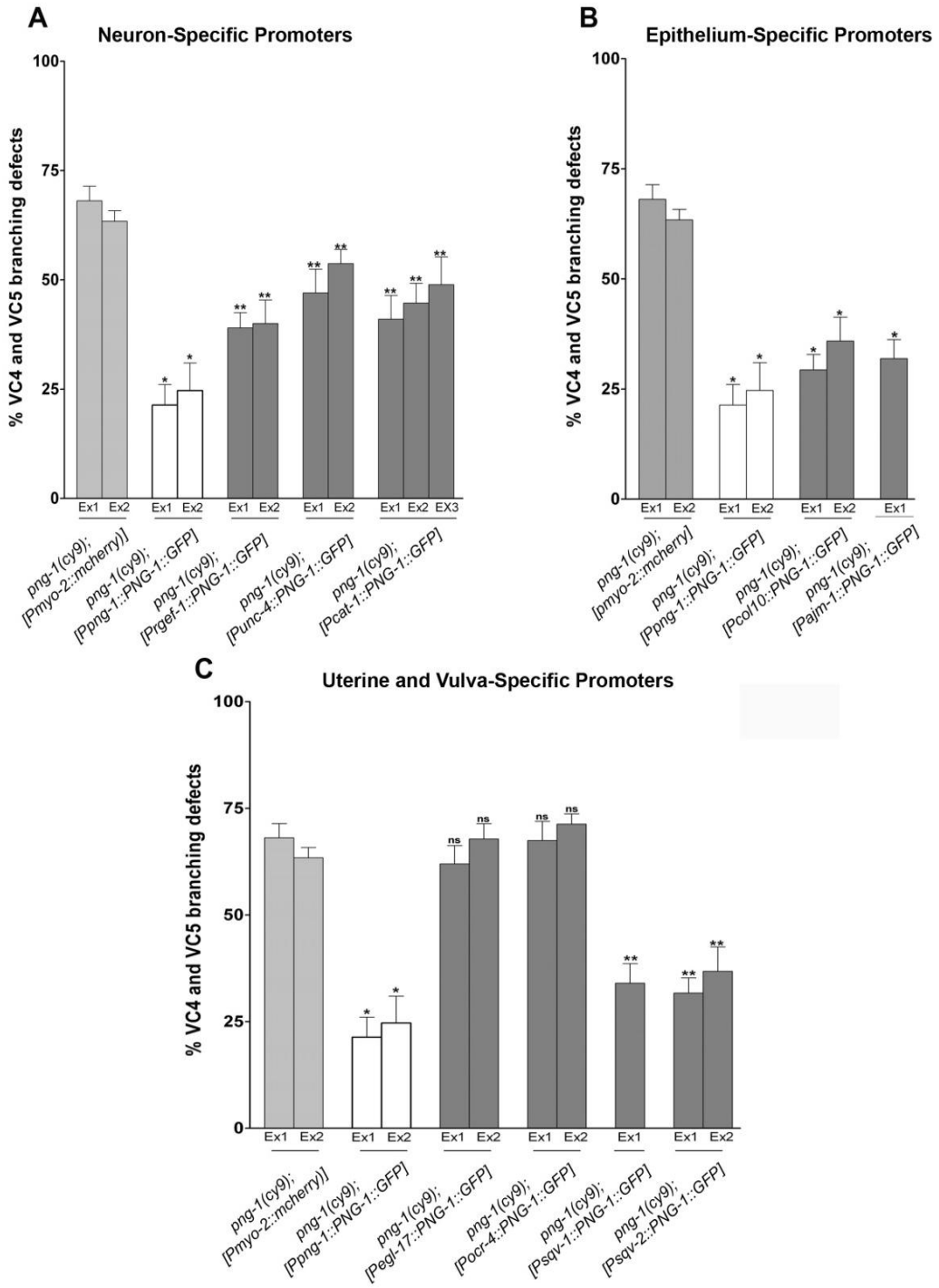
A
Neuron-Specific Promoters
% VC4 and VC5 branching defects
100
75
50
25
0
Ex1 Ex2
Ex1 Ex2
Ex1 Ex2
Ex1 Ex2
Ex1 Ex2 EX3
png-1(cy9); [Pmyo-2::mcherry]
png-1(cy9); [Ppng-1::PNG-1::GFP]
png-1(cy9); [Prgef-1::PNG-1::GFP]
png-1(cy9); [Punc-4::PNG-1::GFP]
png-1(cy9); [Pcat-1::PNG-1::GFP]
B
Epithelium-Specific Promoters
% VC4 and VC5 branching defects
100
75
50
25
0
Ex1 Ex2
Ex1 Ex2
Ex1 Ex2
Ex1
png-1(cy9); [pmyo-2::mcherry]
png-1(cy9); [Ppng-1::PNG-1::GFP]
png-1(cy9); [Pcol10::PNG-1::GFP]
png-1(cy9); [Pajm-1::PNG-1::GFP]
C
Uterine and Vulva-Specific Promoters
% VC4 and VC5 branching defects
100
75
50
25
0
Ex1 Ex2
Ex1 Ex2
Ex1 Ex2
Ex1 Ex2
Ex1
Ex1 Ex2
png-1(cy9); [Pmyo-2::mcherry]
png-1(cy9); [Ppng-1::PNG-1::GFP]
png-1(cy9); [Pegl-17::PNG-1::GFP]
png-1(cy9); [Pocr-4::PNG-1::GFP]
png-1(cy9); [Psqv-1::PNG-1::GFP]
png-1(cy9); [Psqv-2::PNG-1::GFP]

Figure 2.7 PNG-1 is required in epithelial and neuronal cells

Cell specific promoters used to drive expression of PNG-1 from multiple tissues and cells. Constructs were injected with *myo-2::mCherry* into *png-1(cy9);cyIs4[Pcat-1::GFP)* animals to generate multiple independent extrachromosomal transgenic lines. Lines expressing PNG-1 from neurons **(A)** and epithelial cells **(B)** rescue VC4-5 branching defects. **C)** PNG-1 expression in vulva cells (*Psqv-1, Psqv-2*) or VC4-5 (*Pcat-1*) is sufficient for rescue, also. Controls were empty vectors injected with *myo-2::mCherry* injection marker. Error bars denote SE of proportion of counts of population of 60-200 animals. *p<0.05, and **p<0.01, *t* test

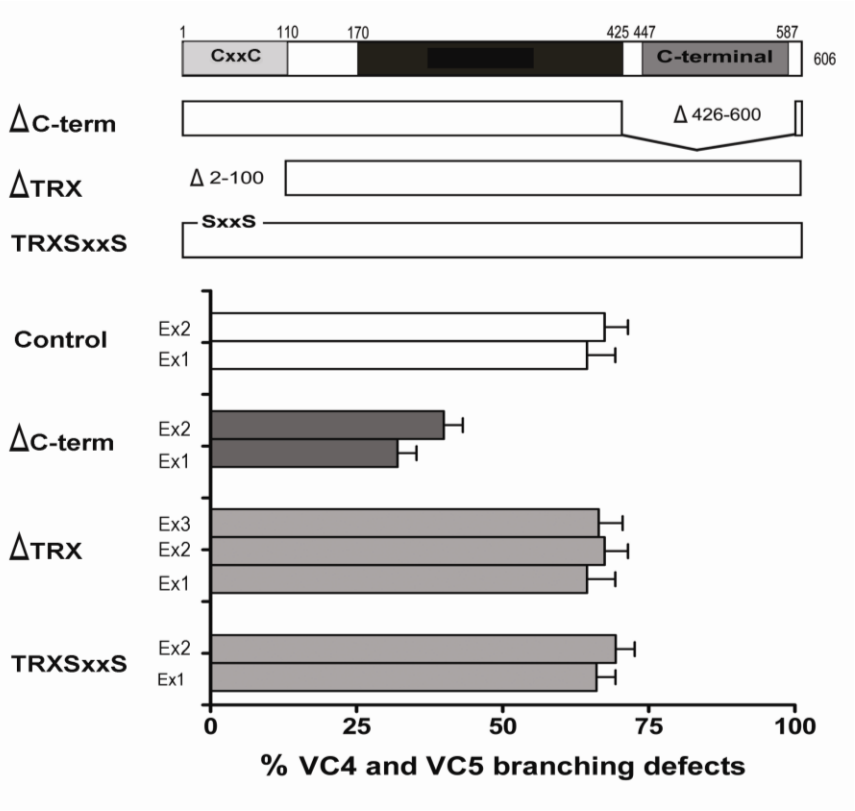

Figure 2.8 C-terminal domain is not essential for axon branching control

PNG-1 structure–function analysis was performed by generating in-frame deletions of the thioredoxin and C-terminal domains and site-directed mutagenesis of the conserved Cys catalytic residues in the thioredoxin domain and scoring for rescue of VC4-5 branching defects in *png-1(cy9); cyIs4*[*Pcat-1::GFP*] animals after germ-line transformation. Multiple Extrachromosomal (Ex) lines were generated for each construct. VC4-5 branching defects were rescued with full-length and C-terminal deleted PNG-1 constructs but not thioredoxin mutants. Constructs were tagged with GFP to verify expression. Error bars denote SEM; N=48 –120 animals

2.3.8 png-1 mutants display branching defects in neurons along the vulval epithelium

To determine the scope and nature of the neuronal defects in *png-1* mutants we used GFP reporter transgenes (Table 2.4) to label subsets of anteroposterior and dorsoventral projecting axon tracts. Axon pathfinding and morphology along the major body axes was found to be normal in *png-1* animals except for the occurrence of inappropriate branches in a subset of ventral cord axons visualized with the *juIs76[Punc-25::GFP]* reporter at sites that correlated precisely with the position of the vulva.

Punc-25::GFP labels all GABAergic neurons, only a subset of which possess processes in the ventral nerve cord that run adjacent to the vulva (DD, VD, AVL, DVB). We therefore isolated AVL using an *unc-30(e191); Punc-25::GFP* background as *unc-25* promoter activity in the DD and VD neurons is silenced in an *unc-30(-/-)* background. We found that AVL which normally projects an unbranched axon from a cell body located in the head to its target in the tail displays inappropriate branches at the vulva in *png-1* mutants (25% in *cy9*, n=150) (Figure 2.9). Branching was only observed in L4 and adult *png-1* alleles.

Additionally the DVB neuron, visualized with an *otIs92 [Pflp-10::GFP]* reporter, which normally projects an axon from a cell body in the tail to a region just posterior to the vulva, displays an axon guidance defect in which axons overextend dorsally along the vulval epithelium or anteriorly past the vulva (36% in *cy9*, n=149) (Figure 2.10 C-E, Figure 2.11 A). A subset of the DVB axons that overextend and reached the vulva also

show inappropriate branching along the vulval epithelium (10% in *cy9*, n=87) (Figure 2-11 B). Similarly, the DVB branching phenotypes were not observed at the L3 stage prior to vulval organogenesis consistent with previous findings that vulval cells provide a branch promoting activity.

In agreement with *png-1* acting in cell-non autonomous manner from multiple tissues to limit neuronal outgrowth and branching, I was able to rescue DVB overextension and branching using constructs driving expression of PNG-1 from neuronal (*Prgef-1*) and epithelial (*Pajm-1*) promoters (Figure 2.11 C, D).

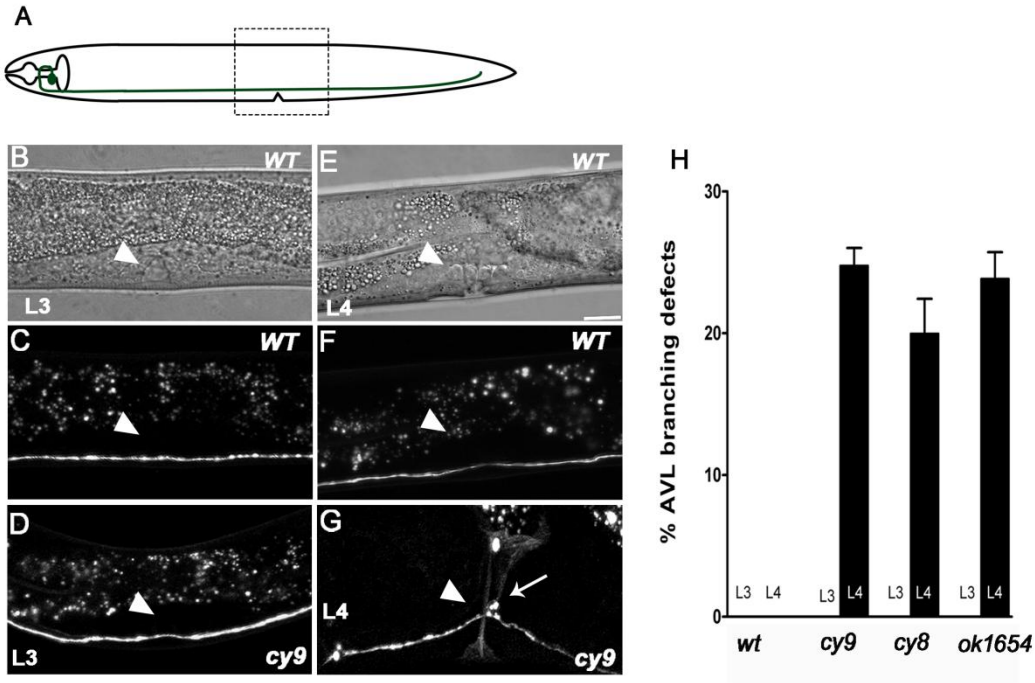

Figure 2.9 AVL motorneuron branching abnormally in *png-1* mutants

A) Schematic of AVL motorneuron in wild type hermaphrodites with images areas boxed. AVL motorneuron is visualized in *Punc-25::GFP; unc-30(e191)* background. In wild type, AVL extends an unbranched axon to the tail. **(B, C)** L3 wild type animals do not display branching in the AVL, as well as *png-1(cy9)* mutants (D). (**G, H)** Branching is only observed in *png-1* mutants at mid-to-late L4 stage in the vulva region, but not before organogenesis at L3 stage. **(E, F)** Wild type does not display similar phenotype in L4 and adult worms. Arrow head denote vulva position, and arrows point to ectopic branch at vulva. Error bars denote SEM of three and/or 4 independent counts (N=50, each). Scale bar, 10μm.

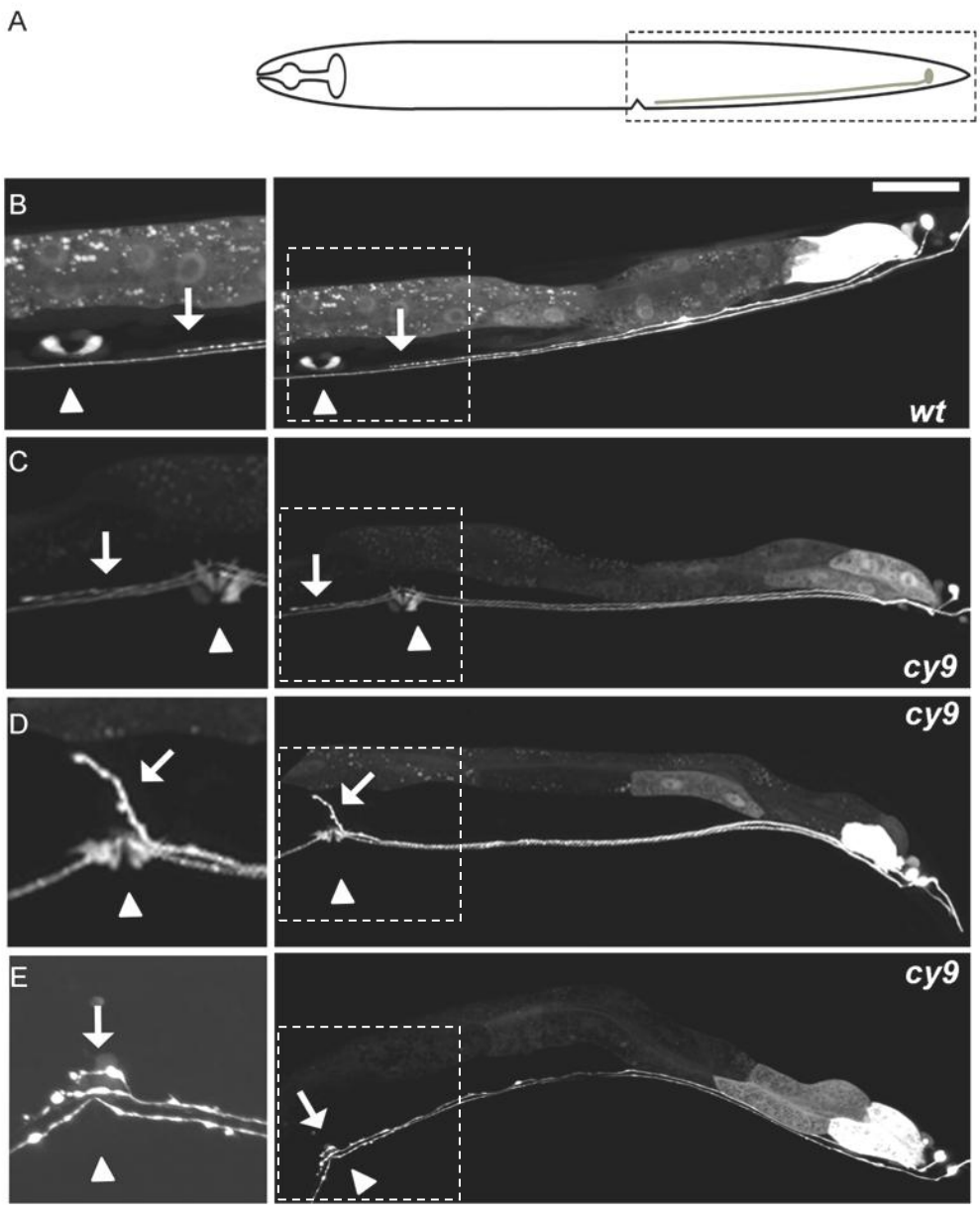
A
B
wt
C
cy9
D
cy9
E
cy9

Figure 2.10 DVB axon overextension and branching in *png-1* mutants

A) Schematic diagram of the DVB motor neuron in wild type hermaphrodites with image site boxed. DVB is visualized with the *otIs92[flp-10::GFP]* reporter transgene. **(B)** In wild type animals, DVB cell body is located in the tail, with an axon extended anteriorly toward the head, terminating at the vulva. **(C, D)** *png-1* mutants display DVB overextension defects where DVB overextends past its termination point and grows past the vulva either anteriorly **(C)**, or dorsally **(D)**. **(E)** DVB motorneuron exhibits branching defects at the distal tip adjacent to the vulva. Arrow head depicts location of vulva, arrow points to DVB defect. Scale bar, 20μm.

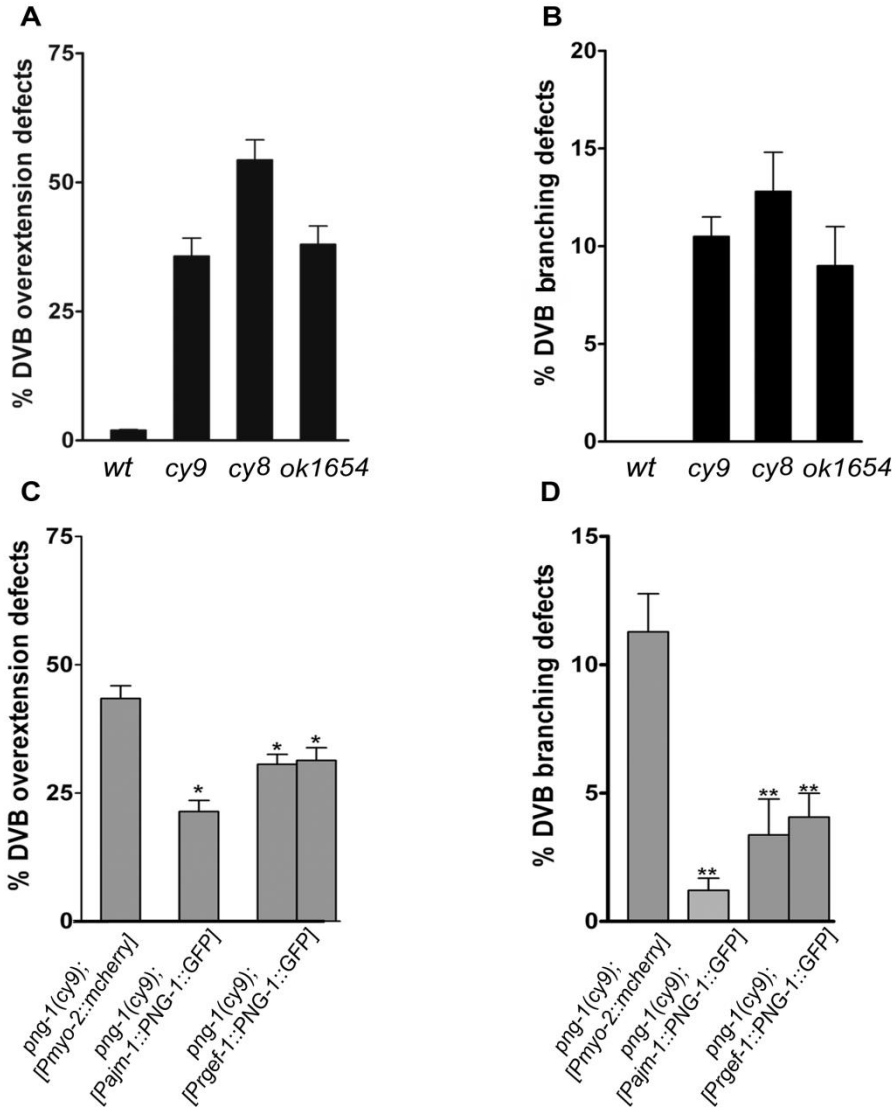
A
% DVB overextension defects
75
50
25
0
wt
cy9
cy8
ok1654
B
% DVB branching defects
20
15
10
5
0
wt
cy9
cy8
ok1654
C
% DVB overextension defects
75
50
25
0
*
*
*
png-1(cy9); [Pmyo-2::mcherry]
png-1(cy9); [Pajm-1::PNG-1::GFP]
png-1(cy9); [Prgef-1::PNG-1::GFP]
D
% DVB branching defects
15
10
5
0
**
**
**
png-1(cy9); [Pmyo-2::mcherry]
png-1(cy9); [Pajm-1::PNG-1::GFP]
png-1(cy9); [Prgef-1::PNG-1::GFP]

Figure 2.11 *png-1* mutant display DVB overextension and branching defects

(A) Worms were scored for DVB overextension if the DVB neuron failed to terminate (near the vulva) and extended pat the vulva either dorsally or anteriorly. **(B)** Branching defects were scored if ectopic branches were observed at the distal tip of the axon in the vulva region. **(C, D)** Overextension and branching defects were rescued with both pan-epithelial (*Pajm-1*) and pan-neuronal (*Prgef-1*) promoters expressing PNG-1. Controls were empty vectors. (A, B) Error bars represent SEM of three and /or 4 independent counts (n=5, each). (C, D) Error bars denote SE of proportion of counts of 60-200 animals. *$P<0.05$, and **$P<0.01$, *t* test

2.4 DISCUSSION

Since the molecular identification of cytoplasmic PNGase as the gene disrupted in an *S. cerevisiae* N-glycanase mutant, highly conserved PNGases have been identified in the genomes of fungi, plants and animals (Suzuki et al., 2000). Several in vitro studies using human cell lines suggests a role for PNGases in the proteasomal-dependent turnover or processing of glycoproteins or glycopeptides that originate in the ER and are retrotranslocated to the cytosol. These roles include the catabolism of misfolded or aberrant glycoproteins during ERAD (Hirsch et al., 2003; Blom et al., 2004; Kim et al., 2006) and the cytoplasmic processing of glycosylated peptide fragments to generate MHC Class I epitopes (Selby et al., 1999; Altrich-VanLith et al., 2006; Kario et al., 2008). However, the developmental and physiological consequences of PNGase deficiency in animal models awaited the phenotypic analysis of knockout mutants. In this chapter I was able to describe for the first time mutations in the sole *C. elegans* PNGase revealing a previously unknown role for a PNGase in regulating neuronal branching during morphogenesis of an organ system.

A striking feature of *png-1* mutants is that axon defects are only found in proximity to the vulva suggesting the disruption of a highly specific pathway associated with innervation of the vulval egg-laying organ. The most prominent defect in *png-1* animals is the overgrowth and increased branching of the VC terminal arbor, the site of synapses to the HSN motor neurons and the vulval muscles (Feinberg et al., 2008).

Current models of egg-laying suggest that acetylcholine release from VC neurons acts to both promote vulval muscle contraction directly while simultaneously inhibiting the stimulatory effect of HSN activity on vulval muscles (Waggoner et al., 1998; Bany et al., 2003). Evidence for an inhibitory role comes from the hyperactive egg-laying phenotype displayed by animals in which VC neurons have been genetically or laser ablated (Bany et al., 2003). In contrast, we find that *png-1* animals display a mild egg-retention phenotype, suggesting that excess branching may contribute to a strengthening of VC inhibition on HSN activity. The opposite phenotype is observed in *png-1; egl-1(gf)* animals that lack HSN neurons, consistent with overstimulation of vulval muscles leading to increased egg laying. PNG-1 activity therefore appears important to limit the extent of VC arborization to prevent overstimulation of the egg-laying circuit

The vulva, a source of innervation and axon branching cues (Li and Chalfie, 1990; Garriga et al., 1993; Shen et al., 2004; Adler et al., 2006), is formed during the third (L3) and fourth larval (L4) stages in a cellular environment occupied by pre-existing axon tracts. The observation that AVL and DVB neurons sprout vulval axon branches *de novo* in *png-1* mutants beginning at L4 from axons that were unbranched at the beginning of vulval organogenesis clearly indicates that normally quiescent axons are intrinsically able to respond to these cues but are normally prevented from doing so. This suggests that PNG-1 may be part of a vulval-organ specific mechanism to limit responses to late acting peripheral innervation cues to neurons involved in egg-laying such as the VC

motor neurons and not to axonal tracts that are present prior to vulval organogenesis. This notion may be similar to mechanisms known to limit or alter neuronal responses to hierarchically acting pathfinding cues during wiring of the central nervous system (Stein and Tessier-Lavigne, 2001).

PNGases are cytoplasmic de-N-glycosylation enzymes. The domain structure of PNG-1 consists of an N-terminal thioredoxin, a central PNGase, and a predicted C-terminal mannose binding domain. The thioreductase and N-glycanase activities of recombinant *C. elegans* PNG-1 have been previously verified (Kato et al., 2007; Suzuki et al., 2007). The disruption of the catalytic Cys (C251Y) in *cy8* is clear evidence that N-glycanase activity is important to mediate axon branching functions. in vitro enzymatic assays using C251Y PNG-1 protein confirm that this mutation specifically abolishes deglycosylation activity without disrupting the thioreductase activity (Suzuki et al., 2007). In addition, the similar phenotypic penetrances of the putative *cy9* null and the *ok1654* deletion allele suggests that the 'glycanase-dead' *cy8* mutation is the equivalent of a complete loss of protein function. The requirement for the thioredoxin domain to rescue branching defects may be related to studies that show a reduced redox state is necessary for optimal PNGase activity (Suzuki et al., 2007).

Our difficulty in detecting expression of a PNG-1::GFP translational fusion, from its endogenous promoter, despite showing transgene expression and functionality by rescuing branching defects, suggests that PNG-1 is normally present in low abundance

or undergoes post-translational regulation to limit protein levels. It could also be due to the toxic effect of wide spread expression, since it is expressed ubiquitously in all larval stages. This mirrors findings from activity assays and immunostaining experiments in yeast, plant, and mammalian cells that also suggest low levels of endogenous PNGase protein (Suzuki et al., 2001; Hirsch et al., 2003; Diepold et al., 2007). Cell-specific analysis also confirmed wide expression pattern in various cells and tissue. Most importantly we observed that PNG-1 is localized in the cytoplasm, when it was expressed from epithelial or neuronal promoters. This is in accordance with studies involving direct visualization, subcellular fractionation, and inferences from the location of deglycosylated substrates is that PNGases are localized to the cytosol or associated with the cytosolic surface of the ER (Spiro, 2004; Suzuki, 2007).

The finding that PNG-1 acts cell non-autonomously from multiple tissues to limit neuronal outgrowth and branching has important mechanistic implications and suggests for the first time that PNGases also participate in intercellular signaling. A cell extrinsic effect can be explained if PNGase activity in epithelial cells influences the secretion or cell-surface expression of an axon branching molecule such that *png-1* deficient cells would present either too much of a branch promoting or too little of a branch inhibitory factor resulting in a hyperinnervation phenotype. At the same time, we cannot entirely exclude a cell autonomous role given that *png-1* defects were also rescued with neuronal-specific expression. However, a cell extrinsic role is not

incompatible with a cellular focus in VC neurons. First, because VC4 and VC5 arbors overlap, each may mutually limit the branching of the other through a lateral inhibitory mechanism akin to that involved in dendritic tiling (Grueber et al., 2002). Alternatively, a factor expressed from VC neurons may act in an autocrine manner to inhibit axon overgrowth and branching. A classic example of autocrine signaling is the action of hepatocytic growth factor on the elongation of sympathetic axons (Yang et al., 1998).

In summary, our findings are consistent with *png-1* acting in a specific and novel pathway to regulate extracellular cues that limit the extent of axon branching during organ innervation in *C. elegans*. Our findings suggest that animal PNGases should be examined for roles in neural wiring and plasticity in addition to their protective 'housekeeping' roles in cellular homeostasis.

Table 2.1 *png-1* sequencing primers

Promoter	Sequence
F56G4.1F	5’-tctttagtctgataaatcggtggc-3’
F56G4.2F	5'-acgtatggaatgaggtctatttgc-3’
F56G4.3F	5’-aaatgatctgatgtcagcgaaag-3’
F56G4.4F	5’-aaaaatttctgggtcccacc-3’
F56G4.5R	3’-caaaactaggccacgcactc-5’
F56G4.6R	3’-aatcgatagggaatttcatggg-5’
F56G4.7R	3’-ctaggccacaaactaaaaatcgg-5’
F56G4.8R	3’-gactggaatatgacatatttgtgtagg-5’

Table 2.2 ***png-1*** **genotyping primers and conditions**

Allele	Primers		Restriction enzyme	Restriction enzyme/PCR fragment size (bp)	
	promoter	sequence		+/+	-/-
cy9	F56G4.8A	5'-gtcgataattttaccgaattttccac-3'	MaeIII	370	230
	F56G4.8B	5'-gtggttgacgtcacttggagata-3'			
cy8	F56G4.8A	5'-gtcgataattttaccgaattttccac-3'	BbvI	320	290
	F56G4.8B	5'-gtggttgacgtcacttggagata-3'			
ok1654	F56G4.OKF1	5'-gtcgataattttaccgaattttccac-3'	NA (deletion)	460	760
	F56G4.OKR	5'- ttgacgtcacttggagata-3'			
	F56G4.OKF2	5'-gtcgataattttaccgaattttccac-3'			

Table 2.3 Cell specific promoter primer list

Translation Construct	Promoter (size)	Expression	Primers
Pcol-10::PNG-1::GFP	*col-10* (1.2kb)	Epithelial cells	5’-gtcgactctagaactagtgg-3’ 3’-ggtaccttattcagtgttac-5’
Pajm-1::PNG-1 ::GFP	*ajm-1* (860bp)	Epithelial cells	5’- cgactcactatagggcgaat -3’ 3’- gtccttggttctgtaaagac -5’
Punc-4::PNG-1::GFP	*unc-4* (2.6kb)	VC1-VC6	5’-ccacctctgtcttcaaggcgacc-3’ 3’-cacttttggaagaagaagatcctc-5’
Pcog-1::PNG-1::GFP	*cog-1* (2.9kb)	Vulva-uterus connection	5’-aagcatttctagaccataagaag-3’ 3’- ctggttatggtagaggggagatt -5’

Translation Construct	**Promoter (size)**	**Expression**	**primers**
Prgef-1::PNG-1::GFP	*rgef-1* (1.5kb)	Pan-neuronal	5’-gcatgctttgaatacggggagcg-3’ 3’-ccggtaccaatagctcacatttcg-5’
Pegl-17::PNG-1::GFP	*egl-17* (2.6kb)	Vulva muscles	5’-gcatgctttgaatacggggagcg-3’ 3’-ccggtaccaatagctcacatttcg-5’
Pcat-1::PNG-1::GFP	*cat-1* (2.4kb)	VC4-VC5	5’-ccaaggctctgcagggtacctatg-3’ 3’-gtacgacatacctccttcttccaag-5’
Pocr-4::PNG-1::GFP	*ocr-4* (400bp)	Uterine	5’-ggcttggtgatacctttgatg-3’ 3’-ctagatgcattacccattaatacaag-5’
Psqv-1::PNG-1::GFP	*sqv-1* (1.3 kb)	Vulva	5’-tactagttaaggtgaagcac-3’ 3’-gcgcgttgattattgattgg-5’

Table 2.4 Neuronal reporter lines used for phenotypic analysis

Neuronal reporter*	Neurons examined	Phenotype observed in png-1 mutants
cyIs4 [cat-1::GFP]	VC4,VC5, PDE	Increased VC4-5 axon branching at the vulva
kyIs179 [unc-86::GFP]	HSN	None
evIs79 [unc-129::GFP]	DA, DB	None
otIs92 [flp-10::GFP] †	DVB, PQR, PVR	DVB axon overextension defect and inapropriate DVB axon branching at the vulva
oyIs14 [sra-6::GFP]	ASH, PVQ	None
*unc-30(e191); juIs76***	AVL, DVB	AVL axon branching at the vulva
zdIs5 [mec-4::GFP]	ALM, PLM, AVM, AVM	None

* all reporters crossed into a *png-1(cy9)* background.

** *unc-30(e191);juIs76* background used to silence DD,VD expression.

† *otIs92* also shows GFP expression in vulD vulva cells.

CHAPTER 3: GENETIC INTERACTORS OF *png-1*

Sections (3.1-3.5) of this chapter associated with *rad-23* and *png-1* have been modified with permission from:

The N-glycanase *png-1* act to limit axon branching during organ formation in *C. elegans*

Nasrin Habibi-Babadi, Anna Su, Carlos E. De Carvalho, Antonio Colavita

J of Neurosci, Feb 3; 30(5): 1766-1776 (2010)

Reprinted from the Journal of Neuroscience with permission from the Society of Neuroscience Copyright Clearance Center (Appendix A)

Contribution to this chapter:

Laboratory of Dr. Maria Gallegos at California State University mapped *sax-2(zy16)*

ABSTRACT

png-1 encodes a Peptide: N-glycanase, a highly conserved cytosolic enzyme that cleaves N-glycans from misfolded glycoproteins. *png-1* was found to regulate axon outgrowth and branching in *C. elegans*. In this study, I used a candidate gene approach to identify genes that interact with *png-1* to regulate neuronal morphology. A deletion allele of the DNA repair gene, r*ad-23*, orthologues of which are known to physically interact with PNGases in yeast and mammals, displayed similar axon branching defects. Analysis of *png-1;rad-23* double mutants displayed axonal defects that were indistinguishable from single mutants, indicating that *png-1* and *rad-23* are components of a common pathway. Additionally, I reveal how mutations in the NDR kinase pathway genes *sax-1* and *sax-2* resulted in *png-1* like phenotypes. Furthermore, I show through genetic analysis that *png-1; sax-1* and *png-1*; *sax-2* double mutants displayed enhanced defects compared to single mutants, suggesting that *png-1* and *sax-1*/*sax-2* act in parallel pathways to regulate axon and branch overgrowth. In summary, this chapter reveals novel pathways in the regulation of neuronal branching during development.

3.1 INTRODUCTION

Assembly of neuronal networks relies on axon growth, guidance, and branching. Axons are guided to their final targets by a variety of extracellular cues and receptor families that modulate axonal growth cone behaviors (Tessier-Lavigne and Klodkin, 2010). Numerous studies describe a role for conserved families of axon guidance cues in axon branching, albeit through different mechanisms (Ma and Tessier-Lavigne, 2007; Dent et al., 2001). In addition to regulating axon outgrowth during development, netrin-1promotes branch formation in cortical neurons (Kalil and Hutchins, 2011; Dent and Kalil, 2001). Even though branching is important in neuronal development, molecular pathways controlling branch formation are not well defined.

png-1 encodes the Peptide: N-glycanase (PNGase) in *C. elegans*. This Cytoplasmic PNGase catalyzes the removal of bulky N-linked glycans from glycoproteins or glycopeptides prior to degradation by the proteasome (Suzuki et al., 2000, 2002, 2007). Mutation in *png-1* resulted in abnormal branching of the VC neurons during the development of the egg-laying organ (Habibi-Babadi et al., 2010). *png-1(-/-)* worms displayed an increase in the number and complexity of branches in VC4-5 motor neurons. Additionally, *png-1* mutants developed ectopic branches in the normally unbranched AVL and DVB motor neurons. These observations suggested that *png-1* functions to limit axon branching and outgrowth in a subset of neurons.

Prior to our work, a role for PNGases was established in the proteasomal-dependent degradation of glycoproteins that are formed in the ER and retrotranslocated to the cytosol. This included the processing of misfolded proteins during endoplasmic reticulum associated degradation (ERAD) (Kim et al., 2006), as well as the cytoplasmic processing of N-glycosylated peptide fragments required for Major Histocompatibility complex (MHC) Class I antigenic activity (Shatz, 2009; Kario et al., 2008; Altrich-vanLith et al., 2006). Yeast and mammalian PNGases were reported to bind directly to the 26S proteasome through interaction with Rad23 (Suzuki et al., 2001b; Madura et al., 2001; Ortolan et al., 2000; Zhao et al., 2007). Notably, PNGase homologues in higher eukaryotes have extended domains at the C- and N-termini (not found in yeast PNGase), that are found to recognize and bind to ubiquitin moieties as well as components of the 26S proteasome (Suzuki et al., 2001a, 2002).

Characterization of *png-1* mutants in *C. elegans* provided evidence that *png-1* glycosylation activity is required to limit neuronal branching at the vulva (Habibi-Babadi et al., 2010, Suzuki et al, 2007). Conversely, our work present evidence that *png-1* acts cell non-autonomously from the epithelia to regulate axon branching in neurons, a significant departure from the cell-intrinsic roles PNGases perform in ERAD and MHC pathways. These results suggest an additional and novel developmental role for PNGases involving intracellular signalling. Thus to understand the role of PNG-1 in neuronal development it is important to identify the upstream and downstream

components and the mechanisms by which PNGases mediate axon outgrowth and branching. I used two parallel approaches to gain new insight into PNG-1 activity in neuronal development. I first used a candidate gene approach examining the function of *C. elegans* axon guidance cues, receptors, and conserved signalling pathways in the development of the egg-laying neuronal circuitry. I also examined the role of the ERAD pathway in regulating axon outgrowth and branching. As these pathways are highly conserved, I utilized the availability of mutants of the genes involved in these pathways and performed a phenotypic screen of their neuroanatomy. This approach revealed that mutations in *rad-23*, the *C. elegans* homologue of Rad23, caused axon outgrowth and branching defects similar to *png-1*.

In the second approach I performed a modifier genetic screen to search for mutants that either suppressed or enhanced branching defects in *png-1* mutants. This screen should identify components of PNG-1 pathway or parallel pathways that regulate neuronal development. *sax-2*, a component of the NDR kinase pathway, was recovered as a mutant that caused synergistic enhancement of VC4-5 branching in *png-1* mutant background. This observation suggests that *sax-2* and *png-1* act in parallel pathway to regulate VC4-5 branching. Combined, these studies suggest that at least two pathways act to limit axon outgrowth and branching in VC neurons: a PNG-1 dependent pathway including RAD-23, and a PNG-1 independent pathway including SAX-2.

3.2 MATERIALS AND METHODS

3.2.1 Nematode strains and genetic methods

C. elegans strains were grown on nematode growth medium (NGM) plates inoculated with *Escherichia coli* strain OP50 (Brenner, 1974). Strains were maintained at at 15°C, 20°C or 25°C, depending on the experimental requirements.

The wild-type N2 (Bristol) strain was used as standard reference, and the following mutant alleles were used: LGI: *png-1 (ok1654), rpn-10(tm1349), lin-44(n1792), unc-40(e271), unc-11(e47), mab-20(ev778), let-502(sb118ts), unc-73(e936);* LGII: *ire-1(ok799), rad-23(tm2595), cwn-1(ok546), cdc-48(tm544), dsh-2(e225), cam-1(gm122), plx-2(ev773), max-2(nv162), vab-1(e2), rga-1(ok204); mig-5(rh14);* LGIII: *hrd-1(tm1743), sax-2(ky491), mig-1(ct41), mig-10(ct41); inft-1(gk386), strd-1(ok2283); unc-119(ed3), cdh-1(gk747), cdh-3(pk87), cdh-4(ok1323);* LGIV: *unc-5(e53), plx-1(nc37), jnk-1(gk7), ced-10(n3246), egl-20(n585), cwn-2(ok895), unc-43(n498), wsp-1(gm324), lin-3(e1417), daf-18(e1375), rho-1(vc40174), unc-44(e362);* LG V: *rpm-1 (ok364), cfz-2(ok1201), mom-2(ne874), unc-34(e566), vab-8(e1017);* LG X: *pek-1(ok275), sax-1(ot10), derlin-1(gk443), slt-1(eh15), lin-18(e620), unc-6(ev400), sax-3(ky200), pkc-2(ok328), kin-20(ok505), sek-1(km4), mig-15(rh148),cgef-1(gk261), mig-2(mu28), egl-15(n484), egl-17(e1313), bar-1(ga80).* Extrachromosomal transgenic line(s): *png-1::cyIs4; Ex1*[*Ppng-1::PNG-1::GFP; Poder-1::dsRed*].

The following green fluorescent protein (GFP) reporter transgenes were used to visualize and score neuroanatomy: *cyIs4[Pcat-1::GFP, rol-6(su1006]* to label VC4-5, and

PDE, *unc-30(e191); juIs76[Punc-25::GFP]* to label AVL and DVB, and o*tIs92[Pflp-10::GFP]* to label DVB. All strains were backcrossed at least three times.

3.2.2 Transgenic lines and genotyping

Neuron specific GFP reporter strains were crossed into the following mutants: *rpn-10(tm1349), lin-44(n1792), unc-40(e271), unc-11(e47), mab-20(ev778), let-502(sb118ts), unc-73(e936), ire-1(ok799), rad-23(tm2595), cwn-1(ok546), dsh-2(e225, cam-1(gm122), plx-2 (ev773), max-2(nv162), vab-1(e2), rga-1(ok204, mig-5(rh14), hrd-1(tm1743), sax-2(ky491), mig-1(ct41), mig-10(ct41), inft-1(gk386), strd-1(ok2283); unc-119(ed3), cdh-1(gk747), cdh-3 (pk87), cdh-4(ok1323), unc-5(e53), plx-1(nc37), jnk-1(gk7), ced-10(n3246), egl-20(n585), cwn-2 (ok895), unc-43(n498), wsp-1(gm324), lin-3(e1417), daf-18(e1375), rho-1(vc40174), unc-44 (e362), rpm-1 (ok364), cfz-2(ok1201), mom-2(ne874), unc-34(e566), vab-8(e1017), pek-1 (ok275), sax-1(ot10), cup-2(gk443), slt-1(eh15), lin-18(e620), unc-6(ev400), sax-3 (ky200), kin-20(ok505), sek-1(km4), mig-15(rh148), cgef-1(gk261), mig-2(mu28), egl-15(n484), egl-17(e1313),* and *bar-1(ga80)* using standard genetic methods (Brenner, 1974). Double homozygous animals were verified using polymerase chain reaction (PCR) for deletion or restriction fragment polymorphism (RFLP) genotyping.

3.2.3 Plasmid construction and molecular cloning

Rescuing RAD-23 constructs were prepared using standard cloning procedures. The transcriptional *Prad-23::RFP* (pAC109) reporter was made by PCR amplifying approximately 1300bp upstream of the predicted *rad-23* starting methionine and cloned

upstream of RFP start codon in pBluecript plasmid. Full length *rad-23* cDNA (1064bp) was generated by RT-PCR from N2 RNA extracts using primers 5′-atggttttgtccgttacattc caggactctc-3′, and 3′-tcctcatcctgaaataattaaaaattaaac-5′ and inserted between the RFP and the *rad-23* promoter in pAC 109. Genomic region containing the *rad-23* promoter and *rad-23* coding region, approximately 2800bp, was amplified using primers 5′-cttgctaaaac caatgcatcggaaagttc-3′ and 3′-agcacatggaactgaatgtgttattatc-5′. Cloning accuracy was verified by restriction enzyme analysis and sequencing.

3.2.4 Transgenic animals and germ line transformation

Extrachromosomal arrays were generated following standard microinjection techniques (Mello et al., 1991). Zeiss Axiovert microscope equipped with 20X and 40X objective lens, and an Eppendorf FemtoJet Microinjector system were used for injecting young adult hermaphrodites with plasmids, genomic PCR fragments, or PCR fusion products.

Gene rescue analysis was performed by testing for the rescue of DVB overextension and branching defects in *rad-23(tm2595);otIs92* animals after germline transformation. *rad-23* mutant worms were injected with 1 *ng/ul* of DNA. PBluecript SK and pPD95.77 (Fire lab vector kit) were injected as controls. Co-injection markers used for making transgenic lines were: *rol-6(at 20-25 ng/ul), Podr-1::dsRed*, expressed in the sensory neurons in the head (at 20-30 *ng/ul)* or *Pmyo-2::mCherry* expressed in the

pharynx (at 5-10 *ng/ul).* Transgenic lines were confirmed in the F2 progeny by transmission of the co-injection markers.

3.2.5 png-1 modifier screen

For mutagenesis, staged homozygous *png-1(cy9);cyIs4* L4 animals were spun at 2000 rpm and resuspended in 4ml M9 buffer. 20µl of ethylmethanesulfonate (EMS, Sigma-Aldrich) was added to a final concentration of 50mM. The worms were incubated for 4h at room temperature on a rotating wheel. Following mutagenesis, the parental generation (P_0) was washed four times with M9 buffer and then placed on fresh seeded plates to recover and produce self progeny (F1 generation). Three F1 adult hermaphrodites were transferred to several individual worm plates to generate the F2 progeny. Plates were allowed to grow at 20°C for three days, after which approximately 50 worms were randomly picked and mounted on slides. F2 worms were visually screened for changes in VC4-5 branching defects using epifluorescenc Zeiss Axioplan2 microscope. Mutants that displayed notable suppression or enhancement of *png-1* ectopic branching defects were recovered from the slide and transferred to new plates and allowed to self propagate. The self-progeny were then re-examined to confirm suppression or enhancement. Mutant strains were backcrossed twice to the wild type (N_2) strain to remove the *png-1* mutant background.

3.2.6 Phenotypic analysis of neuronal morphologies

Worms expressing *cyIs4 [Pcat::GFP]* were scored for VC4-5 neurite branching, axon outgrowth and branching defects using the same criteria described in Chapter 2 (section 2.2.5).

Worms expressing *unc-30(e191);juIs76[Punc-25::GFP]* were used to score for AVL and DVB defects. Worms expressing *otIs92 [Pflp-10::GFP]* were scored *for* DVB motor neurons defects. DVB terminate a short distance posterior to the vulva. A termination defect was scored as any DVB process that extends dorsally along the vulva epithelium or anteriorly past the vulva. To rule out the possibility that DVB overextension defects was caused by a decrease in total body length or possible anterior displacement of the DVB cell body, we measured total body length, DVB cell body position, and DVB axon length in young adult wild type and mutant animals.

Axons were scored as displaying an axon branch if a distinct axonal protrusion at least 3-5μm in length (approximately one neuronal cell body diameter) was observed. All worms were staged accordingly to vulval developmental milestones and verified accordingly using differential interference contrast (DIC) microscopy.

3.2.7 UPR stress analysis

Adult worms were placed on NGM plates containing 0-7.5 μg/ml tunicamycin (per concentration)(Calbiochem) and allowed to lay eggs for four hours at 20°C. Eggs were counted and progenies were monitored three days later for growth and

development, in addition to neuroanatomical analysis (Shen et al, 2001). Results reported from 3 independent assays.

3.2.8 Microscopy and imaging

Worms were mounted on 2% agarose pads in M9 buffer and immobilized with 10mM levamisole (Sigma). Neurons were visualized by epifluorescenc using a Zeiss AxioplanII microscope. Images were captured using a Zeiss LSM510 confocal microscope. Z-stack images of neurons were captured using 20X, 40X, and 63X objective lenses and were collapsed into a single image. Worms were staged with respect to developmental stages as described (Riddle et al, 1997).

3.2.9 Statistical analysis

All experiments were performed at least 3 times, unless noted otherwise noted. The number of worms scored in each experiment is listed in each figure. Data was analyzed using Prism V program (Graphpad). Data are reported as mean , or mean . Differences between strains were investigated with ANOVA followed by the Bonferroni post Hoc test. P values of < 0.05 were considered significant.

3.3 RESULTS

3.3.1 Candidate gene approach for png-1 interactors

A candidate gene screen was performed to study the effects of conserved molecules that mediate neuronal development on VC4-5 branching. We crossed in the *Pcat-1::GFP* reporter transgene into loss of-function mutants of these genes and analyzed their VC4-5 morphology (Table 3.1). The majority of the examined mutants exhibited wild type branching phenotypes with the exception of few that displayed mild, less penetrant defective branching phenotypes. These results suggest that branching at the vulva is mediated through molecules (and pathways) independent of well known neuronal guidance and signalling pathways.

3.3.2 rad-23 mutants display outgrowth and branching defects

PNGases act on misfolded glycoproteins targeted for degradation by ER quality control pathways. Therefore, we wanted to investigate the possibility that VC4-5 branching defects were not a non-specific effect of misregulated cellular processes caused by intracellular accumulation of misfolded proteins. There are numerous known components involved in the retrotranslocation, ubiquitination, and processing of misfolded proteins. We analyzed the following genes for their conserved role in ER quality control pathways in *C. elegans*: *Derlin-1, hrd-1, pek-1, ire-1, rpn-10,* and *rad-23*.

Derlin-1 (also known as *cup-2* in *C. elegans*) binds to misfolded and ubiquitinated proteins in *C. elegans*, and its inactivation causes ER stress (Ye et al., 2004). Hrd-1 is an

E3 ligase in *C. elegans* that is involved in endoplasmic reticulum quality control and ERAD (Shen et al., 2006, 2007; Sasagawa et al., 2007). Subsequently after exiting from the ER lumen, some substrates encounter deglycosylating PNGases, which remove large bulky glycans chains from these substrates. These substrates are recognized by Rad23/HR23 which binds directly to RPN-10 (*C. elegans* homologue of RPN-4) subunit of the proteasome to facilitate transfer of substrates to the regulatory core of the proteasome. Numerous in vitro and in vivo studies report PNGases in complex with Rad23, RPN4, and Derlin-1 (Katiyar et al., 2005, 2004; Suzuki et al., 2003; Zhao et al., 2006).

Accumulation of misfolded proteins in the ER triggers three signalling pathways mediated by IRE1, PERK and ATF6 which correspond to *ire-1*, *pek-1*, and *atf-6* in *C. elegans* (reviewed in Chapter 1, section 1.3). Activation of PERK inhibits protein synthesis, while IRE1 and ATF signalling lead to splicing of the X-box binding (XBP1), a potent transcription factor, resulting in increase of transcription of folding and ERQC components (i.e. chaperones) (Shen et al., 2001; Urano et al., 2000b, 2002). We crossed our GFP reporters into mutants that disrupt the unfolded protein response (UPR) and ERAD adaptive response pathways to ER stress in *C. elegans* and studied their neuronal morphologies for defects similar to *png-1* mutants (Table 3.2). Examination of VC4-5, AVL, and DVB neuronal morphologies in *cup-2(gk443), hrd-1(tm1743), ire-1(ok799),* and *pek-1(ok275)* worms failed to detect obvious axonal outgrowth and branching defects

except for *ire-1(ok799)* and *rad-23 (tm2595)* mutants. *ire-1(ok799)* mutants displayed 8% (n=75) DVB overextension defects; no branching defects were detected in VC4-5 or DVB. *rad-23(tm2595),* a deletion mutation displayed neuronal defects similar to *png-1 (-/-)* animals (Table 3.2). VC4-5 neuronal morphology appeared normal in *rad-23(tm2595)* mutants and there was no enhancement in VC4-5 branching defects in *png-1(cy9);rad-23(tm2595)* or *png-1(ok1654);rad-23(tm2595)* double mutants (Figure 3.1).

We focused our study on characterization of *rad-23* mutants since *ire-1* mutants did not display strong, more penetrant overextension and branching defects such as *rad-23* mutants. AVL neurite length was examined at L3, L4, and adult animals, while branching defects were examined in L4 and adult worms. Approximately 6% of *rad-23* mutants were observed to develop a single inappropriate branch near the vulva (Figure 3.2 A-D). 40% of DVB motorneuron displayed overextension defects in *rad-23* mutants. Of those only 6% displayed ectopic branches at the vulva (Figure 3.2 E-J). These phenotypes were similar to phenotypes observed in *png-1* mutants.

DVB overextension and branching defects in *rad-23* mutants were not observed at L3 stage prior to vulval organogenesis. Additionally, homozygous r*ad-23(tm2595)* mutants were viable, and displayed no alteration of morphology, development, motility, egg-laying, or life-span.

Table 3.1 Candidate gene screen for VC4-5 branching defects+

Gene	Identity	VC4-5 morphology
Wnt pathway components		
lin-44	Wnt	*Pcat-1::GFP* expression off*
egl-20	Wnt	Normal
cwn-1	Wnt	Normal
cwn-2	Wnt	Normal
mom-2	Wnt	Normal
cfz-2	Frizzled	Normal
mig-1	Frizzled	Normal
mom-5	Frizzled	Normal
mig-5	Dishevelled	*Pcat-1::GFP* expression off*
dsh-2	Dishevelled	Normal
cam-1	ROR receptor tyrosine kinase	Normal
lin-18	Ryk/Derailed tyrosine kinase-related	Normal
bar-1	Beta-catenin	*Pcat-1::GFP* expression off*
Axon guidance genes		
unc-6	Netrin	Axons fail to extend laterally along the vulva
unc-5	UNC5 homologue	Normal
unc-40	DCC homologue	Axons fail to extend laterally along the vulva
slt-1	Slit homologue	Normal
sax-3	ROBO homologue	Mild branching defects
vab-1	Ephrin receptor	Normal
vab-2	Ephrin	Normal
mab-20	Semaphorin homologue	Normal
plx-1	Plexin ortholog	Normal
plx-2	Plexin ortholog	Normal

Table 3.1 Continued

Gene	Identity	VC4-5 morphology
Kinase/Phosphatases		
max-2	P21-activated kinase (PAK) homologue	Normal
pak-1	P21-activated kinase (PAK) homologue	Normal
jnk-1	Serine-threonine kinase (JNK)	Mild axon guidance defects
sax-1	NDR kinase	Cell shape and mild axon branching defects
unc-43	CaMKII homologue	Normal
unc-51	Serine-threonine kinase Atg1p	Normal
kin-20	Casein kinase I	Normal
sek-1	MAPKK family	Normal
mig-15	NIK kinase	Mild axon guidance defects
Cytoskeleton remodeling genes		
mig-10	Lamellopodin homologue	Axon guidance defects
rho-1	GTPase orthologous to RhoA	Normal
ced-10	GTPase orthologous to Rac1	Normal
let-502	Rho-associated kinase homologue	Normal
cgef-1	Putative GEF for Rho and Rac GTPases	Normal
wsp-1	WASP homologue	Normal
unc-34	Enabled/VASP homologue	Axons fail to extend laterally along vulva
unc-73	RhoGEF Trio homologue	Normal
mig-2	Rho GTPase	Normal
rga-1	Cdc42 RhoGAP	Normal
rga-6	RhoGAP	Normal
inft-1	Inverted formin related	Normal
frl-1	Formin related	Normal

Table 3.1 Continued

Gene	Identity	VC4-5 morphology
Other		
lin-3	EGF ligand	*Pcat-1::GFP* expression off
rpm-1	E3 ubiquitin ligase highwire homologue	Normal
sax-2	Homologue of Drosophila furry	Cell shape and mild axon branching defects
strd-1	STRAD pseudokinase homologue	Normal
unc-11	Clathrin-adaptor protein AP180	Normal
unc-119	Novel highly conserved protein	Normal
vab-8	Atypical kinesin-like motor	Normal
daf-18	PTEN tumor suppressor homologue	Mild axon guidance defects
unc-44	Ankyrin	Normal
cdh-1	Cadherin daschsous homologue	Normal
cdh-3	Similar to FAT3 and FAT4 cadherin	Normal
cdh-4	Similar to FAT3 and FAT4 cadherin	Normal
egl-15	Fibroblast growth factor receptor	Mild axon guidance defects
egl-17	Fibroblast growth factor-like	Mild axon guidance defects

* VC4-5 morphology in *lin-44, lin-17, mig-5, and bar-1* mutants visualized using *Punc-4::GFP*.

Pcat-1::GFP was used to visualize VC4-5 in all other mutants.

+ >30 animal counted

Table 3.2 UPR and ERAD candidate gene screen for neuronal defects

		% Neuronal Defects			
Gene/strain	**Function**	**VC4-5**	**AVL**	**DVB overextension**	**DVB branching**
ire-1(ok799)	UPR	0[a]	0[b]	8[c]	0[c]
pek-1(ok275)	UPR	0[a]	0[b]	0[c]	0[c]
rpn-10(tm1349)	ERAD	0[a]	0[b]	0[c]	0[c]
hrd-1(tm1743)	ERAD	0[a]	0[b]	0[c]	0[c]
cup-2(gk479)	ERAD	0[a]	0[b]	0[c]	0[c]
rad-23(ok2595)	ERAD	0[a]	6[b]	40[b]	6[b]

a, b : n>100 scored for each gene

c : n>70 counted for each gene

3.3.3 rad-23 encodes the sole RAD23 orthologue in C. elegans

RAD23 is a member of the highly conserved Radiation sensitivity 23 family involved in transferring ubiquitinated proteins to the proteasome for degradation. BLAST analysis revealed a sole homologue of Rad23 in *C. elegans* (Figure 3.3). Worm RAD-23 is a 372 amino acid protein, sharing the same characteristic domain structure with mouse and human HR23A/hHR23A and HR23B/hHR23B, along with 36% overall sequence homology(Figure 3.3, and Figure 1.4). RAD-23 consists of two ubiquitin associated (UBA) domains, a single ubiquitin-like (UBL) domain and the xeroderma pigmentosum complementation group C binding (XPC) domain (Figure 3.3A). *rad-23(tm2595)* is a deletion/insertion mutation that results in the removal of both the UBA and XPC binding domains (exon2 and exon3), and is predicted to produce a small truncated protein (96 amino acid)(Figure 3.4) (Hannes and Vermeulen, 2011).

3.3.4 RAD-23 expression pattern

To further characterize *rad-23* a transcriptional fusion construct was prepared consisting of 1300 bp upstream promoter region that was sufficient to rescue DVB defects in *rad-23(tm2595)* mutants (Figure 3.4). The *rad-23* promoter was fused to red fluorescent protein (RFP) to generate *Prad-23::RFP* which was injected into wild type animals. Analysis of transcriptional fusion constructs confirmed a ubiquitous expression of *rad-23* in L3, L4 and adults similar to *png-1* promoter expression, where

RFP expression was observed in body wall muscles, vulva cells, as well as neurons (Figure 3.5).

The translational RFP fusion construct, *Prad-23::RAD-23::RFP* was also prepared to determine RAD-23 expression and localization. We were able to get rescue with this construct at very low concentration (1µg/mL), however we could not detect RFP fluorescence in the transgenic animals. Overexpression analysis also failed as it caused lethality in the animals.

3.3.5 rad-23 interacts with png-1 in a common genetic pathway

The findings that *png-1* and *rad-23* mutants share similar AVL and DVB phenotypes suggested that they may act in the same genetic pathway. If indeed they are components of a common pathway we would not expect to see an enhancement in their associated defects. Therefore we made *png-1;rad-23* double mutants and examined them for genetic interactions. The penetrance of AVL branching defects did not significantly differ in the *png-1(cy9);rad-23(tm2595)* double mutants(23%; *n*) (Figure 3.6 A-C) compared with the *png-1(cy9)* single (25%) mutant. Similarly, the penetrance of DVB defects in the *png-1(cy9);rad-23(tm2595)* doubles were not significantly different from the *png-1 (cy9)* (36% overextension, and 10% branching) and *rad-23(tm2595)* (40% overextension and 6% branching) single mutants (Figure 3.7). Similar results were observed in the doubles with *png-1(ok1654)* worms also. DVB overextension and branching defects in *rad-23 (-/-)* worms were rescued with a genomic fragment,

containing the promoter and coding sequence of r*ad-23* gene from 40% and 6% to 23% and 3%, respectively (Figure 3.7). These results indicate that *rad-23* and *png-1* act in the same genetic pathway to prevent AVL and DVB motorneurons from branching or overextending at the vulva.

3.3.6 png-1 mutants are not sensitive to ER stress

Impairment of protein folding in the ER leads to accumulation of misfolded proteins which in turn impair ER assisted proteasomal degradation activity. The UPR has been studied widely for its protective role following accumulation of misfolded proteins using pharmacological compounds that induce ER stress (Schroder and Kaufman, 2005). To assess if VC4-5 branching is due to signalling through UPR we treated *ire-1(ok799), pek-1(ok275),* and *png1(cy9)* with various concentrations of tunicamycin and monitored their survival and development (Figure 3.8). Tunicamycin is a natural compound which inhibits N-linked glycosylation in proteins and induces ER stress due to accumulation of misfolded proteins.

Previous studies in *C. elegans* reported increased sensitivities of *ire-1* and *pek-1* mutants to elevated ER stress (Shen et al., 2001). *ire-1* mutants were reported to arrest at or prior to larval stage L3 under ER stress conditions (Shen et al., 2001). Therefore, it was no surprise when we noted similar hypersensitivity in tunicamycin treated *ire-1(ok799)* (Figure 3.8). At low tunicamycin concentration (2.5 μg/ml), the majority of wild type animals were sensitive to ER stress and arrested during development (79%

arrested at or prior to L3 stage, while 11% were dead). At a similar concentration, only 9% of *ire-1(ok799)* and 22% of *pek (ok275)* mutants matured into adults. An overwhelming majority of these two mutants arrested at higher concentrations (5 and 7.5 μg/ml).

Notably, *png-1(cy9),* displayed an unusual resistance to ER stress. 21% of *png-1* mutants were not able to develop past L3 stage, while more than 78% matured into adults at low concentration (2.5 μg/ml). ER stress resistance in *png-1* mutants was also observed at higher concentrations of 5 and 7.5 μg/ml; 21% and 12% of *png-1* mutants matured into adulthood, respectively.

Furthermore, analysis of VC4-5 in worms that survived to adulthood did not exhibit significant changes in branching morphology. Our results confirm previous reports of hypersensitivity of *ire-1* and *pek-1* mutants to ER stress (Shen et al, 2001), but do not indicate a strong role for PNG-1 in proteasome-dependant pathways. Loss of PNG-1 activity appears to be protective in ER stress, which could indicate a mechanism of PNG-1 activity independent of ERAD.

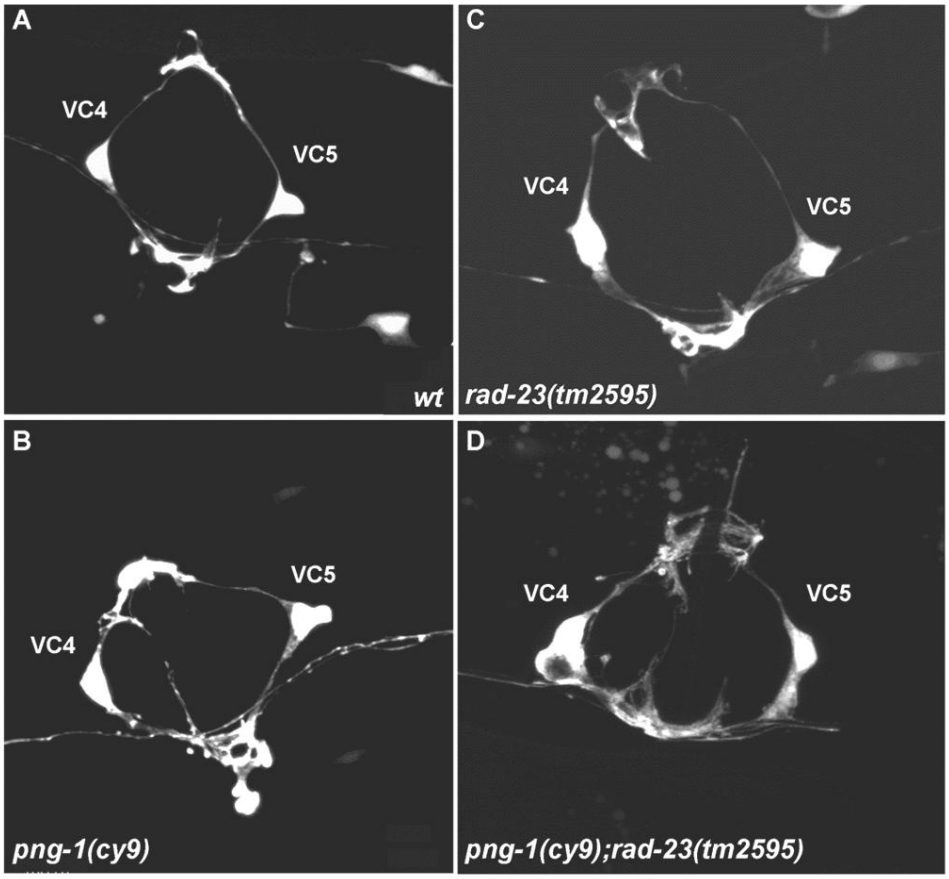

Figure 3.1 *rad-23* mutants display normal VC4-5 branching phenotype

VC4-5 neurons were visualized using *cyIs4* [(*Pcat-1::GFP*)] neuronal reporter. **A)** VC4-5 in adult wild type and **(B)** *png-1(cy9)* mutant animals. **(C)** *rad-23(tm2595)* mutants display wild type like branching morphology. **(D)** VC4-5 branching in *png-1(cy9); rad-23(tm2595)* is not enhanced, but is similar to *png-1* mutants.

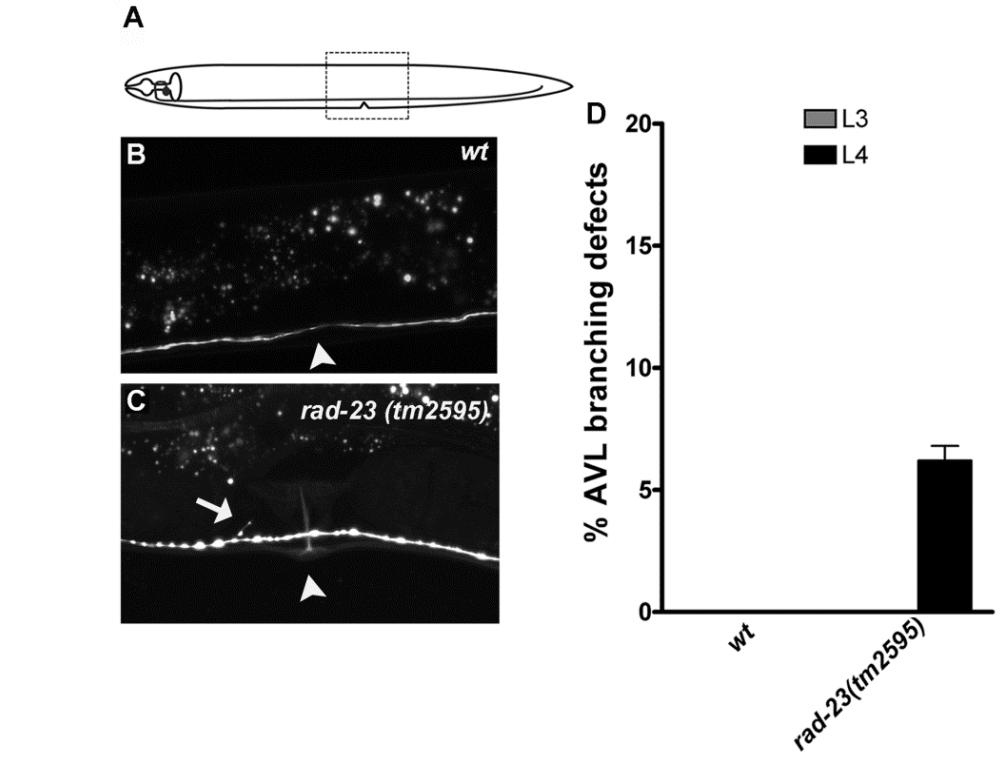
A
B
wt
C
rad-23 (tm2595)
D
L3
L4
% AVL branching defects
20
15
10
5
0
wt
rad-23(tm2595)

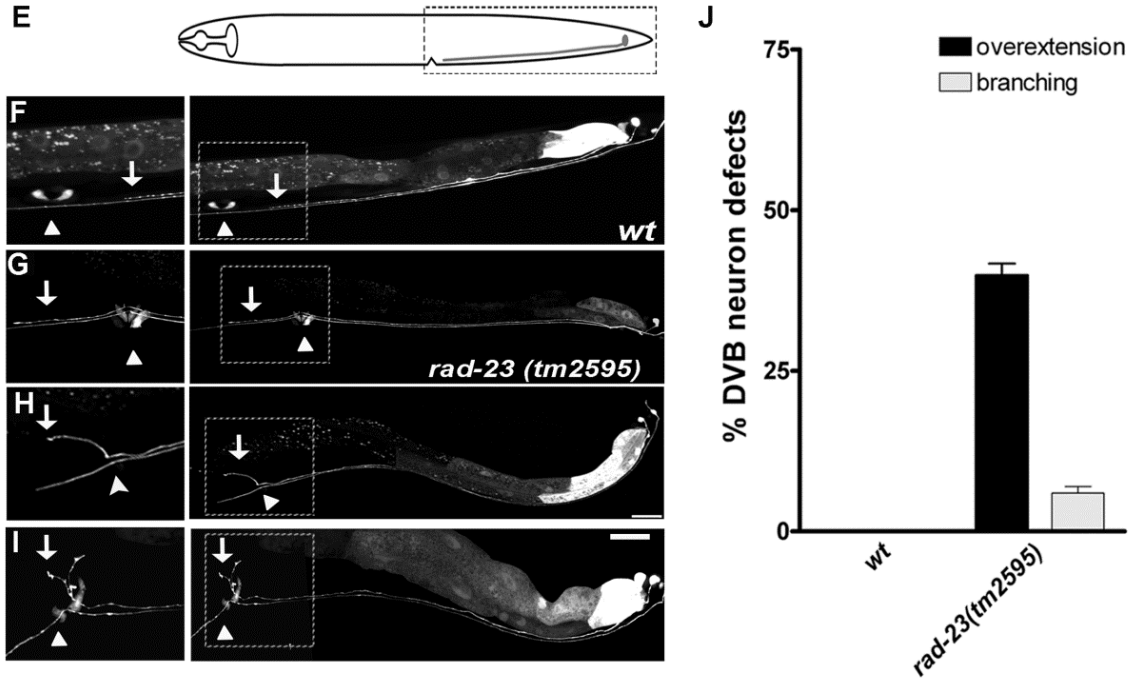
E
F
wt
G
rad-23 (tm2595)
H
I
J
overextension
branching
% DVB neuron defects
75
50
25
0
wt
rad-23(tm2595)

Figure 3.2 AVL and DVB defects in *rad-23* mutants

(A) Schematic diagram of the AVL motorneuron in a wild type hermaphrodite with the imaged area boxed. AVL motorneuron is visualized in *Punc-25::GFP;unc-30(e191)* background. **(B)** In wild type AVL extends an unbranched axon to the tail. **(C, D)** Branching is only observed in mid-to-late L4 stages in the vulva region, but not before vulva organogenesis at L3 stage. **(E)** Schematic diagram of the DVB motorneuron in a wild type hermaphrodite with the image site boxed. DVB is visualized with the *otIs92* [*Pflp-10::GFP*] reporter transgene. **(F)** In wild type animals DVB cell body is located at the tail, with an axon extended anteriorly toward the head, terminating near the vulva. **(G)** Mutant *rad-23(tm2595)* display DVB overextension defects where the DVB overextends past its termination point and grows past the vulva either anteriorly **(G)**, or dorsally **(H)**. **(I)** DVB motorneuron exhibits branching defects at the distal tip adjacent to the vulva. Arrow head depicts location of the vulva, arrow points to AVL and DVB branching and overextension defects. Scale bar, 20μm.

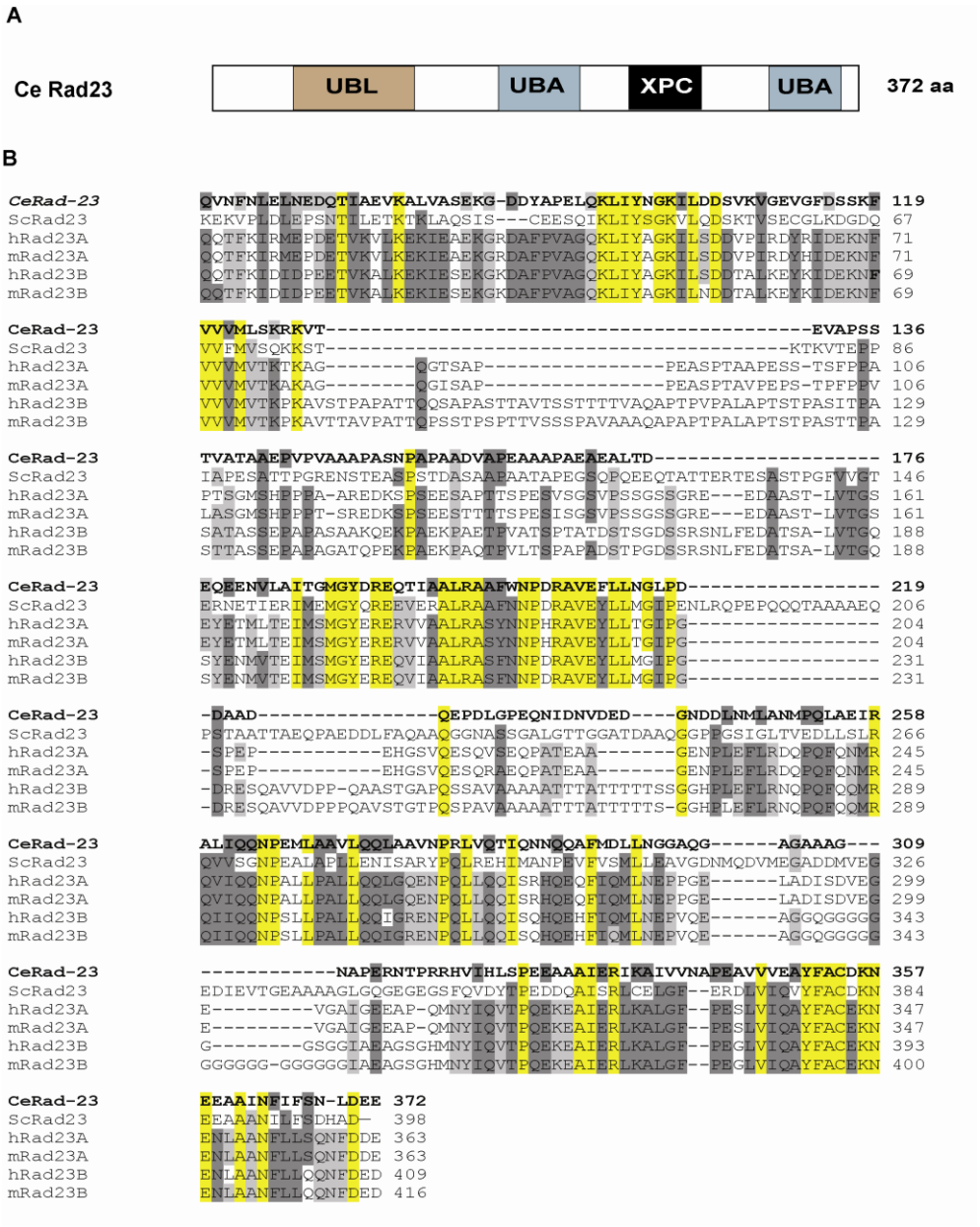
A
Ce Rad23
UBL
UBA
XPC
UBA
372 aa
B
CeRad-23 QVNFNLELNEDQTIAEVKALVASEKG-DDYAPELQKLIYNGKILDDSVKVGEVGFDSSKF 119
ScRad23 KEKVPLDLEPSNTILETKTKLAQSIS---CEESQIKLIYSGKVLQDSKTVSECGLKDGDQ 67
hRad23A QQTFKIRMEPDETVKVLKEKIEAEKGRDAFPVAGQKLIYAGKILSDDVPIRDYRIDEKNF 71
mRad23A QQTFKIRMEPDETVKVLKEKIEAEKGRDAFPVAGQKLIYAGKILSDDVPIRDYHIDEKNF 71
hRad23B QQTFKLDIDPEETVKALKEKIESEKGKDAFPVAGQKLIYAGKILSDDTALKEYKIDEKNF 69
mRad23B QQTFKLDIDPEETVKALKEKIESEKGKDAFPVAGQKLIYAGKILNDDTALKEYKIDEKNF 69
CeRad-23 VVVMLSKRKVT----------EVAPSS 136
ScRad23 VVFMVSQKKST----------KTKVTEPP 86
hRad23A VVVMVTKTKAG---------QGTSAP----------PEASPTAAPESS-TSFPPA 106
mRad23A VVVMVTKAKAG---------QGISAP----------PEASPTAVPEPS-TPFPPV 106
hRad23B VVVMVTKPKAVSTPAPATTQQSAPASTTAVTSSTTTTVAQAPTPVPALAPTSTPASITPA 129
mRad23B VVVMVTKPKAVTTAVPATTQPSSTPSPTTVSSSPAVAAAQAPAPTPALAPTSTPASTTPA 129
CeRad-23 TVATAAEPVPVAAAPASNPAPAADVAPEAAAPAEAEALTD---------- 176
ScRad23 IAPESATTPGRENSTEASPSTDASAAPAATAPEGSQPQEEQTATTERTESASTPGFVVGT 146
hRad23A PTSGMSHPPPA-AREDKSPSEESAPTTSPESVSGSVPSSGSSGRE---EDAAST-LVTGS 161
mRad23A LASGMSHPPPT-SREDKSPSEESTTTTSPESISGSVPSSGSSGRE---EDAAST-LVTGS 161
hRad23B SATASSEPAPASAAKQEKPAEKPAETPVATSPTATDSTSGDSSRSNLFEDATSA-LVTGQ 188
mRad23B STTASSEPAPAGATQPEKPAEKPAQTPVLTSPAPADSTPGDSSRSNLFEDATSA-LVTGQ 188
CeRad-23 EQEENVLAITGMGYDREQTIAALRAAFWNPDRAVEFLLNGLPD---------- 219
ScRad23 ERNETIERIMEMGYQREEVERALRAAFNNPDRAVEYLLMGIPENLRQPEPQQQTAAAAEQ 206
hRad23A EYETMLTEIMSMGYERERVVAALRASYNNPHRAVEYLLTGIPG---------- 204
mRad23A EYETMLTEIMSMGYERERVVAALRASYNNPHRAVEYLLTGIPG---------- 204
hRad23B SYENMVTEIMSMGYEREQVIAALRASFNNPDRAVEYLLMGIPG---------- 231
mRad23B SYENMVTEIMSMGYEREQVIAALRASFNNPDRAVEYLLMGIPG---------- 231
CeRad-23 -DAAD----------QEPDLGPEQNIDNVDED----GNDDLNMLANMPQLAEIR 258
ScRad23 PSTAATTAEQPAEDDLFAQAAQGGNASSGALGTTGGATDAAQGGPPGSIGLTVEDLLSLR 266
hRad23A -SPEP----------EHGSVQESQVSEQPATEAA-------GENPLEFLRDQPQFQNMR 245
mRad23A -SPEP----------EHGSVQESQRAEQPATEAA-------GENPLEFLRDQPQFQNMR 245
hRad23B -DRESQAVVDPP-QAASTGAPQSSAVAAAAATTTATTTTTSSGGHPLEFLRNQPQFQQMR 289
mRad23B -DRESQAVVDPPPQAVSTGTPQSPAVAAAATTTATTTTTS-GGHPLEFLRNQPQFQQMR 289
CeRad-23 ALIQQNPEMLAAVLQQLAAVNPRLVQTIQNNQQAFMDLLNGGAQG------AGAAAG--- 309
ScRad23 QVVSGNPEALAPLLENISARYPQLREHIMANPEVFVSMLLEAVGDNMQDVMEGADDMVEG 326
hRad23A QVIQQNPALLPALLQQLGQENPQLLQQISRHQEQFIQMLNEPPGE------LADISDVEG 299
mRad23A QVIQQNPALLPALLQQLGQENPQLLQQISRHQEQFIQMLNEPPGE------LADISDVEG 299
hRad23B QIIQQNPSLLPALLQQIGRENPQLLQQISQHQEHFIQMLNEPVQE------AGGQGGGGG 343
mRad23B QIIQQNPSLLPALLQQIGRENPQLLQQISQHQEHFIQMLNEPVQE------AGGQGGGGG 343
CeRad-23 ----------NAPERNTPRRHVIHLSPEEAAAIERIKAIVVNAPEAVVVEAYFACDKN 357
ScRad23 EDIEVTGEAAAAGLGQGEGEGSFQVDYTPEDDQAISRLCELGF--ERDLVIQVYFACDKN 384
hRad23A E---------VGAIGEEAP-QMNYIQVTPQEKEAIERLKALGF--PESLVIQAYFACEKN 347
mRad23A E---------VGAIGEEAP-QMNYIQVTPQEKEAIERLKALGF--PESLVIQAYFACEKN 347
hRad23B G--------GSGGIAEAGSGHMNYIQVTPQEKEAIERLKALGF--PEGLVIQAYFACEKN 393
mRad23B GGGGGG-GGGGGGIAEAGSGHMNYIQVTPQEKEAIERLKALGF--PEGLVIQAYFACEKN 400
CeRad-23 EEAAINFIFSN-LDEE 372
ScRad23 EEAAANILFSDHAD- 398
hRad23A ENLAANFLLSQNFDDE 363
mRad23A ENLAANFLLSQNFDDE 363
hRad23B ENLAANFLLQQNFDED 409
mRad23B ENLAANFLLQQNFDED 416

Figure 3.3 *rad-23* encodes a highly conserved gene

(A) *rad-23* encodes a 372 aa protein consisting of a ubiquitin-like domain (UBL), two ubiquitin associated domains (UBAs), and a xeroderma pigmentosum complementation group C (XPC) binding domain. **(B)** Alignment of Rad23 homologues. Yellow shading indicates sequence identity. Sequence similarity indicated by dark grey shading. *C. elegans* (Ce, GeneBank no. CAA93780), *S. cerevisiae* (Sc, AAB28441), human (h, AAB5117, and AAH20973 for A and B isoforms), mouse (m, AAB45373A and AAH68193 for A and B isoforms). ClustalW alignment (version 6.0).

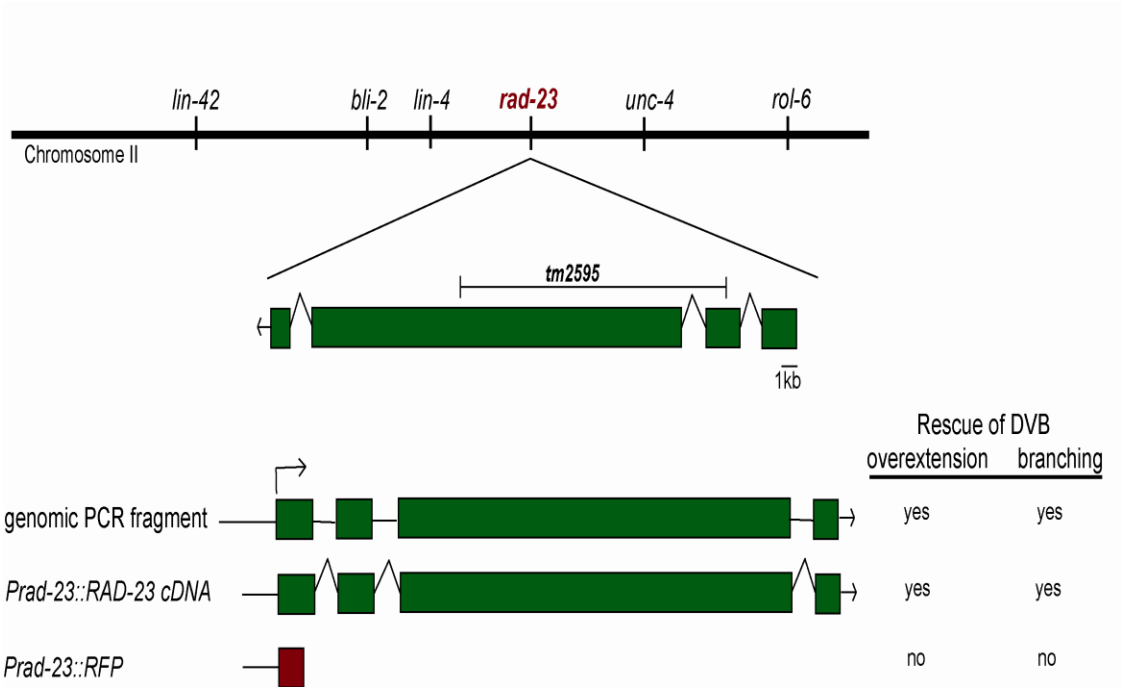

Figure 3.4 Positional cloning of *rad-23*

Genetic position of *rad-23* gene on chromosome II and its exon-intron structure with the position of the *tm2595* mutation shown. Genomic PCR fragment containing *rad-23* gene and plasmid construct containing *Prad-23::RAD-23* cDNA rescued DVB overextension and branching defects in mutant *rad-23(tm2595)*animals.

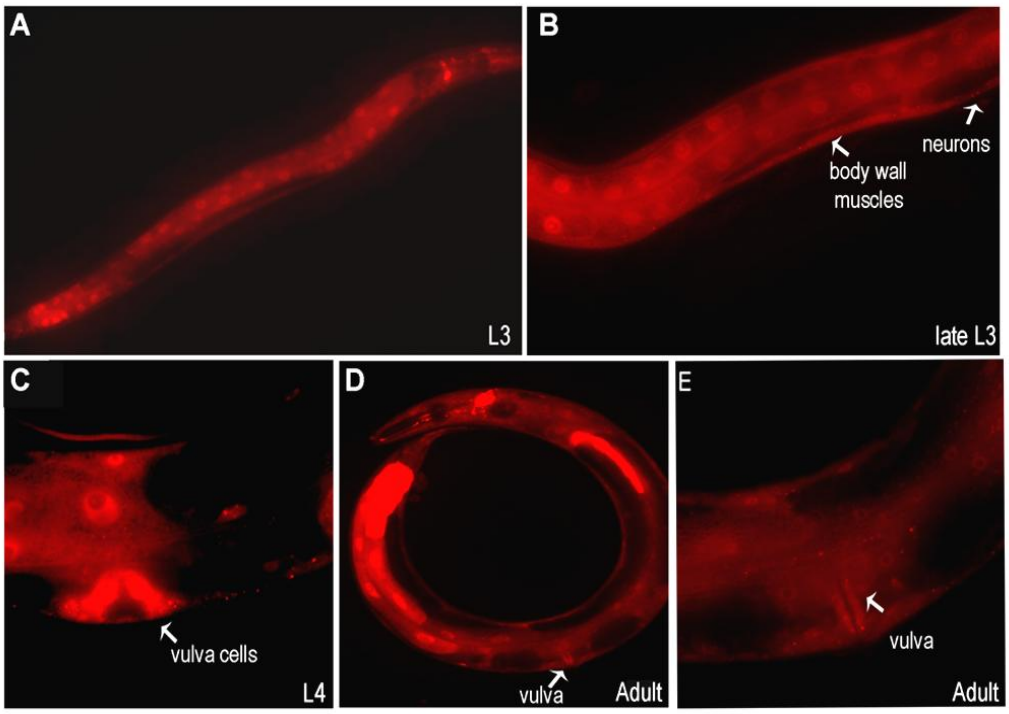

Figure 3.5 Expression of *Prad-23::RFP*

(A-E) *rad-23* promoter expression was observed in L3, L4, in **(B)** body wall muscles, neurons, **(C)** vulva cells, and the vulva **(D, E)**.

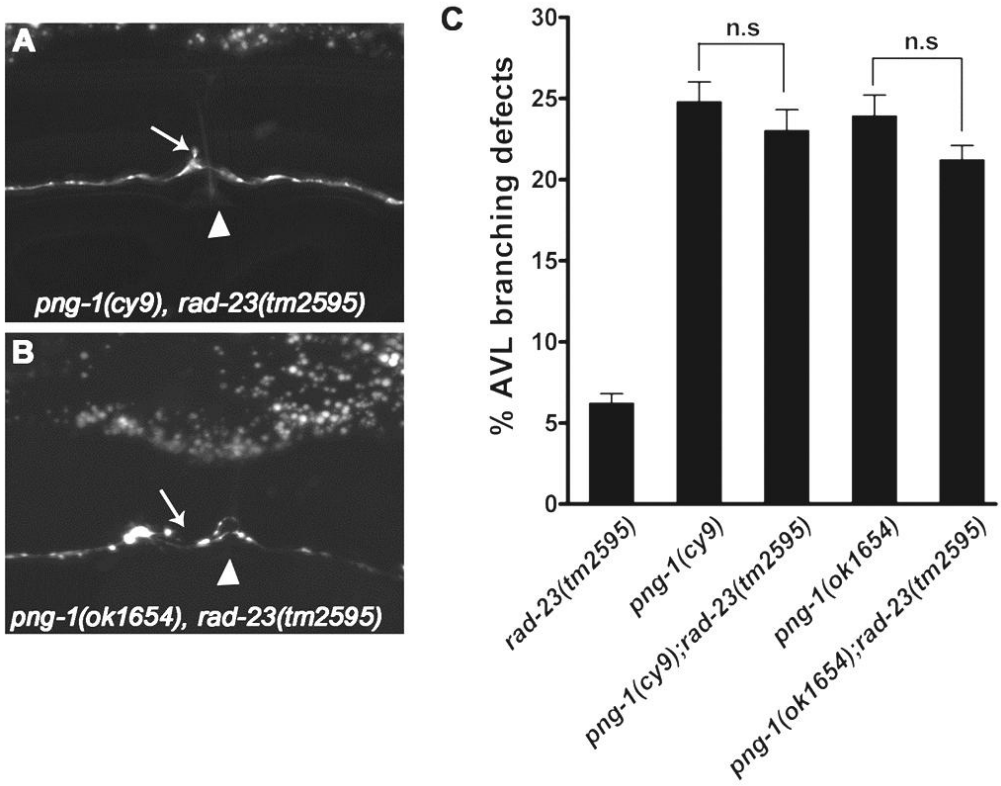

Figure 3.6 *png-1* and *rad-23* interact genetically in a common pathway to limit AVL motorneuron branching

---

(A, B) AVL motorneuron, visualized in *Punc-25::GFP;unc-30(e191)* background, displayed a single branch (arrow) at the vulva(arrow head) in *png-1* and *rad-23* double mutants. **(C)** Penetrance of AVL branching defects at the vulva do not differ significantly in *png-1* single and *png-1;rad-23* double mutants, indicating that these genes interact in the same genetic pathway to prevent ectopic AVL branching at the vulva. Error bars denote SEM of three independent counts (n=50, each).

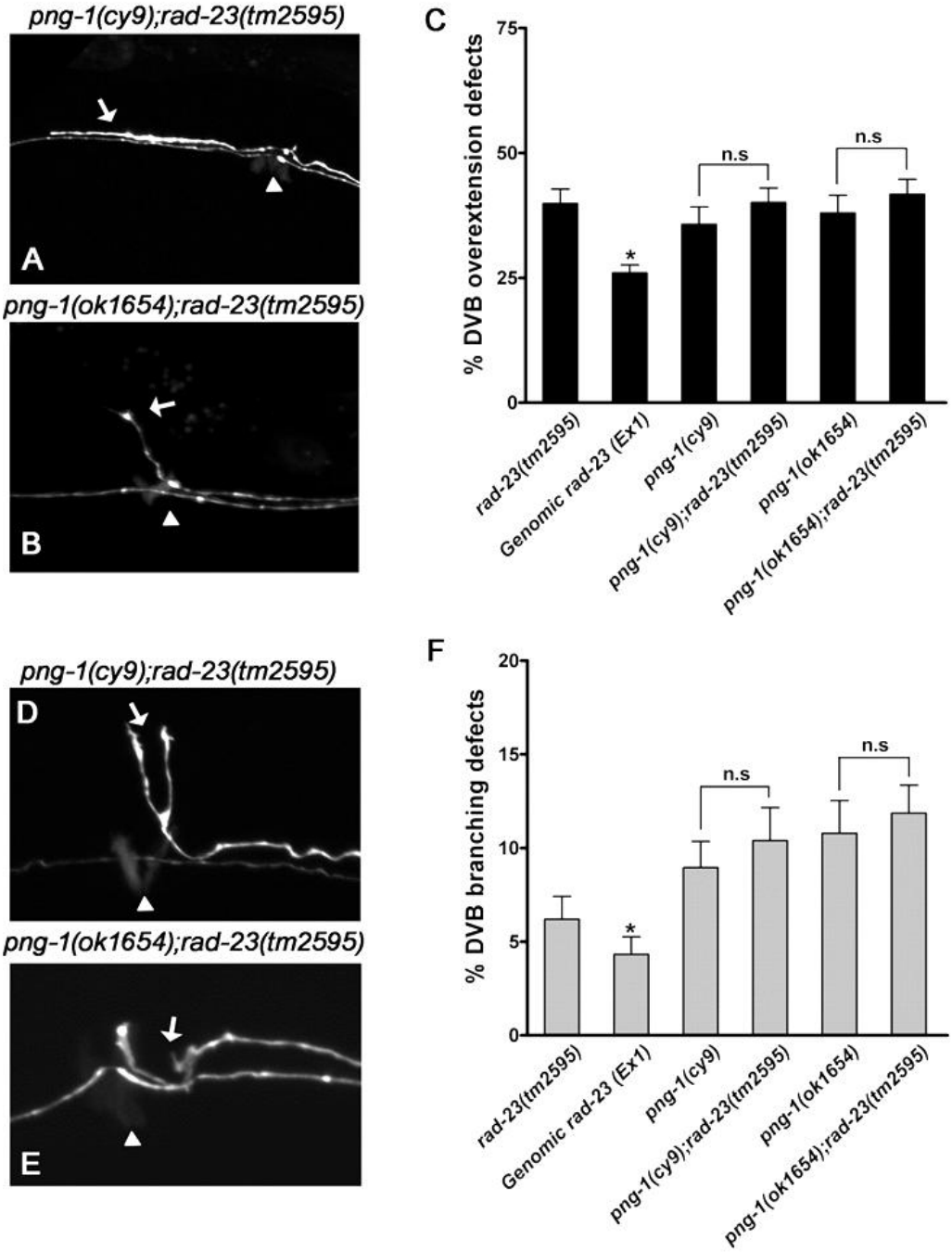
png-1(cy9);rad-23(tm2595)
A
png-1(ok1654);rad-23(tm2595)
B
C
% DVB overextension defects
75
50
25
0
n.s
n.s
*
rad-23(tm2595)
Genomic rad-23 (Ex1)
png-1(cy9)
png-1(cy9);rad-23(tm2595)
png-1(ok1654)
png-1(ok1654);rad-23(tm2595)
png-1(cy9);rad-23(tm2595)
D
png-1(ok1654);rad-23(tm2595)
E
F
% DVB branching defects
20
15
10
5
0
n.s
n.s
*
rad-23(tm2595)
Genomic rad-23 (Ex1)
png-1(cy9)
png-1(cy9);rad-23(tm2595)
png-1(ok1654)
png-1(ok1654);rad-23(tm2595)

Figure 3.7 *png-1* and *rad-23* interact genetically in a common pathway to limit DVB motorneuron overextension and branching

---

(A, B) DVB motorneuron, visualized in *otIs92 [Pflp-10::GFP]* background, displayed a neurite that failed to stop at its termination point and overextended (arrow) past the vulva (arrow head), either anteriorly **(A)**, or dorsally **(B)** in *png-1;rad-23* double mutants. **(C)** The penetrance of DVB overextension in the double mutants were not significantly different than in *png-1* single mutants indicating that these genes act in the same genetic pathway to limit DVB overextension. DVB overextension defects were reduced when a PCR fragment containing *rad-23's* endogenous promoter and coding region was injected in mutant *rad-23* worms. **(D, E)** A subset of overextended DVB motorneurons were also observed to display axon branching (arrow) at the distal tip of the axon at a region near the vulva (arrow head) in *png-1;rad-23* double mutants. **(F)** *rad-23* and *png-1* function in the same genetic pathway to limit DVB branching, also. The penetrance of DVB branching in double mutant worms was not significantly different than in *png-1* single mutants. Branching defects were also rescued in extrachromosomal transgenic animals carrying endogenous *rad-23* promoter and coding sequences. Error bars for *rad-23* genomic rescue denote SE of proportion, $*P< 0.05$, n=51. Error bars for all other data denote SEM of three independent counts (n=50, each). analysis was used to determine that double mutants do not significantly differ (ns) from single mutants.

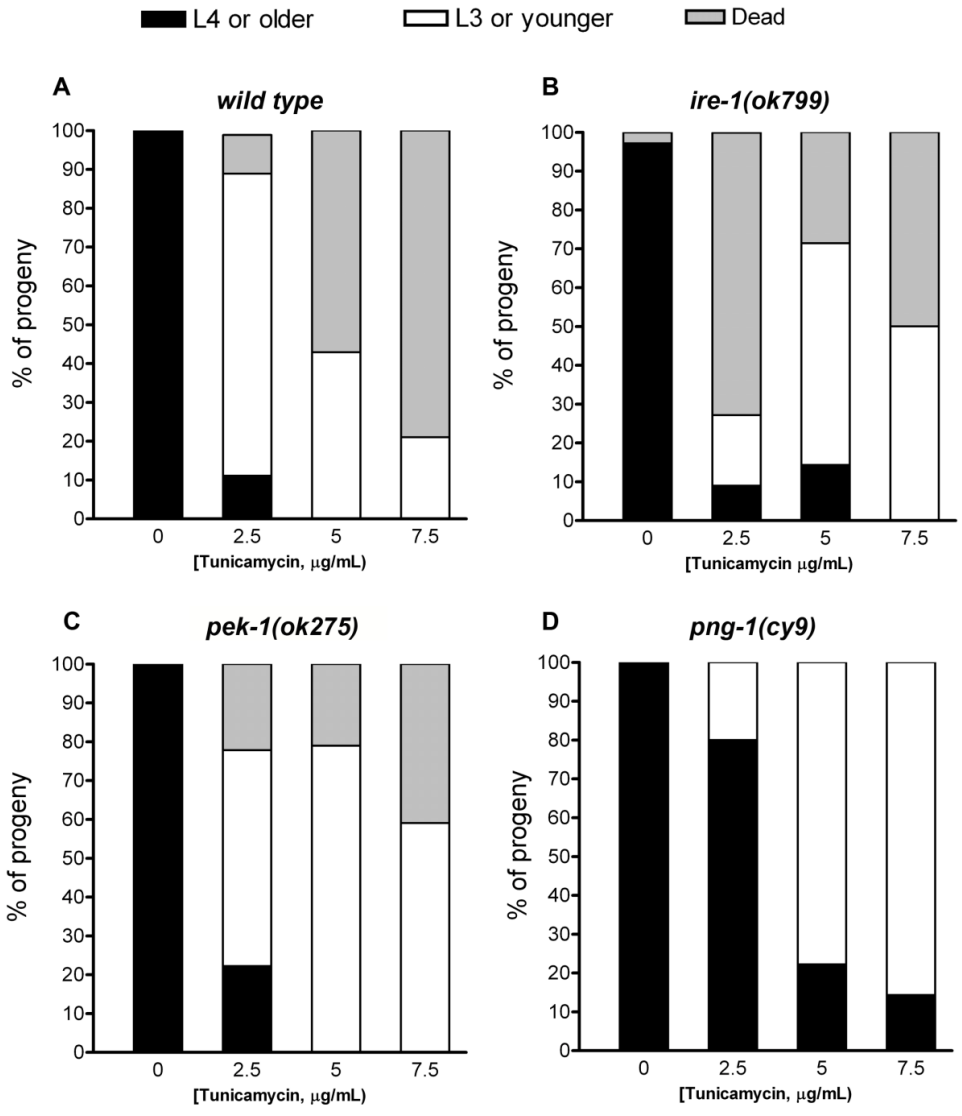
L4 or older
L3 or younger
Dead
A
wild type
B
ire-1(ok799)
C
pek-1(ok275)
D
png-1(cy9)
% of progeny
[Tunicamycin, μg/mL)
0
2.5
5
7.5

Figure 3.8 Quantitative analysis of *png-1(cy9)* sensitivity to ER stress

Each strain was allowed to lay eggs for four hours on plates containing different concentrations of tunicamycin. Progeny was examined 3 days later for survival and development. Progeny analysis was performed by grouping animals into three categories: worms that matured to L4 or older, worms that arrested at/or L3, and dead animals. Percentage progeny that were arrested at indicated stages of development or dead were plotted against the tunicamycin concentrations treated to. **(A)** *wild type*, **(B),** *ire-1(ok799),* **(C)**, *pek-1(ok275),* and **(D)**, *png-1 (cy9). png-1* mutants displayed significant resistance to ER stress.

3.3.7 A modifier screen identifies sax-2 as png-1 enhancer

PNG-1 is the first characterized cytoplasmic deglycosylating enzyme in *C. elegans* with conserved functional thioredoxin and transglutaminase domains (Suzuki et al., 2007; Habibi-Babadi et al., 2010). In addition to describing a novel role for *png-1* in neuronal development, our data suggests a function for PNG-1 independent of ERAD and UPR. Since *png-1* is required for limiting VC4-5 branching during vulva organogenesis, the molecule(s) that signals outgrowth and branching at the vulva would also be required for *png-1* dependent activity. To identify potential upstream and downstream effectors of *png-1*, I performed a genetic modifier screen. I searched for mutants that suppressed and mutants that enhanced *png-1(-/-)* VC 4-5 branching defects.

png-1(cy9);cyIs4 were mutagenized with EMS (Brenner, 1974) followed by a visual screen for nematodes displaying normal and enhanced VC4-5 branching morphologies. After screening approximately 8600 haploid genomes only one enhancer mutation, *(zy16)*, but no suppressors were identified (Figure 3.9). *zy16* mutants displayed strong enhancement of VC4-5 branching defects in *png-1* mutants. On their own, *zy16* mutants displayed mild ectopic VC4-5 branching defects (Figure 3.9). SNP mapping localized this gene to a genetic interval on chromosome III (data not shown). This region also included the sensory axon guidance-2 (*sax-2*) gene, which encodes a scaffolding protein that was previously characterized in *C. elegans* to play an important role, along with SAX-1, in neuronal development (Zallen et al, 1999, 2000). Mutant *sax-1*

and *sax-2* worms displayed neuronal cell shape defects, as well as axon outgrowth and neurite branching defects (Zallen et al., 1999, 2000; Gallegos and Bargmann, 2004).

Sax-1 belongs to a family of nuclear Db2-related (NDR) kinases, a subclass of evolutionarily conserved serine/threonine AGC group of protein kinases. Numerous genetic and biochemical studies describe a role for NDR kinases and their interacting scaffolding partners, in a variety of cellular processes such as regulation of cell growth and shape, neurite outgrowth, dendritic tiling as well as branching (Zallen et al., 1999, 2000; Gallegos and Bargmann, 2004; Emoto et al., 2004, 2006; Hergovich et al., 2006; He et al., 2005a, 2005b; Geng et al., 2000; Du and Novick, 2002; Jia and Emmons, 2006).

Interestingly, we did examine *sax-2(ot10),* a loss-of-function mutant, in our candidate gene screen for VC4-5 branching defects, previously (Table 3.1). s*ax-2(ot10);cyIs4* mutant worms did display cell shape defects in addition to ectopic branching defects similar to *png-1* mutants, although less penetrant. Thus the question was raised if *zy16* was a mutation in the *sax-2* gene. In collaboration with the laboratory of Dr. Maria Gallegos (California State University at East Bay), *zy16* was fully sequenced and confirmed to be a new allele of *sax-2*. *sax-2(zy16)* is loss-of-function mutation that introduces a stop codon at Q1329 which would be predicted to produce a truncated protein (Figure 3.10).

3.3.8 sax-1 and sax-2 mutants exhibit defective neuronal morphologies

We next examined if *sax-1* and *sax-2* mutants displayed VC4-5 and DVB defects similar to *png-1* mutants. *sax-1 (ky491)* is a candidate null with a 1.3 kb deletion mutation within the conserved kinase domain, while *sax-2(ot10)*, is a point mutation that introduces a stop at *Q809* that is predicted to lead to premature truncation (Figure 3.10) (Zallen 2000; Gallegos and Bargmann, 2004).

Homozygous *sax-1(ky491)* and *sax-2(ot10)* mutants were viable, and did not display abnormal morphology, development, motility, or egg-laying defects. In comparison to wild type, *sax-1(ky491)* and *sax-2(ot10)* mutants displayed 24% and 14% excessive branching defects, respectively (Table 3.3). *sax-1(ky491);sax-2(ot10)* double mutants did not show enhancement in VC4-5 branching (13% n=100), compared to *sax-1* and *sax-2* single mutants (Table 3.3). This suggests that *sax-1* and *sax-2* interact in a common genetic pathway to control neuronal branching.

Examination of DVB morphology in *sax-1(ky491),* and *sax-2(ot10)* as well as *sax-1(ky491); sax-2(ot10)* double mutants revealed no significant DVB overextension and branching defects (Table 3.3).

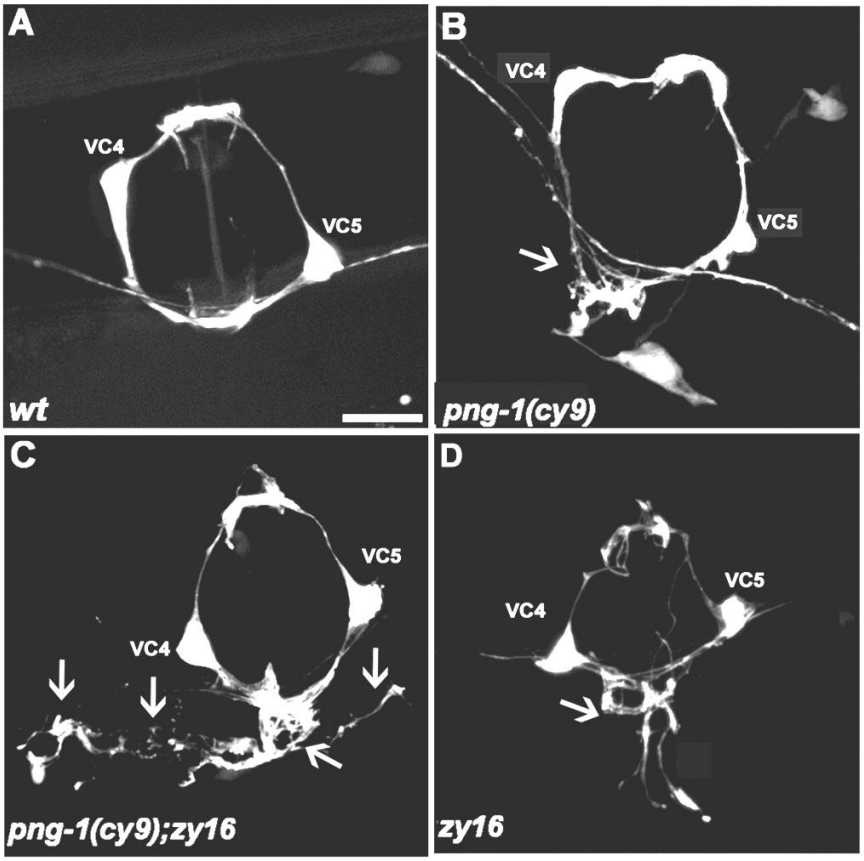

Figure 3.9 *zy16* enhances *png-1* mutant VC4-5 branching defects

(A) Wild type VC4-5 axon typically contain 3-5 branches on the left and right side of the vulva. **(B)** Excessive branching defects are observed in *png-1(cy9)* mutants, where the number of branch defects range between 6-20. **(C)** *png-1(cy9)* enhancer mutant *zy16* displays an increase in the number and complexity of VC4-5 branches in comparison to *png-1* single mutant. **(D)** *zy16* mutants display mild branching defects as well as cell shape defects. Arrow points toward neuronal defects. Ventral view, scale bar, 10μm.

Table 3.3 Phenotypic analysis of *sax-1* and *sax-2* mutants

Gene/strain	% Neuronal Defects			N
	VC4-5	DVB overextension	DVB branching	
wild type	0	0[b]	0[b]	100
sax-1(ky491)	24[a] ± 3	0[b]	0[b]	100
sax-2(ot10)	14[a] ± 2	0[b]	0[b]	100
sax-1(ky491);sax-2(ot10)	13[a] ± 2	0[b]	0[b]	100

[a] Young adult worms were scored for VC4-5 branching defects using the *cyIs4(Pcat-1::GFP]* transgene. Axon branching defects were scored if mutants displayed 6-20 branch defects on either the left or right sides of the vulva. Values represent the mean ± SEM of four independent counts (n=25, each).

[b] Young adult worms were scored for DVB axon outgrowth and branching defects using the *otI92[Pflp-10::GFP]* transgene. Defects were scored if DVB failed to terminate at its regular termination site, and extended past the vulva either dorsally or anteriorly. DVB branching defects were scored if ectopic branch(s) were observed at the distal tip of the axon. Values represent the mean ± SEM of four independent counts (n=25, each).

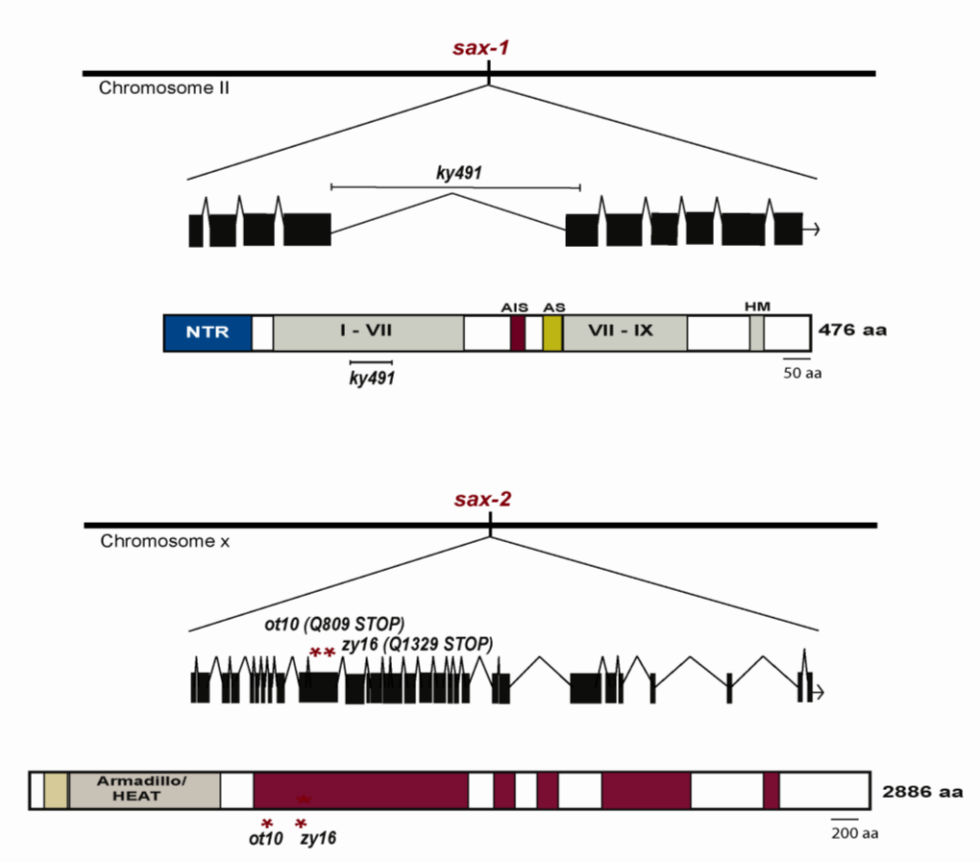

Figure 3.10 *sax-1* and *sax-1* genomic and protein structure

Domain structure of SAX-1 consists of and N-terminal regulatory domain (NTR), a core kinase domain (subdomains I-IX), a putative auto-inhibitory sequence (AIS), an activation segment (AS), and a C-terminal hydrophobic motif (HM). *sax-1 (ky491)* is a candidate null allele with a 1.3kb deletion mutation within the kinase domain. *sax-2* encodes a large scaffolding proteins with N-terminal Armadillo/HEAT repeats and several unknowns domains. O*t10* and *zy16* are both point mutations that are predicted to lead to premature truncation. Genomic structure indicated by lines and boxes (exons). Location of mutations is indicated by asterisks and lines.

3.3.9 sax-1 interacts genetically with png-1

sax-2(zy16) was recovered from a genetic screen where it enhanced VC4-5 branching defects in *png-1(cy9)* mutants. Similarity of neuronal phenotypes in *sax-1(ky491)* and *sax-2(ot10)* mutants prompted us to ask whether mutation in *sax-1* can also enhance VC4-5 branching defects in *png-1* mutants. Additionally, we wanted to know if DVB defects were similarly enhanced in *sax-2;png-1* double mutants. We generated *png-1; sax-2* and *png-1; sax-1* double mutants and examined their VC4-5 and DVB neuronal morphologies. Analysis of VC4-5 branching phenotype in the double mutants was challenging as these mutants displayed a more severe and complex form of branching compared to single mutants that are characterized with excessive branching defect consisting of 6-20 ectopic branches. In the double mutants we commonly saw >20 ectopic VC4-5 branches which prompted us to establish a third branching defect category: if the total number of ectopic branches exceeded 20, the phenotype was described as a "severe" branching defects (Figure 3.11).

Branch examination in both *png-1;sax-1* and *png-1;sax-2* double mutants revealed a synergistic enhancement of VC4-5 branching (Figure 3.12). More than 65% of *png-1;sax-1* worms displayed severe branching defects, and 33% displayed excessive branching defects. Similarly, approximately 46% and 44% of *png-1;sax-2* double mutants displayed severe and excessive axon branching defects respectively. Transgenic lines carrying a PNG-1 transgene displayed a significant reduction in the severe branching,

such that only 8% of *png-1;sax-1*, and 11% of *png-1;sax-21* mutant worms displayed severe branching defects (Figure 3.12).

sax-1(ky491) and *sax-2(ot10)* single mutants did not display DVB overextension or branching defects, however examining DVB morphology in *png-1; sax-1* and *png-1; sax-2* double mutants revealed a significant increase in DVB defects in these worms. More than 81% of *png-1;sax-1* double mutant displayed DVB overextension defects, compared to 36-39% in *png-1* mutants, and 0% in *sax-1(ky491)* single mutants. *png-1;sax-1* and *png-1;sax-2* doubles also displayed enhanced branching in an area adjacent to the vulva, >30% and >47% respectively (Figure 3.13). Our data suggests that *sax-1* and *sax-2* act in a parallel pathway with *png-1* to limit VC4-5 and DVB outgrowth and branching at the vulva.

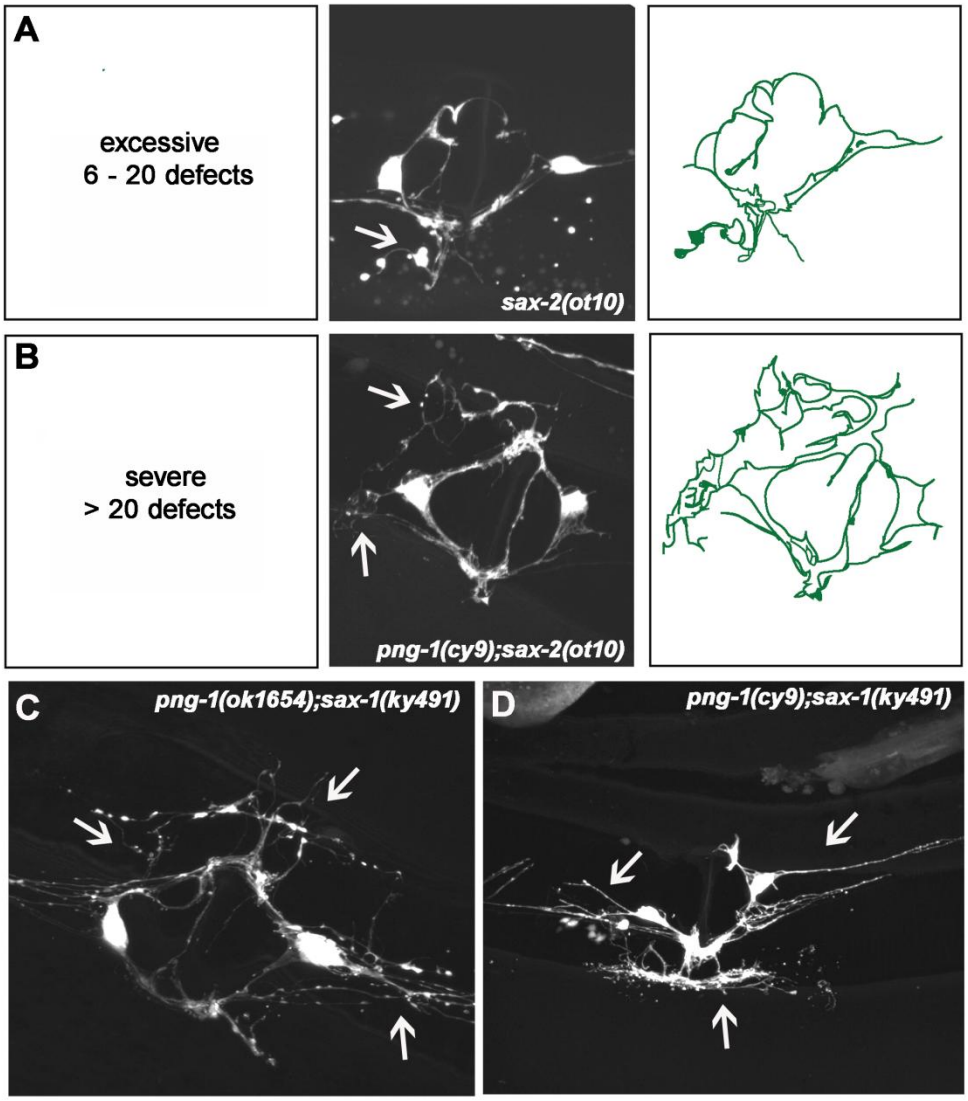
A
excessive
6 - 20 defects
sax-2(ot10)
B
severe
> 20 defects
png-1(cy9);sax-2(ot10)
C
png-1(ok1654);sax-1(ky491)
D
png-1(cy9);sax-1(ky491)

Figure 3.11 *png-1* branching defects are enhanced with *sax-1* and *sax-2*

VC4-5 branching complexity and number is enhanced in *png-1;sax-1* and *png-1;sax-2* double mutants compared to single mutants. **(A)** *png-1, sax-1,* and *sax-2* single mutants display excessive branching, where the number of branch defects observed varies between 5-20. **(B)** Branching defects in *png-1;sax-1* and *png-1;sax-2* double mutants are more severe in comparison to single mutants, where we observe more than 20 ectopic branching defects. Arrows mark branching defects. All images, ventral view of VC4-5, anterior to the left.

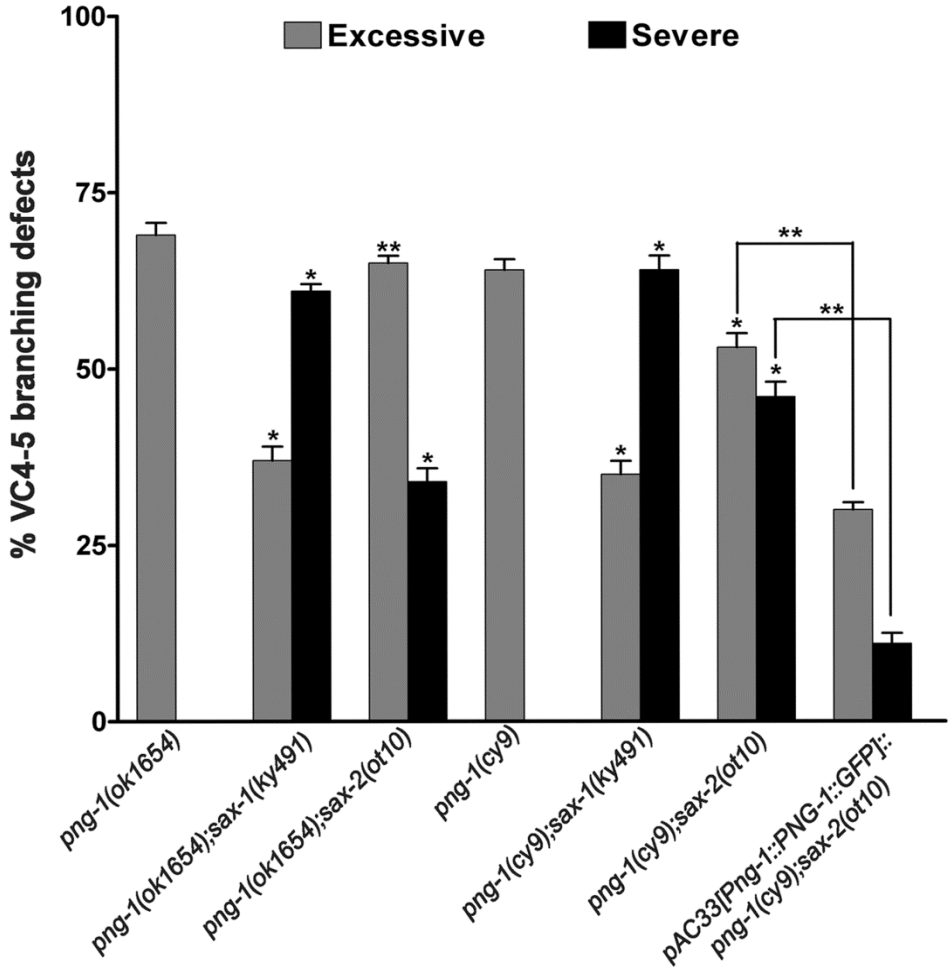
Excessive
Severe
% VC4-5 branching defects
100
75
50
25
0
*
**
png-1(ok1654)
png-1(ok1654);sax-1(ky491)
png-1(ok1654);sax-2(ot10)
png-1(cy9)
png-1(cy9);sax-1(ky491)
png-1(cy9);sax-2(ot10)
pAC33[Png-1::PNG-1::GFP]::
png-1(cy9);sax-2(ot10)

Figure 3.12 Quantitative analysis of VC4-5 branch enhancement

In comparison to single mutant *png-1*, double mutant *png-1;sax-1* and *png-1;sax-2* displayed significant enhancement of branching defects. Error bars represent SEM of four independent counts (=25, each). *$P< 0.05$, and **$P<0.01$ compared to *png-1* single mutant using one-way analysis of variance Bonferroni's multiple comparison test. Error bars for pAC33 extrachromosomal transgenic line denote SE of proportion (n>75), **$P< 0.01$, compared to *png-1(cy9);sax-2(ot10)* using analysis of variance and Bonferroni's multiple comparison post hoc test.

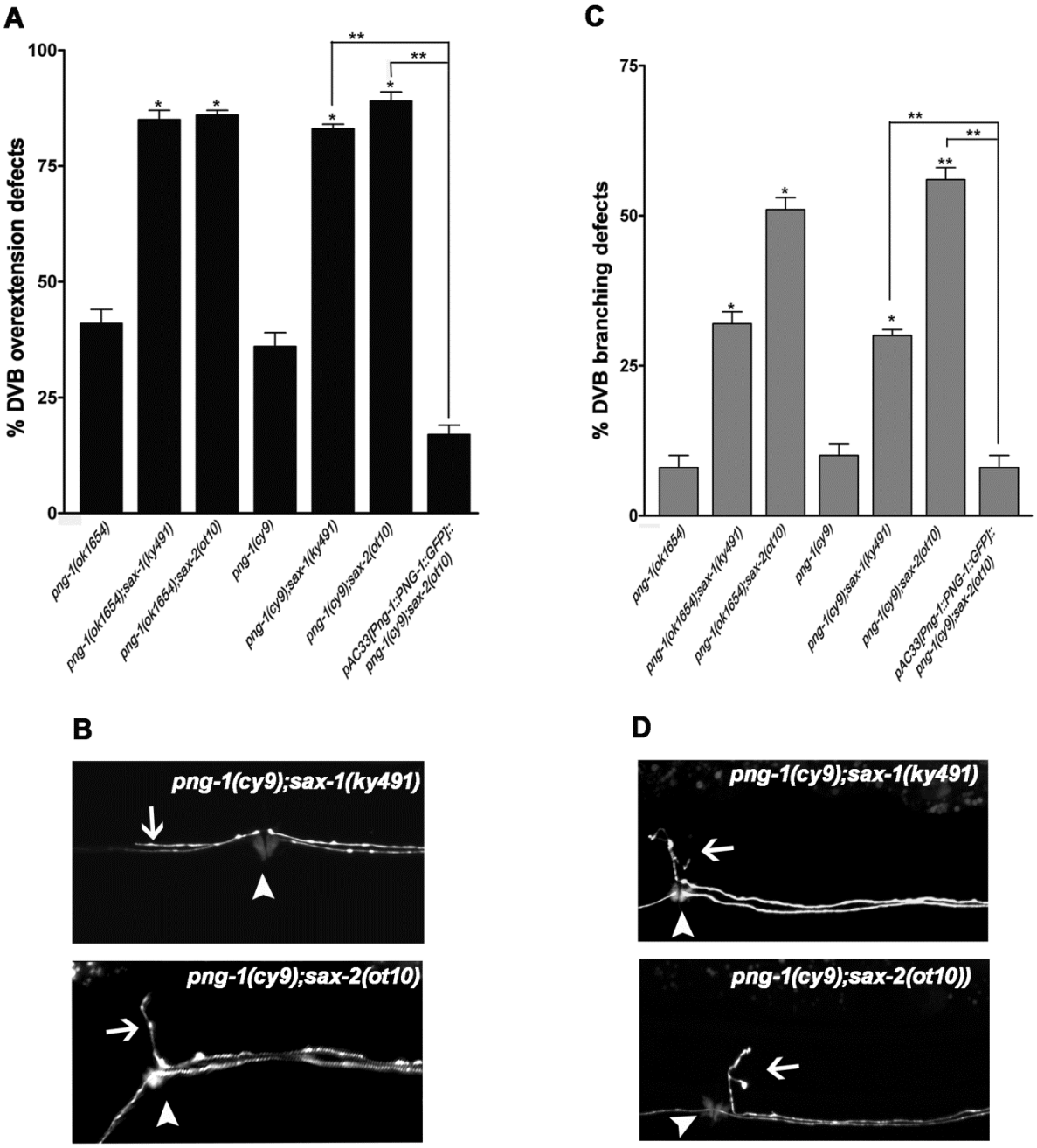
A
% DVB overextension defects
100
75
50
25
0
png-1(ok1654)
png-1(ok1654);sax-1(ky491)
png-1(ok1654);sax-2(ot10)
png-1(cy9)
png-1(cy9);sax-1(ky491)
png-1(cy9);sax-2(ot10)
pAC33[Png-1::PNG-1::GFP];
png-1(cy9);sax-2(ot10)
C
% DVB branching defects
75
50
25
0
B
png-1(cy9);sax-1(ky491)
png-1(cy9);sax-2(ot10)
D
png-1(cy9);sax-1(ky491)
png-1(cy9);sax-2(ot10))

Figure 3.13 *sax-1* and *sax-2* act in parallel to *png-1* in to limit DVB overgrowth and branching

---

DVB motorneuron defects are significantly enhanced in the double mutants *png-1:sax-1 and png-1:sax-2.* **(A)** DVB overextension defects were significantly increased in the double mutants *png-1;sax-1* and *png-1;sax-2* in comparison to *png-1* single mutants **(B)** In the double mutants, DVB overextends past its termination point and extends past the vulva, either dorsally or anteriorly. **(C)** DVB branching defects were also significantly higher in the double mutants in comparison to *png-1 (-/-)* animals**. (B, D)**Arrow head indicate location of the vulva, arrows indicate DVB defects. Error bars denote SEM of four independent counts (n=25, each). *$P< 0.05$ compared to *png-1* single mutant using one-way analysis of variance Bonferroni's multiple comparison test. Error bars for pAC33 extrachromosomal transgenic line denote SE of proportion (n>80), **$P< 0.01$, compared to *png-1(cy9);sax-2(ot10)* using analysis of variance and Bonferroni's multiple comparison post hoc test.

3.4 DISCUSSION

Formation of neuronal circuits is largely influenced by axon branching, but the mechanisms that regulate this process remain unknown. A genetic screen for branching abnormal genes in the egg-laying circuitry in *C. elegans* identified *png-1* to play a crucial role in the outgrowth and branching of VC4-5 during vulva organogenesis. PNG-1 is a highly conserved cytoplasmic PNGase that catalyzes the removal of N-linked sugar moieties from glycoproteins and glycopeptides prior to degradation by the proteasome (Suzuki et al., 2001). Cytoplasmic PNGases in yeast and mammals have been implicated in endoplasmic reticulum associated degradation (ERAD), a multi-step cellular process that identifies and retrotranslocates misfolded aberrant proteins from the ER to the cytosol where they are ubiquitylated prior to degradation by the proteasome (Suzuki et al., 2001-2007; Park et al., 2001; Hirsch et al., 2003; Blom et al., 2004). Yeast and mammalian PNG-1 orthologues bind indirectly to the proteasome via their interaction with multiple components of ERAD, such as Rad23 and Derlin-1.

Mutation in the *C. elegans* PNGase, *png-1*, resulted in abnormal outgrowth and branching of neurons at locations near or adjacent to the vulva, a known source for branch inducing signals (Li and Chalife, 1999). This has prompted us to ask whether *png-1* acts through a proteasome-dependent pathway to regulate branching at the vulva. To answer this question we employed a candidate gene approach analyzing neuronal morphology in mutants that disrupt highly conserved components of the unfolded

protein response (UPR) and ERAD. The worm homologues of several conserved UPR pathway components such as Ire1, Pek1/Perk (Shen et al., 2001), and Hrd1/Der3 (Sasagawa et al., 2007) have recently been shown to function in the cellular responses to ER stress in *C. elegans*. Inactivation of these genes by mutation or RNAi depletion triggers the widespread expression of a UPR inducible *Phsp-4::GFP* reporter indicative of elevated levels of ER stress throughout the animal (Calfon et al., 2002; Sasagawa et al., 2007). ERAD components such as *hrd-1* (Carvalho et al., 2010), *Derlin-1* (Katiyar et al, 2005), *rpn-10* (Elsasser et al., 2004), and *rad-23* (Suzuki et al., 2002-07) have also been reported to facilitate protein ubiquitylation, retrotranslocation and degradation. With the exception of *rad-23* and *ire-1*, mutations in *pek-1, hrd-1, cup-2, and rpn-10* displayed wild type VC4-5 and DVB morphology.

rad-23 mutants displayed neuronal defects similar to *png-1 (-/-)* animals. RAD-23, the only Rad23 homologue in *C. elegans,* is a member of the Radiation sensitivity 23 family of proteins that function in nucleotide excision repair (NER) and in the transport of ubiquitylated substrates to the proteasome (Suzuki et al., 2001, 2005). In *C. elegans*, r*ad-23* encodes a protein comprised of an N-terminal ubiquitin-like domain and two ubiquitin associated domains flanking an XPC binding domain. The role of *rad-23* in *C. elegans* NER or ERAD is not well defined. As in mammals, NER in *C. elegans* removes helix-distorting DNA lesions caused by UV irradiation that can interfere with transcription and replication (Lans and Vermeulen et al., 2011). Interaction of *rad-23* and

xpa-1 has been reported to be critical in the response to UV damage during development (Lans and Vermeulen et al., 2011). Mammalian Rad23 has been reported to form a complex with Rad4/XPC through the XPC binding domain specifically.

Here we describe for the first time a previously unknown role for *rad-23* in regulating axon outgrowth and branching during development. *rad-23 (-/-)* animals displayed axon branching in the AVL and DVB neurons and DVB overextension similar to *png-1* mutants. These defects were not enhanced in *png-1;rad-23* double mutants indicating the disruption of a common genetic pathway. In vitro and in vivo studies (Leanarz et al., 2004; Suzuki et al., 2001-2007) have shown that PNGases in yeast and mammals indirectly interact with the proteasome through physical association with Rad23. Our results using presumptive null alleles of *png-1* and *rad-23* represent genetic evidence that the physical interaction between PNG-1 and RAD-23 homologues in mammals and yeast is likely conserved in *C. elegans.* Moreover, we observed strong *rad-23* promoter expression in the vulva at L4 and adults. However, RAD-23 appears to be expressed in low amounts since overexpression caused embryonic lethality in transgenic lines. PNG-1 was also shown to be expressed in various tissue and cells, including the vulva at L3, L4 and adult stage (Habibi-Babadi et al., 2010).

Surprisingly, *rad-23 (-/-)* animals did not display the excessive VC4-5 neuronal branching phenotype that is so prominent in *png-1 (-/-)* animals suggesting that PNG-1 must also have RAD-23 independent axon branching functions. Genetic redundancy

would not account for the latter observation as both PNGase and RAD-23 are encoded by single genes in the worm genome. Recent functional studies in yeast have also provided evidence for parallel Rad23-dependent and independent PNGase pathways in the ER-associated degradation of a glycosylated substrate (Kim et al., 2006, 2004). Those pathways were defined as a deglycosylation pathway mediated by Rad23-free Png1 and a proteasomal degradation pathway mediated by the Png1-Rad23 complex.

A limited survey of mutants that are known to disrupt ERAD or the adaption to ER stress in *C. elegans* did not reveal axon branching phenotypes following treatment with tunicamycin. In fact, *png-1* (-/-) animals showed resistance to induced ER stress, suggesting that *png-1* and *rad-23* may indeed identify a novel pathway independent of their known function in maintaining ER-homeostasis. These results are consistent with several genetic screens performed in our laboratory that resulted in the recovery of only *png-1* mutants with VC4-5 axon branch overgrowth phenotypes (A. Colavita, unpublished results).

PNG-1 includes a unique thioredoxin domain at its N-terminus, which differs from other animal PNGases, such as those of flies and mammals that contain a PUB domain at their N-terminus (Suzuki et al., 2007). The PUB domain in mouse N-glycanase is the site of interactions with several known ERAD components including the AAA ATPase p97, the ubiquitin protein ligase AMFR, and Derlin1 (Katiyar et al., 2005; Li et al., 2005, 2006). The absence of this domain in PNG-1 may suggest that axon

branching functions may be largely independent of possible PNG-1 roles in maintaining ER homeostasis. Similarly, the predicted mannose binding C-terminal domain, which in mouse PNGase has been shown to influence the rate of deglycosylation of an ERAD substrate *in vitro* (Zhou et al., 2006), was shown to be dispensable for axon branching in *C. elegans* (Habibi-Babadi et al., 2010) suggesting other roles to account for its conservation in PNG-1. Furthermore, the absence of more widespread neuronal defects outside of the vulval region in *png-1* mutants as might be expected from loss of a general ER quality control component and the lack of branching phenotypes in mutants with elevated levels of ER stress are also consistent with an ERAD-independent role for PNG-1 in axon branching.

My effort to gain further insight into PNG-1 mediated axon branching pathways through genetic screens was successful in identifying a single mutation that enhanced VC4-5 branching defects significantly in *png-1* mutants. Enhancer and suppressor screens are useful genetic tools for uncovering components of molecular pathways and in this study it identified *zy16*, a mutation in the conserved *sax-2* gene that is known to play a significant role in axonal and dendritic branching and arborization (Zallen et al., 1999, 2000).

Sensory axon guidance, *sax-1* and *sax-2* were initially identified in a genetic screen for mutants with abnormal neuronal morphology in *C. elegans* (Zallen et al., 1999). Mutant *sax-1* and *sax-2* worms display neuronal cell shape defects, as well as

axon outgrowth and neurite branching defects (Zallen et al., 1999, 2000; Gallegos and Bargmann, 2004). *sax-1* belongs to a family of nuclear NDR kinases, a subclass of evolutionarily conserved serine/threonine AGC group of protein kinases that are involved various cellular functions such as regulation of cell morphology and growth as well as cell division. NDR kinases, like other kinases, have a complex structure that contains an N-terminal regulatory (NTR) domain, an insert of multiple residues between VII and VIII subdomains of the core catalytic kinase domain, and finally a C-terminal hydrophobic motif (HM) (Figure 3.10). All NDR kinases share two main regulatory phosphorylation sites: the activation segment (AS)(Ser281 of human NDR1/Ser909 of human LATS1) located upstream of VIII subdomain; the second phosphorylation site is located within the HM domain (Thr444 of human NDR1/ Thr1079 in human LATS1) (Hergovich et al., 2006). NDR kinases require the phosphorylation of the conserved Ser/Thr residues for activation (Hergovish et al., 2006, 2005).

Several members of the NDR kinase family have been reported to interact both genetically and physically with members of the Furry proteins (He et al, 2005a; Emoto et al., 2004; Hergovich et al., 2006). These are conserved scaffolding proteins that include Tao3 and Nud1 in *S. cerevisiae,* Salvador and Fry in Drosophila, SAX-2 in *C. elegans,* and hWW45, hFURRY1, and hFURRY2 in humans (Hergovich et al., 2006). In fact these scaffolding proteins facilitate localization and activation of NDR kinases (He et al., 2005b; Emoto et al., 2004). In *C. elegans*, *sax-2* encodes a large conserved protein with

HEAT/Armadillo repeats (Figure 3.10) (Gallegos and Bargmann, 2004). Numerous genetic and biochemical studies describe a role for NDR kinases and their interacting scaffolding partners in regulation of neuronal development, specifically neuronal cell shape, neurite outgrowth, dendritic tiling as well as branching (Bidlingmaier et al., 2001; Zallen et al., 1999, 2000; Emoto et al., 2004, 2006; Gallegos and Bargmann, 2004; Jia and Emmons, 2006).

Characterization of *sax-1* and *sax-2 (-/-)* animals revealed similar neuronal defects as described previously in *png-1* mutants, where the most prominent defects were increased axonal overgrowth and excessive branching in VC4-5. Consistent with our data, mutation in the *trc* and *fry*, the fly homologs of *sax-1*, and *sax-2*, resulted in branching of neuronal and cellular processes (Emoto et al., 2004). Trc inhibits the growth of epidermal hairs, sensory bristles, and antenna in Drosophila, in addition to regulating sensory neuron branching and dendritic arborization (Emoto et al., 2004; He and Adler, 2002). Similarly, mutation in Cot-1, *sax-1* homologue in *N. crassa*, results in excessive hyphal branching (Tamaskovic et al, 2003). Overall, our results further support a conserved role for *sax-1* and *sax-2* in limiting neuronal outgrowth and branching during development in *C. elegans*.

Similarities in neuronal defects between *png-1*, *sax-1* and *sax-2* mutants prompted further analysis of genetic interaction between these mutants. Analysis of *sax-1;sax-2* double mutants revealed neuronal defects that were not enhanced in comparison

to single *sax-1* and *sax-2* mutants, suggesting that these two function within the same genetic pathway to regulate axon outgrowth and branching. This interaction is consistent with reports in other model organisms. Studies in *C. elegans*, Drosophila and *S. cerevisiae* report that *Trc/Cbk-1 fry/Tao3*, homologues of *C. elegans sax-1* and *sax-2*, are components of a common molecular pathway (Zallen et al, 2000; Emoto et al, 2004; He et al., 2005; Du and Novick 2002). Mutation in *trc* and *fry* caused similar neuronal defects that were indistinguishable from *trc;fry* double mutants (Emoto et al., 2004). In vivo analysis of Cbk-1 and Orb6 in yeast show they interact physically with the *sax-2* orthologs Mor2 and Pag1 (Du and Novick, 2002; Seiler et al., 2006). Thus, our data provides further support to the conserved interaction between *sax-1* and *sax-2* and their homologous which is required for proper neuronal development.

Several studies have shown that the vulva epithelium is a source of branch promoting cues (Garriga et al., 1993; Li and Chalfie, 1990; Shen et al., 2004). Characterization of *png-1, sax-1,* and *sax-2* mutants suggest a vital role for these genes in limiting axonal branching during vulva organogenesis. In *C. elegans, sax-1* was reported to function cell-autonomously from neurons to inhibit secondary neurite outgrowth (Zallen et al., 2000); in Drosophila, *sax-1* homologue also functions intrinsically within neurons to limit dendritic branching and tilling (Emoto et al., 2004). Conversely, we reported earlier (Chapter two) that PNG-1 acts within epithelial cells to limit neuronal branching. Examination of VC neurons in *png-1:sax-1* and *png-1;sax-2* double mutants

showed strong synergistic phenotypes, where double mutants displayed significant enhancement of VC morphology defects compared to either the single mutants. Based on the genetic analysis reported in this study and differences in the function and site of action of PNG-1 and SAX-1/SAX-2, we propose that these genes function through two independent parallel pathways, the PNG-1 pathway and SAX-1 pathway, to limit axonal branching and overgrowth, by controlling a common cellular process that regulates cytoskeleton dynamics (Figure 3.14).

The extrinsic activity of PNG-1 within epithelial vulva cells may influences cell surface expression or secretion of branching molecules (Habibi-Babadi et al., 2010). Mutation in PNG-1 can present either excessive amounts of branch promoting factor or little branch inhibitory factor that results in excessive branching phenotypes. This branching factor could be derived from a specific N-glycoprotein or glycopeptide that is retrotranslocated from the ER lumen and processed into a bioactive peptide by a combination of PNGase activity and proteolytic degradation. The resulting active peptide can interact directly by inhibiting axon branching, or indirectly by interacting with cell surface receptors that trigger intracellular signalling pathways that regulate cytoskeleton remodeling and consequently neuronal morphology. Although ERAD substrates have been identified and characterized in yeast and mammals (Suzuki et al., 2002; Hughes et al., 1997; Halaban et al., 1997; Yu et al., 1997), the identity of potential substrate(s) in *C. elegans* remains unknown. In vitro and in vivo studies suggest a direct

role for the NDR kinase pathway in mediating cytoskeleton dynamics by regulating Rho GTPase expression and activity (He and Adler, 2002; Emoto et al., 2004; Chiba et al., 2009). In Drosophila, Trc kinase activity inhibits antenna and hair branching through Rho GTPase signalling (Emoto et al., 2004). Furthermore, dominant negative mutation in Rho GTPases causes similar neuronal defects as *sax-1* mutation in *C. elegans* (Zallen et al., 2000). Therefore I propose that PNG-1 pathway is also involved in a similar process, where the disruption of these two pathways can result in axon branching and overgrowth due to overactive branch promoting signaling mechanisms and cytoskeleton dynamics. Further experiments dissecting these two pathways are needed to determine how they mediate neuronal development.

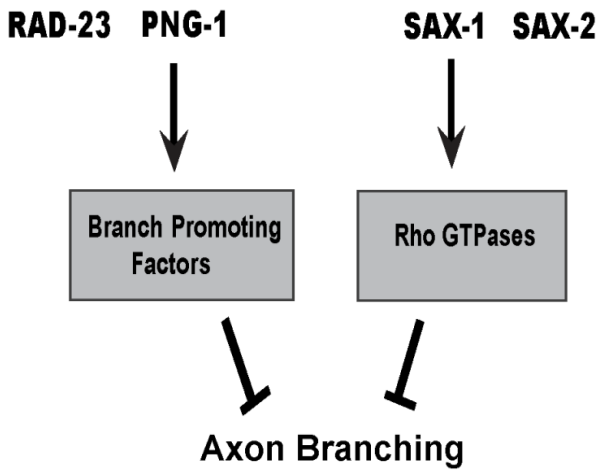

Figure 3.14 PNG-1 and SAX-1 mediated pathways to regulate axon branching

PNG-1 and SAX-1 function through parallel pathways to regulate cytoskeleton dynamics that underlie axon branching. In these pathways, PNGases regulate the turnover of branch promoting factors secreted by vulva epithelial cells, and combined with SAX-1 regulation of Rho GTPases, both pathways limit axon over branching.

CHAPTER 4: CONCLUSION AND FUTURE DIRECTIONS

4.1 Summary and Conclusion

Axon branching patterns are important determinants of neuronal circuit assembly in the nervous system. Although studies in model organisms identified novel genes and alternative functions for conserved guidance cues in this process, the molecular mechanisms that regulate branching remain unknown. The egg-laying neuronal system of *C. elegans* is an excellent system for the dissection and identification of molecular mechanism and signalling molecules that regulate axon branching and arborization. Consisting of eight motorneurons, 2 HSNs and 6 VC cells, this system develops following an organized and specific pattern to innervate the egg laying vulva muscles, and subsequently control egg-laying behavior in nematodes. Of the 6 VC neurons, which normally orient anteroposteriorly, VC4 -5 orient mediolaterally, and extend their axons along the vulva forming a circular tract with distinct stereotypical branches (Schafer, 2006). VC4-5 are among the most branched neurons in *C. elegans*.

png-1 was identified in a genetic screen for VC4-5 axon branch morphology defects. PNG-1 encodes Peptide: N-glycanase (PNGase), a cytosolic enzyme that removes N-linked sugar moieties from glycoproteins and glycopeptides (Suzuki et al., 2000, 2005). Cytosolic PNGases were identified to play a significant role in the degradation of misfolded proteins through the conserved ERAD system that prevents the accumulation of misfolded proteins (Park et al., 2001). The ER quality control system actively retains misfolded aberrant proteins in the ER, and retrotranslocates them to the

cytosol for degradation by the proteasome. Cytosolic PNGases deglycosylate ERAD-targeted proteins to facilitate their transfer to the proteasome. Mammalian and yeast PNGases interact directly with RAD23, an adaptor protein, which binds directly with the proteasome to shuttle misfolded proteins into the proteolytic core (Suzuki et al, 2005; Katiyar et al., 2004). Consistent with a role in ERAD, mutation in PNGase orthologous in yeast leads to a decrease in the rate of degradation of misfolded protein (Suzuki et al., 2000, 2002). The work presented in this thesis describes a novel role for the conserved PNG-1 in the regulation of axon outgrowth and branching during development.

In Chapter two, examination of *png-1 (-/-)* animals revealed excessive axon branching and ectopic neurite outgrowth in VC4-5 neurons as well as branching in the normally unbranched AVL and DVB motor neurons. Additionally, these mutants displayed DVB axons frequently extending past their normal termination sites. Mutation in *png-1* also effected egg-laying behavior where *png-1* (-/-) animals displayed a decrease in the egg-laying and *in utero* egg retention phenotypes. *png-1* promoter activity was observed embryonically and post embryonically in neurons, pharynx, intestine, body wall muscles, vulval epithelial cells, and gonads. A PNG-1 translational fusion to GFP revealed cytoplasmic localization, consistent with other animal model PNGases.

Domain analysis revealed PNG-1 to contain a conserved thioredoxin and transglutaminase domains whose function is vital for *png-1* regulation of axon

branching. Cell specific rescue studies determined that *png-1* acts cell-non autonomously from vulval epithelial cells to regulate axon branching in addition to functioning cell autonomously from neurons, also. These results reveal a novel role PNGase in neuronal development.

In Chapter three, I provided insight into PNG-1 mediated pathways in regulating neuronal development in *C. elegans*. I identified mutations in RAD-23, the sole homolog of RAD23 in *C. elegans*, to cause axonal outgrowth and branching defects similar to *png-1 (-/-)* animals. DVB and AVL motor neurons displayed ectopic branching in an area adjacent to the vulva. These mutants also exhibited DVB overextension defects. The effect of the double mutation on AVL and DVB phenotype was indistinguishable from what was observed in single *png-1(-/-)* and *rad-23(-/-)* animals suggesting that these two genes function in the same pathway to limit axon outgrowth and branching. This data is consistent with previously reported physical interaction between RAD23 and PNG1 (Suzuki et al, 2001, 2005, 2007; Katiyar et al., 2004). This work shows for the first time a role for RAD-23 in neuronal development, where it works with PNG-1 in a common pathway to regulate axonal outgrowth and branching independent of ERAD.

In Chapter three, I presented evidence for genetic interactions between *png-1* and *sax-1*/*sax-2*. *sax-1(-/-)* mutants were recovered from a *png-1* modifier genetic screen. Prior to this work, a role for *sax-1* and *sax-2* was reported in regulating neuronal outgrowth, in addition to axonal and dendritic branching and arborization in *C. elegans*

(Zallen et al, 1999, 2000; Gallegos and Bargman, 2004). *sax-1* encode a highly conserved NDR kinase, while *sax-2* encodes a large protein with Armadillo/HEAT repeats that are also found in scaffolding proteins. NDR kinases and their scaffolding proteins are important for the development of cellular processes and neuronal morphology. Loss of *sax-1* and *sax-2* homologs in Drosophila, *trc* and *fry*, results in neurite overextension, dendritic and axonal branching, and cell body shape defects in a subset of neurons (Emoto et al., 2004). *trc* and *fry* are also involved the development and branching of sensory bristles, antennas, and epidermal hairs (Geneg et al., 2000;, Huang et al, 2005; Emoto et al., 2004; He et al, 2005). Similarly a mutation in Cot-1, yeast homologs of *sax-1*, causes hyphal branching (Maerz et al., 2008).

Examination of neuronal phenotypes in *sax-1* and *sax-2 (-/-)* mutants revealed neuronal defects similar to *png-1(-/-)* mutants, albeit less penetrant. Our analysis of *png-1, sax-1* and *png-1;sax-2* double mutants showed strong synergistic phenotypes indicating *png-1* and *sax-1*/*sax-2* function in two parallel pathways to regulate axon branching and outgrowth.

4.2 Future Directions

The proposed pathways for regulation of axon branching presents a challenge as it suggests multiple components and possible mechanisms are involved. Future experiments will be required to dissect each of these pathways separately to identify these components.

As mutation in *png-1*, *rad-23*, *sax-1* and *sax-2* resulted in similar neuronal defects, it is possible that these pathways act on the same substrate, albeit through different mechanisms. Thus it is important to identify the branch promoting factor secreted by the vulva epithelial cells to gain more information about the proposed pathways. Yeast two-hybrid (Y2H) systems are powerful and efficient techniques to identify proteins-protein interactions. A yeast two-hybrid screen utilizing full length PNG-1 and C-terminal, a construct containing an in-frame deletion of the C-terminal, as baits against a *C. elegans* cDNA library (prey) will identify proteins that interact with PNG-1. Structure/function analysis showed that the PNG-1 C-terminal domain is not required for axon outgrowth and branching. Even though Y2H screens are very useful, they are also known to result in many false positives. To overcome this problem, interactions can be validated by examining available mutants and analyze their neuronal morphologies and genetic interactions with *png-1*. Furthermore, RNAi knockdown can be performed to test candidate interactors and genes with no mutants available, for abnormal neuronal morphologies.

Given that *sax-1* and *sax-2* act in parallel pathways to *png-1* in limiting axon outgrowth and branching, it is important to identify new component of these pathways. Genetic screens can be helpful in identifying such components. Screening for *sax-1* and *sax-2* enhancers of VC4/5 and DVB defects would identify new components of the *png-1* pathway. In fact an enhancer screen of *sax-1* performed in our laboratory identified

several mutants that displayed branching defects similar to *png-1 (-/-)* mutants (Claudia Arauz, Master's thesis, 2010). Characterization of these mutants would provide further insight into PNG-1 pathway. As VC4-5 branching defects are easy to visualize but harder to score, enhancer screens should be performed in the *otIs92 [Pflp-10::GFP]* reporter background. This reporter transgene is used to visualize the DVB motorneuron. DVB overextension and branching defects were significantly enhanced in *png-1;sax1* and *png-1;sax-2* mutants.

An important discovery in this study was the identification of *sax-2* as an enhancer of *png-1* branching defects. *sax-1* and *sax-2* have been widely characterized in neuronal development *C. elegans*. Even though I show a role for *sax-1* and *sax-2* in limiting neuronal outgrowth and branching, it is important to identify how they do so. Therefore modifier genetic screens for enhancer and suppressor of *png-1* would be valuable in recovering components of this pathway. Furthermore, it will be interesting to know if Rho GTPases play a role in VC4-5 branching. Translational fusion constructs driving the expression of dominant negative forms of *Rho-1* in VC4-5 and DVB motorneurons will shed some light on the possibility that defects at these neurons is due to cytoskeleton remodeling mediated through Rho GTPases.

In summary, this thesis represents the first description of the role of conserved cytoplasmic PNG-1 in neuronal development, where it revealed for the first time a role for cytoplasmic PNGases in regulating axon morphology and branching. The results

reported in this thesis shed more insight about novel pathways and genes that are involved in the formation of neuronal circuits. Understanding the molecular pathways involved in axon branching is vital for the development of therapeutic treatments for neurodevelopmental diseases such as Autism and mental retardation.

APPENDIX A: COPY-RIGHT PERMISSION

Fed of Am Societies for Experimental Bio (FASEB) LICENSE TERMS AND CONDITIONS

Dec 13, 2013

This is a License Agreement between Nasrin Habibi-Babadi ("You") and Fedn of Am Societies for Experimental Bio (FASEB) ("Fedn of Am Societies for Experimental Bio (FASEB)") provided by Copyright Clearance Center ("CCC"). The license consists of your order details, the terms and conditions provided by Fedn of Am Societies for Experimental Bio (FASEB), and the payment terms and conditions.

All payments must be made in full to CCC. For payment instructions, please see information listed at the bottom of this form.

License Number	3283120940862
License date	Dec 06, 2013
Licensed content publisher	Fedn of Am Societies for Experimental Bio (FASEB)
Licensed content title	The FASEB journal
Licensed content date	Jan 1, 1987
Type of Use	Thesis/Dissertation
Requestor type	Publisher, not-for-profit
Format	Print, Electronic
Portion	chart/graph/table/figure
Number of charts/graphs/tables/figures	1
Title or numeric reference of the portion(s)	Figure 1.5
Title of the article or chapter the portion is from	Chapter 1: Wiring of the nervous system
Editor of portion(s)	N/A
Author of portion(s)	Nasrin Habibi-Babadi
Volume of serial or monograph.	N/A
Issue, if republishing an article from a serial	N/A
Page range of the portion	56-60
Publication date of portion	December 2013
Rights for	Main product

Duration of use	Life of current edition
Creation of copies for the disabled	no
With minor editing privileges	yes
For distribution to	Canada
In the following language(s)	Original language of publication
With incidental promotional use	no
The lifetime unit quantity of new product	0 to 499
Made available in the following markets	Education
Specified additional information	I will be including this figure in my dissertation, which will be printed into 5 paper copies and published on-line
The requesting person/organization is:	Nasrin Habibi-Babadi
Order reference number	
Author/Editor	Nasrin Habibi-Babadi
The standard identifier	Nasrin HB's Thesis, Chapter 1
Title	PNG-1, a Peptide: N-glycanase limits axon outgrowth and branching in Caenorhabditis Elegans
Publisher	University of Ottawa
Expected publication date	Apr 2014
Estimated size (pages)	190
Billing Type	Invoice
Billing address	
Total (may include CCC user fee)	4.25 USD

Confirmation Number: 11141830
Order Date: 12/03/2013

Customer Information

Customer: Nasrin Habibi-Babadi
The FASEB journal

Invoiced: RLNK501176116

- **Order detail ID:** 64176853
- **ISSN:** 1530-6860
- **Publication Type:** e-Journal
- **Volume:**
- **Issue:**
- **Start page:**
- **Publisher:** Federation of American Societies for Experimental Biology
- **Author/Editor:** Federation of American Societies for Experimental Biology ; HighWire Press
- **Permission Status:** **Granted**
- **Permission type:** Republish or display content
- **Type of use:** Thesis/Dissertation

Job Ticket:	500820139
Order License Id:	3283120940862
Requestor type	Publisher, not-for-profit
Format	Print, Electronic
Portion	chart/graph/table/figure
Number of charts/graphs/tables/figures	1
Title or numeric reference of the portion(s)	Figure 1.5
Title of the article or chapter the portion is from	Chapter 1: Wiring of the nervous system
Editor of portion(s)	N/A
Author of portion(s)	Nasrin Habibi-Babadi
Volume of serial or monograph	N/A
Issue, if republishing an article from a serial	N/A
Page range of portion	56-60
Publication date of portion	December 2013
Rights for	Main product
Duration of use	Life of current edition
Creation of copies for the disabled	no

With minor editing privileges	yes
For distribution to	Canada
In the following language(s)	Original language of publication
With incidental promotional use	no
Lifetime unit quantity of new product	0 to 499
Made available in the following markets	Education
Specified additional information	I will be including this figure in my dissertation, which will be printed into 5 paper copies and published on-line
The requesting person/organization	Nasrin Habibi-Babadi
Order reference number	
Author/Editor	Nasrin Habibi-Babadi
The standard identifier	Nasrin HB's Thesis, Chapter 1
Title	PNG-1, a Peptide: N-glycanase limits axon outgrowth and branching in Caenorhabditis Elegans
Publisher	University of Ottawa
Expected publication date	Apr 2014
Estimated size (pages)	190
Billing Type	Invoice
Note:	This item was invoiced through CCC'S
RightsLink service.	
Total order items:	1
Order Total:	$4.25

Society for Neuroscience LICENSE
TERMS AND CONDITIONS

Dec 13, 2013

This is a License Agreement between Nasrin Habibi-Babadi ("You") and Society for Neuroscience ("Society for Neuroscience") provided by Copyright Clearance Center ("CCC"). The license consists of your order details, the terms and conditions provided by Society for Neuroscience, and the payment terms and conditions.

All payments must be made in full to CCC. For payment instructions, please see information listed at the bottom of this form.

License Number	3283261022569
License date	Dec 06, 2013
Licensed content publisher	Society for Neuroscience
Licensed content title	The journal of neuroscience : the official journal of the Society for Neuroscience
Licensed content date	Jan 1, 1981
Type of Use	Thesis/Dissertation
Requestor type	Academic institution
Format	Print, Electronic
Portion	chapter/article
Title or numeric reference of the portion(s)	Chapter 2: 2.1 introduction, 2.2 Materials and methods, 2.3 Results, 2.4 Discussion. Chapter 3: 3.1 introduction, 3.1 materials and methods, 3.3 Results, 3.4 discussion
Title of the article or chapter the portion is from	Chapter 2: characterization of png-1 function in nervous system development in C. elegans. Chapter 3: Genetic interactors of PNG-1
Editor of portion(s)	n/a
Author of portion(s)	Nasrin Habibi-Babadi
Volume of serial or monograph.	n/a
Issue, if republishing an article from a serial	n/a
Page range of the portion	
Publication date of portion	Jan 2014
Rights for	Main product

Duration of use	Current edition and up to 5 years
Creation of copies for the disabled	no
With minor editing privileges	yes
For distribution to	Canada
In the following language(s)	Original language of publication
With incidental promotional use	no
The lifetime unit quantity of new product	0 to 499
Made available in the following markets	Education
Specified additional information	I am the author of this research article, and I intend use its contents and divided into two sections to be used in two chapters in my thesis. I intend to use all words, and images used in this journal, with modification to text and figures
The requesting person/organization is:	Nasrin Habibi-Babadi
Order reference number	n/a
Author/Editor	Nasrin Habibi-Babadi
The standard identifier	Nasrin HB's Thesis Chapter 2 and 3
The proposed price	n/a
Title	PNG-1, Peptide-N:glycanase limit axon outgrowth and branching in Caenorhabditis Elegans
Publisher	University of Ottawa
Expected publication date	Jan 2014
Estimated size (pages)	190
Total (may include CCC user fee)	0.00 USD

Confirmation Number: 11141844
Order Date: 12/03/2013

Customer Information

Customer: Nasrin Habibi-Babadi

The journal of neuroscience: the official journal of the Society for Neuroscience

- **Order detail ID:** 64177121
- **ISSN:** 1529-2401
- **Publication Type:** e-Journal
- **Volume:**
- **Issue:**
- **Start page:**
- **Publisher:** SOCIETY FOR NEUROSCIENCE
- **Author/Editor:** Society for Neuroscience
- **Permission Status:** **Granted**
-
- **Permission type:** Republish or display content
- **Type of use:** Republish in a thesis/dissertation

Job Ticket:	500820155
Order License Id:	3283261022569
Requestor type	Academic institution
Format	Print, Electronic
Portion	chapter/article
Title or numeric reference of the portion(s)	Chapter 2: 2.1 introduction, 2.2 Materials and methods, 2.3 Results, 2.4 Discussion. Chapter 3: 3.1 introduction, 3.1 materials and methods, 3.3 Results, 3.4 discussion
Title of the article or chapterthe portion is from	Chapter 2: characterization of png-1 function in nervous system development in C. elegans. Chapter 3: Genetic interactors of PNG-1
Editor of portion(s)	n/a
Author of portion(s)	Nasrin Habibi-Babadi
Volume of serial or monograph	n/a
Issue, if republishing an article from a serial	n/a
Page range of portion	
Publication date of portion	Jan 2014
Rights for	Main product
Duration of use	Current edition and up to 5 years

Creation of copies for the disabled	no
With minor editing privileges	yes
For distribution to	Canada
In the following language(s)	Original language of publication
With incidental promotional use	no
Lifetime unit quantity of new product	0 to 499
Made available in the following markets	Education
Specified additional information	I am the author of this research article, and I intend use its contents and divided into two sections to be used in two chapters in my thesis. I intend to use all words, and images used in this journal, with modification to text and figures
The requesting person/organization	Nasrin Habibi-Babadi
Order reference number	n/a
Author/Editor	Nasrin Habibi-Babadi
The standard identifier	Nasrin HB's Thesis Chapter 2 and 3
The proposed price	n/a
Title	PNG-1, Peptide-N:glycanase limit axon outgrowth and branching in Caenorhabditis Elegans
Publisher	University of Ottawa
Expected publication date	Jan 2014
Estimated size (pages)	190
Note: **RightsLink service.**	This item was invoiced through CCC'S More info $ 0.00
Total order items: 1	Order Total: $0.00

From: **Sue Chamberlain**

Sent: December 03-10 5:14:16 AM

To : Nasrin Habibi

RE: PERMISSION TO USE A FIGURE FROM DEVELOPMENT

Dear Nasrin,

Permission is granted with no charge.

The acknowledgement should state "reproduced / adapted with permission" and give the source journal name - the acknowledgement should either provide full citation details or refer to the relevant citation in the article reference list - the full citation details should include authors, journal, year, volume, issue and page citation.

Where appearing online or in other electronic media, a link should be provided to the original article (e.g. via DOI):-

Development: dev.biologists.org

Best wishes,

Sue Chamberlain

This email was sent by Sue Chamberlain on behalf of the Company of Biologists.

permissions@biologists.com

Sue Chamberlain
For and on behalf of The Company of Biologists
Bidder Building
140 Cowley Road
Cambridge
CB4 0DL
UK

http://www.biologists.com/index.html
http://twitter.com/J_Exp_Biol
http://twitter.com/dmm_journal

On 29/11/13 21:08, "Nasrin Habibi" :

Hello,

My name is Nasrin Habibi-Babadi and I am writing in regards of using a figure published in **Development,** in a **review** by **Daniel A. Gibson** and **Le May (2011), vol.138 pages 183-195**. I would like to get your permission to use **Figure 1** as a part of PhD thesis. I am completing my revisions now and plan to submit my thesis by December 15. As for any fees involved in this process, please advise me of the established method by your organization in order to complete the process.

Thank you,

Nasrin

REFERENCES

Acebes A, Ferrus A. (2000). Cellular and molecular features of axon collaterals and dendrites. Trends Neurosci, 23(11):557-565.

Adler CE , Fetter RD, Bargmann CI (2006). UNC-6/Netrin induces neuronal asymmetry and defines the site of axon formation. Nat Neurosci 9:511-518.

Araujo SJ , Tear G.(2003). Axon guidance mechanisms and molecules: lessons from invertebrates. Nat Rev Neurosci , 4:910-922.

Arauz, C. (2010). Genes required for normal neuronal morphology in *Caenorhabditis elegans.* Master's Thesis, University of Ottawa

Arber S, Barbayannis FA, Hanser H, Schneider C, Stanyon CA, Bernard O, Caroni P. (1998). Regulation of actin dynamics through phosphorylation of cofilin by LIM-kinase. Nature, 393:805-809.

Altrich-Van Lith ML, Ostankovitch M, Polefrone JM, Mosse CA, Shabanowitz J, Hunt DF, Engelhard VH. (2006). Processing of class I-restricted epitope from tyrosinase requires peptide: N-glycanase and the cooperative action of endoplasmic reticulum aminopeptidase 1 and cytosolic proteases. J Immunol, 177: 5440-5450.

Amano M, Chihara K, Kimura K, Fukata Y, Nakamura N, Matsura Y, Kaibuchi K. (1997). Formation of actin stress fibers and focal adhesions enahnced by Rho-kianse. Science, 275: 1308-1311.

Amano M, Chihara K, Nakamura N. (1998). Myosin II activation promtes neurite retractin during the action of Rho and Rho-kinase. Genes Cells, 3: 177-188.

Amano M, Ito M, Kimura K, Fukata Y, Chihara K, Nakano T, Matsuura Y, Kaibuchi K . (1996). Phosphorylation and activation of myosin by Rho-associated kinase (Rho-kinase). J Biol Chem, 271: 20246-20249.

Ambros V. (2000). Control of developmental timing in Caenorhabditis elegans. Curr Opin Genet Dev, 10: 428-433.

Anderson P. (1995). Mutagenesis. Methods Cell Biol , 48: 31-58.

Araki K, Nagata K. (2011). Protein folding and quality control in ER. Cold spr Harb Perspect Biol, 3: a007526.

Araujo SJ, and Tear G. (2003a). Axon guidance mechanisms and molecules: lessons from invertebrates. Nat Rev Neurosci, 4: 910-922.

Araujo SJ, Tear G. (2003b). Cellular and molecular features of axon collaterals and dendrites. Nat Rev Neurosci , 4:910-922.

Bagnard D, Lohrum M, Uziel D, Puschel AW, Bolz J. (1998). Sempahrins act as attractive and repulsive guidance signals during the development of cortical projections. Development , 125: 5043-5053.

Bagri A, Cheng HJ, Yaron A, Pleasure SJ, Tessier-Lavign M. (2003). Stereo-typed pruning of long hippocampal axon branches triggered by retraction inducers of teh semaphorin family. Cell, 113: 285-299.

Bagri A, Marin O, Plump AS, Mak J, Pleasure SJ, Rubenstein JL, Tessier-Lavigne M. (2002). Slit proteins prevent midline crossing and determine the dorsoventral position of major axonal pathways in the mammalian forebrain. Neuron, 33:233-248.

Bastmeyer M, and O'Leary DD. (1996). Dynamics of target recognition by interstitial axon branching along developing cortical axons. J Neurosci , 16:1450–1459.

Bastmeyer M, Daston MM, Possel H, O'Leary DD (1998) Collateral branch formation related to cellular structures in the axon tract during corticopontine target recognition. J Comp Neurol, 392:1-18.

Baas PW. (2002) Neuronal polarity: microtubules strike back. Nat Cell Biol, 4: E194-195.

Barnes AP, Polleux F. (2009). Establishment of axon-dendrite polarity in developing neurons. Annu Rev Neurosci, 32:347-381.

Bear MF, Connors BW, Paradiso MA. (2001). Neurosciecne Exploring the brain 2nd Ed. Philadelphia: Lippincott.

Bentley D, and Toroian-Raymond A. (1986). Disoriented pathfinding by pioneer neurone growth cones deprived of filopodia by cytochalasin treatment. Nature , 323: 712-715.

Bernstein BW, and Bamburg JR. (2003). Actin-ATP hydrolysis is a major energy drain for neuron. J. Neurosci , 23: 1-6.

Berridge Mj, Lipp P, Bootman MD. (2000). The versatility and universality of calcium singalling. Nat Rev Mol Cell Biol , 1: 11-21.

Bertolotti A, Zhang Y, Hendershot LM, Harding HP, Ron D. (2000). Dynamic interaction of BiP and ER stress transducers in the unfolded-protein response. Nat Cell Biol , 2: 326-332.

Bilimoria PM, de la Torre-Ubieta L, Ikeuchi Y, Becker EB, Reiner O, Bonni A. (2010). A JIP3-

regualted GSK3 beta/DCX signalling pathway restricts axon branching. J Neurosci , 30: 16766-16776.

Bichsel SJ, Tamaskovic R, Stegert MR, Hemmings BA. (2004). Mechanism of activation of NDR (nuclear Dbf2-related) protein kinase by the hMOB1 protein. J Biol Chem, 79:35228-35235.

Bidlingmaier S, Weiss EL, Seidel C, Drubin DG, Snyder M. (2001). The Cbk1p pathway is important for polarized cell growth and cell separation in Saccharomyces cerevisiae. Mol Cell Biol, 21:2449-2462.

Bishop AL, Hall A. (2000). Rho GTPases and their effector proteins. Biochem J, 348 Pt 2:241-255.

Bischof LJ, Kao CY, Los FCO, Gonzalez MR, Shen Z, Briggs SP, Van der Goot FG, Aroian RV. (2008). Activation of the unfolded protein response is required for defences against bacterial pore-forming toxin in vivo. PLOS Pahog , 4: e1000176 doi: 10:1371/journal.ppat.1000176.

Biswas S, Katiyar S, Li G, Zhou X, Lennarz WJ, Schindelin H. (2004). The N-terminus of yeast peptide: N-glycanase interacts with the DNA repair protein Rad23. Biochem Biophys Res Commun, 323:149-155.

Blom D, Hirsch C, Stern P, Tortorella D, Ploegh HL. (2004). A glycosylated type I membrane protein becomes cytosolic when peptide: N-glycanase is compromised. EMBO J, 23:650-58.

Bos JL, Rehmann H, Wittinghofer A. (2007). GEFs and GAPs: critical elements in the control of small G proteins. Cell, 129:865-877.

Bondeva T, Pirola L, Bulgarelli-Leva G, Rubio I, Wetzker R, Wymann MP. (1998). Bifurcation of lipd and protein kinase signals of PI3Kgamma to the protein kinases PKB and MAPK. Science, 282: 293-296.

Bourn HR, Sanders DA, McCormick F. (1991). The GTPase superfamily: conserved structure and molecular mechanism. Nature, 349: 117-127.

Bouquet C, Nothias F. (2007). Molecular mechanisms of axonal growth. Adv Exp Med Biol, 621:1-16.

Boyle M, Nighorn A, Thomas JB. (2006). Drosophila Eph receptor guides specific axon branches of mushroom body neurons. Development , 133: 7204-7213.

Brenner S. (1974). The genetics of Caenorhabditis elegans. Genetics, 77:71-94.

Brittis PA, Lu Q, Flanagan JG (2002). Axonal protein synthesis provides a mechanism for

localized regulation at an intermediate target. Cell, 110:223-235.

Brose K, Tessier-Lavigne M. (2000). Slit proteins: key regulators of axon guidance, axonal branching, and cell migration. Curr Opin Neurobiol, 10:95-102.

Buchberger A, Howard MJ, Proctor M, Bycroft M. (2001). The UBX domain: a widespread ubiquitin-like module. J Mol Biol , 307: 17–24.

Burgess RW, Petersen KA, Johnson MJ, Roix JJ, Welsh IC, O'Brien TP. (2004). Evidence for a conserved function in synapse formation reveals Phr1 as a candidate gene for respiratory failure in newborn mice. Mol Cell Biol, 24: 1096-1105.

Bustelo XR, Sauzeau V, Berenjeno IM. (2007). GTP-binding proteins of the Rho/Rac family: regulation, effectors and functions in vivo. BioEssays, 29: 356-370.

Calfon M, Zeng H, Urano F, Till JH, Hubbard SR, harding HP, Clark SG, Ron D. (2002). IRE couples endplsasmic reticulum load to secretory capcity by processing the XBP-1m RNA. Nature, 415: 92-96.

Carlvalho P, Stanley AM, Rapoport TA. (2010). Retrotranslocation of a misfolded luminal ER protein by the ubiquitin ligase Hrd1p. Cell, 143: 579-591.

Challacombe JF, Snow DM, Letourneau PC. (1996). Actin filament bundles are required for microtubule reorientation during growth cone turning to avoid an inhibitoryguidance cue. J Cell Sci, 109: 2031-2040.

Chao DL, Ma L, Shen K. (2009). Transietn cell-cell interaction in neuronal circuit formation. Nature, 10: 262-269.

Chen L, Janetopoulos C. (2003). Two phases of actin polymerization display different dependencies on PI(3,4,5) P3 accumulation and have unique roles during chemotaxis. Mol Biol Cell, 14: 5028-5037.

Chen L, Shinde U, Ortolan TG, Madura K. (2001). Ubiquitin-associated (UBA) domain in Rad23 bind ubiquitin and promotes inhibition of multi-ubiquitin chan assembly. EMBO , 2: 933-938.

Chen YM, Wang QJ, Hu HS, Yu PC, Zhu J, Drewes G, Piwnica-Worms H, Luo ZG. (2006). Microtubule affinity-regulating kinase 2 functions downstream of the PAR-3/PAR-6/atypical PKC complex in regulating hippocampal neuronal polarity. Proc Natl Acad Sci U S A 103:8534-8539.

Cheng PL, Lu H, Shelly M, Gao H, Poo MM. (2011). Phosphorylation of E3 ligase smurff1 switches its substrate preferecne in support of axon development. Neuron , 69: 231-243.

Chien CB, Rosenthal DE, Harris WA, Holt CE. (1993). Navigational errors made by growth cones without filopodia in the embryonic Xenopus brain. Neuron, 11: 237-251.

Chiba S, Ikeda M, Katsunuma K, Ohashi K, Mizuno K. (2009). MST2- and Furry-mediated activation of NDR1 kinase is critical for precise alignment of mitotic chromosomes. Curr Biol, 19:675-681.

Ciechanover A. (1998). The ubiquitin-proteasome pathway: on protein death and cell life. The EMBO Jour , 24: 7151-7160.

Colativa A, Tessier-Lavigne M. (2003). A Neurexin-related protein, BAM-2, terminates axonal branches in C. elegans. Science, 302: 293-296.

Colavita, A, and Culotti JG. (1998). Suppressors of Ectopic UNC-5 growth cone steering identify eight genes involved in axon guidance in caenorhabditis elegans. Dev Biol, 194: 72-85.

Colicelli J. (2004). Human RAS superfamil proteins and related GTPases. Sci STKE , 2004: RE13.

Cong J, Geng W, He B, Liu J, Charlton J, Adler PN. (2001). The furry gene of Drosophila is important for maintaining the integrity of cellular extensions during morphogenesis. Development 128:2793-2802.

Corsi AK. (2006). A biochemist's guide to Caenorhabdtis elegans. Anal Biochem, 359:1-17.

Corriveau RA, Huh GS, Shatz CJ. (1998). Regulation of class I MHC gene expression in the developing and mature CNS by neuronal activity. Neuron, 21: 505:520.

Cox JS, Walter P. (1996). A novel mechanism for regulating activity ofa transcription factor that controls the unfolded protein response. Cell, 87: 391-404.

Da Silva JS, Medina M, Zuliani C, Di Nardo A, Witke W, Dotti CG. (2003). RhoA/ROCK regulation of neuritogenesis via profilin IIa-mediated control of actin stability. J Cell Biol, 162: 1267-1279.

Das M, Wiley DJ, Chen X, Shah K, Verde F. (2009). The conserved NDR kinase Orb6 controls polarized cell growth by spatial regulation of the small GTPase Cdc42. Curr Biol, 19:1314-1319.

Desai A, Mitchison T. (1997). Microtubule polymerization dynamics. Annu Rev Cell Dev Biol, 13: 83-117.

Dent EW, Gertler FB. (2003). Cytoskeletal dynamics and transport in growth cone motility and axon guidance. Neuron , 40: 209-227.

Dent EW, Barnes AM, Tang F, Kalil K. (2004). Netrin-1 and Semaphorin 3A promote or inhibit

cortical axon branching, repectively, by reorganization of the cytoskeleton. J Neuro, 24: 3002-3012.

Dent EW, Tang F, Kalil K. (2003). Axon guidance by growth cones and branches: common cytoskeletal and signaling mechanisms. The Neuroscientist, 9: 343 - 353.

Dent EW, Kalil K. (2001). Axon branching requires interactions between dynamic microtubules and actin filaments. J Neurosci, 21:9757-9769.

Dent EW, Callaway JL, Szebenyi G, Baas PW, Kalil K. (1999). Reorganization and movement of microtubules in axonal growth cones and developing interstitial branches. J Neurosci, 19:8894-8908.

Deshaies RJ, Joazeiro CA. (2009). RING domain E3 ubiquitin ligases. Annu Rev Biochem, 78: 399-434.

Deveraux Q, Ustrell V, Pickart C, Rechsteiner M. (1999). A 26S proteasome subunit. J Biol Chem, 269: 7059-7061.

Di Cola A, Frigerio L, Lord JM, Roberts LM, Ceriotti A. (2005). Endoplasmic reticulum-associated degradation of ricin A chain has unique and plant-specific features. Plant Physiol, 137: 287–296.

Dickson BJ. (2001). Rho GTPases in grwoth cone guidance. Curr Opin Neurobio , 11: 103-110.
Diepold A, Li G, Lennarz Wj, Numberger T, Brunner F. (2007). The Arabidopsis AtPNG1 gene encodes a peptide:N-glycanase. Plant J, 52: 94-104.

Ditlevsen DK, Kohler LB, Pederesen MV, Risel M, Kolkova K, Meyer M, Berezin V, Bock E. (2003). The role of phosphatidylinositol 3-kinase in neural cell adhesion molecule-mediated neuronal differentiation and survival. J Neurochem, 84: 546-556.

D'Souza J, Hendricks M, Guyader S, Subburaju S, Grunewald B, Scholich K, Jesuthasan S. (2005). Formation of the retinotectal projection requires Esrom, an ortholog of PAM (protein associated with Myc). Development, 132: 247-256.

Dougan SK, Hu CCA, Paquet ME, Greenblatt MB, Kum J, Liley B, Watson N, Ploegh H. (2011). Derlin-2 Deficient Mice Reveal an Essential Role for Protein Dislocation in Chondrocytes. Mol Cell Biol, 31: 1145-1159.

Drinjakovic J, Jung H, Campbell DS, Strochlic L, Dwivedy A, Holt CE . (2010). E3 ligase Nedd4 promotes axon branching by downregulating PTEN. Neuron , 65: 341–357.

Du LL, Novick P. (2002). Pag1p, a novel protein associated with protein kinase Cbk1p, is required for cell morphogenesis and proliferation in Saccharomyces cerevisiae. Mol Biol Cell, 13:503-514.

Duerr JS, Frisby DL, Gaskin J, Duke A, Asermely K. (1999). The cat-1 gene of Caenrohabditis elegans encodes a vesicular monoamine transporter required for specific monoamine-dependent behaviors. J Neurosci, 19:72-84

Duerr JS, Gaskin J, Rand JB. (2001). Identified neurons in C. elegans coepxress vesicular transporters for acetylcholine and monoamines. Am J Physiol Cell Physiol, 280: C1616-C1622.

Eastman C, Horvitz HR, Jin Y. (1999). Coordinated transcriptional regulation of the unc-25 glutamic acid decarboxylase and the unc-47 GABA vesicular transporter by the Caenorhabditis elegans UNC-30 homeodomain protein. J Neurosci, 19: 6225-6234.

Ellgaard L, Helenius A. (2003). Quality control in the endoplasmic reticulum. Nature Rev Mol Cell Biol, 4: 181-191.

Elsasser S, Chandler-Militell D, Muller B, Hanna J, and Finley D. (2004). Rad23 and Rpn10 serve as alternative ubiquitin receptors for the proteasome. J Biol Chem, 279: 26817–26822.

Elsasser, S., and Finley, D. (2005). Delivery of ubiquitinated substrates to protein-unfolding machines. Nat Cell Biol, 7: 742–749.

Emoto K, Parrish JZ, Jan LY, Jan YN. (2006). The tumour suppressor Hippo acts with the NDR kinases in dendritic tiling and maintenance. Nature, 443:210-213.

Emoto K, He Y, Ye B, Grueber WB, Adler PN, Jan LY, Jan YN. (2004). Control of dendritic branching and tiling by the Tricornered-kinase/Furry signaling pathway in Drosophila sensory neurons. Cell, 119:245-256.

Esposito C and Caputo. (2005). Mammalian transglutaminases Identification of substrates as a key to physiological function and physiopathological relevance. FEBS J , 272: 615-631.

Evan TA, and Bashaw GJ. (2010). Functional diversity of Robo receptor immunogloulin domains promtes distinct axon gudiance decisions. Curr Biol , 20: 567-572.

Feinberg EH, Vanhoven MK, Bendesky A, Wang G, Fetter RD, Shen K, Bargman Ci. (2008). GFP reconstitution across synaptic partners (GRASP) defines cell contact and synapses in living nervous systems. Neuron, 57:353-363.

Finely D. (2009). Recognition and processing of ubiquitin-protein conjugates by the protesome. Annu Rec Biochem , 78: 477-513.

Fire A, Xu S, Montgomery MK, Kostas SA, Driver Se, Mello CC. (1998). Potent and specific genetic interference by double-stranded RNA in Caenorhabditis elegans. Nature , 391: 806-811.

Funakoshi Y, Negishi Y, Gergens P, Seino J, Ishii K, Lennars WJ, Matsuo I, Ito Y, Tanigushi N, Suzuki T . (2011). Evidence for an Essential Deglycosylation-Independent Activity of PNGase in Drosophila melanogaster. PLOS ONE , 5(5): e10545.

Gallegos ME, Bargmann CI, (2004). Mechanosensory neurite termination and tiling depend on SAX-2 and the SAX-1 kinase. Neuron, 44:239-249.

Gallo G, Letourneau PC. (1998). Localized sources of neurotrophins initiate axon collateral sprouting. J Neurosci, 18:5403-5414.

Gallo G. (2011). The Cytoskeletal and Signaling Mechanisms of Axon Collateral Branching. Dev Neurob , 71: 201- 220.

Gallo G, and Letourneau PC. (2004). Regulation of growth cone actin filaments by guidance cues. J Neurobiol , 58: 92-102.

Gallo G, Letourneau PC. (1998). Localized soruces of neuroneurotrophins initiate axon collateral sprouting. J Neurosci , 18: 5403–5414.

Gao FB. (2007). Molecular and cellular mechanisms of dendritic morphogenesis. Curr Opin Neurobiol, 17:525-532.

Garriga No, Desai C, Horvitz HR. (1993). Cell interactions control the direction of outgrowth, branching and fasciculation of the HSN axons of Caenorhabditis elegans. Development, 117: 1071-1087.

Geng W, He B, Wang M, Adler PN. (2000). The tricornered gene, which is required for the integrity of epidermal cell extensions, encodes the Drosophila nuclear DBF2-related kinase. Genetics 156:1817-1828.

Gibson D, Ma K. (2011). Developmental regulation of axon branching in vertebrate nervous system. Development, 138: 183-195. Doi:10.1242/dev.046441

Glamis-Gardikas A, Holmgren A. (2002). Thioredoxin and glutaredoxin isoforms. Methods Enzymol , 347: 286-296.

Glebova NO, Ginty DD. (2005). Growth and survival signals controlling sympathetic nervous system development. Annu Rev Neurosci, 28: 191-222.

Goddard CA, Butts D, Shatz CJ. (2007). Regulation of CNS synapses by neuronal MHC Class I. Proc Natl Acad Sci USA , 104: 6826-6833.

Gossain et al., (2012). Identfication and characterization of peptide: N-glycanase from Dicotyostelim discoideum. *BMC Biochem*., 147:-2091-13-9.

Goodwin M, and Yap AS. (2004). Classical cadherin adhesion moleculres: coordinating cell adhesion, signaling and the cytoskeleton. J Mol Histol , 35: 839-844.

Gue Q, Xie J, Dang CV, LIu ET, Bishop JM. (1998). Identification of a large Myc-binding protein that contains RCC1-like repeats. Proc Natl Acad Sci , 95: 9172-9177.

Guerriero CJ, Brodsky JL. (2012). The delicate balance between secreted protein folding and endoplasmic reticulum-associated degradation in human physiology. Physiol Rev , 92: 537-576.

Guzder SN, Habraken P, Sung L, Prakash S, Prakash L. (1995). Reconstitution of yeast nucleotide excision repair with purified Rad proteins, replication protein A, and transcription factor TFIIH. J Biol Chem , 270: 12973-12976.

Habibi-Babadi N, Su A, de Carvalho CE, Colavita A. (2010). The N-glycanase png-1 acts to limit axon branching during organ formation in Caenorhabditis elegans. J Neurosci, 30:1766-1776

Hagg T. (2006). Collateral sprouting as a target for improved function after spinal cord injury. J Neurosci Res , 14: 3033-3042.

Halaban R, Cheng E, Zhang Y, Moelmann G, Hanlon D, Mischalak M, Setaluri V, Herbert DN. (1997). Aberrant retention of tyrosinase in the endoplasmic reticulum mediates accelerated degradation of the enzyme and contributes to the dedifferentiated phenotypes of ameloanotic melonoma cells. Proc Natl Acad Sci USA, 94: 6210-6215.

Hall A, and Lalli G. (2010). Rho and Ras GTPases in axon growth, guidance, and branching. Cold Spring Harb Perspect Biol , 2: a001818.

Hall D, Altun ZF. (2008). C. Elegans Atlas. New York: Cold Spring Harbor Laboratory Press.
Halloran MC, Kalil K. (1994). Dynamic behaviors of growth cones extending in the corpus callosum of living cortical brain slices observed with video microscopy . J neurosci, 14: 2161-2177.

Hao JC, Yu TW, Fujisawa K, Culotti JG, Gengyo-Ando K, Mitani S, Moulder G, Barstead R, Tessier-Lavigne M, Bargmann CI. (2001). C. elegans slit acts in midline, dorsal-ventral, and anterior-posterior guidance via the SAX-3/Robo receptor. Neuron, 32:25-38.

Harden N, Ricos M, Yee K, Sanny J, Langmann C, Yu H, CHia W, Lim L. (2002). Harden N, Ricos M, Yee K, Sanny J, Langmann C, Yu H, CHia W, Lim L. J cell Sci, 115: 2119-2129.
Harding HP, Ron D. (2002). Endoplasmic reticulum stress and teh development of diabetes: a review. Diabetes, 51: S455-S461.

Harding HP, Zeng H, Zhang Y, Jungries R, Chung P, Plesken H, Sabatini DD, Ron D. (2001). Diabetes mellitus and exocrine pancreatic dysfunctino in perk-/- mice reveals a role for translational control in secretory cell survival. Mol Cell, 7: 1153-1163.

Harding HP, Zhang Y, Bertolotti A, Zeng H, Ron D. (2000). Perk is essential for translatinal regulation and cell survival during the unfolded protein response. Mol Cell, 5:897-904.

Harding HP, Zhang Y, Ron D. (1999). Protein translation and folding are coupled by an endoplasmic-reticulum resident kinase. Nature, 397: 271-274.

Harfield PM, Vierstra RD. (1992). J Biol Chem, 10: 227-236.

Hartman PS, and Herman RK. (1982). Radiation-senstive mutants of Caenorhabditis elegans. Genetics, 102: 159-178.

Hartmann-Petersen R, Tanaka K, Hendil KB. (2001). Quaternary structure of the ATPase complex ofhuman 26Sproteasome determined by chemcial cross-linking.Arch Biochem Biophys,386:89-94.

Hartmann-Peterson R, and Gordon C. (2004 b). Inegral UBL domain proteins: a family of proteasome interacting proteins. Semin Cell Dev Biol, 15: 247-259.

Hartmann-Peterson R, and Gordon C. (2004 a). Proteins interacting with the 26S proteasome. Cell Mol Life Sci, 61: 1589-1595.

Hartman-Petersen, R, Seeger M, Gordon C. (2003). Transferring substrates to the 26S proteasome. Trends Biochem Sci, 28: 26-31.

Heasman SJ, and Ridley AJ. (2008). Mammalian RHo GTPase: new insights into their functin from in vivo studies. Nat Rev Mol Cell Biol , 9: 690-701.

He B, Adler PN. (2002). The genetic control of arista lateral morphogenesis in Drosophila. Dev Genes Evol 212:218-229.

He Y, Fang X, Emoto K, Jan YN, Adler PN .(2005a). The tricornered Ser/Thr protein kinase is regulated by phosphorylation and interacts with furry during Drosophila wing hair development. Mol Biol Cell 16:689-700.

He Y, Emoto K, Fang X, Ren N, Tian X, Jan YN, Adler PN. (2005b). Drosophila Mob family proteins interact with the related tricornered (Trc) and warts (Wts) kinases. Mol Biol Cell 16:4139-4152.

Henley J, Poo MM (2004) Guiding neuronal growth cones using Ca2+ signals. Trends Cell Biol 14:320-330.

Hedge RS, and Pleogh H. (2010). Qualtiy and quantity control at the endoplasmic reticuum. Curr Opin Cell Biol, 22: 437-446.

Hege RS, Kang HL. (2010). The concept of translocational regulation. J Cell Biol , 182: 437-446.

Henley J, and Poo MM. (2004). Guiding neuronal growth cones using Ca2+ signals. Tends Cell Biol , 14: 320-330.

Hergovich A, Bichsel SJ, Hemmings BA. (2005). Human NDR kinases are rapidly activated by MOB proteins through recruitment to the plasma membrane and phosphorylation. Mol Cell Biol 25:8259-8272.

Hergovich A, Stegert MR, Schmitz D, Hemmings BA.(2006). NDR kinases regulate essential cell processes from yeast to humans. Nat Rev Mol Cell Biol 7:253-264.

Hergovich A, Lamla S, Nigg EA, Hemmings BA .(2007). Centrosome-associated NDR kinase regulates centrosome duplication. Mol Cell 25:625-634.

Hiller et al. (2005). Generation and annotation of the DNA sequences of human chromosmes 2 and 4. Nature , 434: 724-731.

Hirose M, Ihizaki T, Watanabe N. (1998). Molecualr dissection of the Rho-associated protein kinase (p160ROCK)-regulated neurite remodeling in neuroblastma N1E-115 cells. J cell Biol , 141: 1625-1636.

Hirsch C, Blom D, Ploegh HL. (2003). A role for N-glycanase in the cytosolic turnover of glycoproteins. EMBO J , 22: 1036–1046.

Hirsch C, Misaghi S, Blom D, Pacold M, Ploegh H. (2004). Yeast N-glycanase distinguishes between native and non-native glycoproteins. EMBO Rep , 5: 201-206.

HodgkinJ, and Barnes TM. (1991). More is not better: brood size and poplation growth in self-fertilizing nemaode. Proc Biol Sci , 246: 19-24.

Hong K, Nishiyama M, Henley J, Tessier-Lavigne M, Poo M. (2000). Calcium signalling in the guidance of nerve growth by netrin-1. Nature , 403: 93-98.

Horvitz HR. (1999). Genetic control of programmed cell death in the nematode Caenorhabditis elegans. Cancer Res , 59: 1701-1706.

Howard J, Hyman AA. (2003). Dynamics and mechanics of the mircrotubule plus end. Nature, 422: 753-758.

Hughes EA, Hammond C, Cresswell P. (1997). Misfolded major histocompatibility complex class I heavy chains are translocated into the cytoplasm and degraded by the proteasome. Proc Natl Acad Sci USA., 94: 1895-1901.

Huh Gs, Boulanger LM, Du H, Riquelme PA, Brotz TM, Shatz CJ. (2000). Functional requriement for class I MHC in CNS development and plasticity. Science, 290: 2155-2159.

Husnjak K, and Dikic I. (2012). Ubiquitin-binding proteins: decoders of ubiquitin-mediated cellular functions. Annu Rev Biochem , 81: 291-322.

Jaffe AB, and Hall A. (2005). Rho GTPases: biochemsitry and Biology. Annu REv CEll Dev Bio, 21: 247-269.

Jarosch E, Taxis C, Volkwein C, Bordallo J, Finley D, Wolf DH, Sommer T. (2002). Protein dislocation from the ER requires polyubiquitination and the AAA-ATPase Cdc48. Nat Cell Biol, 4: 134-139.

Jin Z, and Strittmatter SM. (1997). Rac1 mediates collapsin-1-induced growth cone collapse. J Neurosci, 17: 6256-6263.

Jordan MA, and Wilson L. (2004). Microtubules as a target for anticancer drugs. Nature , 4:253-265.

Jia L, Emmons SW (2006) Genes that control ray sensory neuron axon development in the Caenorhabditis elegans male. Genetics 173:1241-1258.

Jiang H, Guo W, Liang X, Rao Y (2005) Both the establishment and the maintenance of neuronal polarity require active mechanisms: critical roles of GSK-3beta and its upstream regulators. Cell 120:123-135.

Jin Z, Strittmatter SM (1997) Rac1 mediates collapsin-1-induced growth cone collapse. J Neurosci 17:6256-6263.

Joshi S, Katiyar S, Lennarz WJ (2005) Misfolding of glycoproteins is a prerequisite for peptide: N-glycanase mediated deglycosylation. FEBS Lett 579:823-826.

Kalil K, Dent EW. (2005). Touch and go: guidance cue ssignal to the growth cone cytoskeleton. Curr Opin Neurobiol, 15: 521–526.

Kalil K, Li L, Hutchines B. (2011). Signaling mechansims in cortical axon growth, guidance and branching. Front Neuroanat, 5: 62.

Kalil K, Szebenyi G, Dent EW. (2000). Common mechanisms underlying growth cone guidance and axon branching. J Neurobiol, 44: 145–158.

Kario E, Tirosh B, Ploegh HL, Navon A. (2008). N-linked glycosylation does not impair proteasomal degradation but affects class I major histocompatibility complex presentation. J Biol Chem, 283: 244-254.

Kamath RS, Fraser AG, Dong Y, Poulin G, Durbin R, Gotta M, Kanapin A, Le bot N, Moreno S., Sohrmann M, Welchman DP, Zipperlen P, Ahringer J. (2003). Systematic functional analysis of the Caenorhabditis elegans genome using RNAi . Nature , 421: 231-237.

Kaminoka M, and Feigon J. (2004). Structure of the XPC binding domain of hHR23A reveals hydrophobic patches for protein interaction. Protein Sci , 13: 2370-2377.

Katiyar S, Joshi S, Lennarz WJ. (2005). The retrotranslocation protein Derlin-1 binds. Mol Biol Cell, 16: 4584-4594.

Katiyar S, Li G, Lennarz WJ. (2004). A complex between peptide: N-glycanase and two proteasome-linked proteins suggest a mechansim for the degradation of misfolded glycoproteins. Proc Natl Acad Sci USA, 101: 13774-13779.

Kato T, Kawahara A, Ashida H, Yamamoto K. (2007). Unique peptide: N-glycanse in *Caenorhabditis elegans* has activity of protein disulphide reductases as well as of deglycosylation. J Biochem, 142-175-181.

Kaufman RJ. (1999). Stress signaling from the lumen of the endoplasmic reticulum: coordination of gene transcriptional and translational controls. Gene Dev , 13: 1211-1233.

Kaufman RJ, Malhotra JD. (2007). The endoplasmic reticulum and the unfolded protein response. Sem in Cell and devel biol , 18: 716-731.

kaufman RJ, Scheuner D, Schroder M, et al. (2002). The unfolded protein response in nutrient sensing and diferentiation. Nat Rev Mol Cell Biol , 3: 411-421.

Ketschek A, and Gallo G. (2010). Nerve growth factor induces axonal filopida through localized microdomains of phosphoinositide 3-kinase activity that drive the formation of cytoskeletal precursors to filopodia. J Neurosci , 30: 12185-12197.

Kim J, Poole DS, Waggoner LE, Kempf A, Ramirez DS. (2001). Genes affecting the activity of nicotinic receptors involved in Caenorhabditis elegans egg-laying behavior. Genetics, 157: 1599-1610.

Kim I, Ahn J, Liu C, Tanabe K, Apodaca J, Suzuki T, Rao H. (2006b). the Png-1-Rad23 complex regultes glycoprotein turnover. J Cell Biol, 172:211-219.

Kim WY, Zhou FQ, Zhou J, Yokota Y, Wang YM, Yoshimura T et al. (2006a). Essential roles of GSK-3s and GSK-3-primed substrates in neurotrophin-induced and hippocampal axon growth. Neuron , 52: 981-996.

Kitajima K, Suzuki T, Kouchi Z, Inoue S, Inoue Y. (1995). Identification and distribution

of peptide: N-glycanase (PNGase) in mouse organs. Arch Biochem Biophys, 319: 393-401.

Koppen M, Simske JS, Sims PA, Firestein Bl, Hall DH, Radice AD, Rongo C, Hardin JD. (2001). Cooperative regulation of AJM-1 controls junctional integrity in Caenorhabditis elegans epithelia. Nat Cell Biol, 3: 983-991.

Klodkin A, Tesseir-Lavigne M. (2011). Mechanisms and molecules of neuronal Wiring: a primer. Cold Spring Harb Perspect Biol, 3:a001727.

Knop M, Finger A, Braun T, Hellmuth K, Wolf DH. (1996). Der1, a novel protein specifically required for endoplasmic reticulum degradation in yeast. EMBO J, 15: 753-763.

Kny M, Standera S, Hartmann-Petersen R, Kloetzel PM, Seeger M. (2011). Herp regulates Hrd1-mediated ubiquitylation in a ubiquitin-like domain-dependent manner. J Biol Chem, 286: 5151-5156.

Korobova F, and Svitkina T. (2010). Molecular architecture of synaptic actin cytoskeleton in hippocampal neurons reveals a mechanism of dendritic spine morphogenesis. Mol Biol Cell, 21:165–176.

Korobova F, Svitkina T. (2008). Arp2/3 complex is important for filopodia formation, growth cone motility, and neuritogenesis is neuronal cell. Mol Biol Cell, 19: 1561-1571.

Krasilnikov MA. (2000). Phosphatidylinositol-3 kianse dependent pathways: the role in control of cell growth, survival, and malignant transformation. Biochemistry, 65: 59-67.

Kruger RP, Arandt J, Guan KL. (2005). Sempahorins command cells to move. Nat Rev , 6: 789-800.
Kureishy N, Sapountzi V, Prag S, Anilkumar N, Adams JC. (2002). Fascins, and their roles in cell structure and function. Bioessays, 24: 350-360.

Kwon CH, Luikart BW, Powell CM, Zhou J, Matheny SA, Zhang W, Li Y. (2006). Pten regulates neuronal arboriarborization and social interaction in mice. Neuron , 50:377–388.
La Brasseur N. (2007). PKA steers growth coens. J Cell Biol, 176:2.

Kurischko C, Weiss G, Ottey M, Luca FC .(2005). A role for the Saccharomyces cerevisiae regulation of Ace2 and polarized morphogenesis signaling network in cell integrity. Genetics, 171:443-455.

Kurischko C, Kuravi VK, Wannissorn N, Nazarov PA, Husain M, Zhang C, Shokat KM, McCaffery JM, Luca FC.(2008). The yeast LATS/Ndr kinase Cbk1 regulates growth via Golgi-dependent glycosylation and secretion. Mol Biol Cell, 19:5559-5578.

Lal AA, Korn ED, and Brenner SL. (1984). Rate constants for actin polymerization in ATP determined using crosslinked actin trimers as nuclei. J Biol Chem, 259:8794-8800.

Lans H, Vermeulen W. (2011). Nucleotide excision repair in Caenorhabditis elegans. Mol Biol Inter, 2011: ID542795.

Lambertson D, Chen L, Madura K. (1999). Pleiotropic growth and proteolytic defects caused by the loss of of the proteasome-interacting factors Rad23 and Rpn10 of Saccharomyces cerevisiae. Genetics, 153: 69-79.

Lasorella A, Stegmuller J, Guardavaccaro D. (2006). Degradation of Id2 by the anaphase-promoting complex couples cell cycle exit and axonal growth. Nature , 442: 417-474.

Lee JH, Choi JM, Lee C, Yi KJ, Cho Y. (2005). Structure of a peptide:N-glycanase–Rad23 complex:Insight into the deglycosylation for denatured glycoproteins. Prec Nat Acad of Sci USA, 102: 9144–9149.

Lee K, Tirasophon W, Shen X, Michalak M, Prywes K, Okada T, Yoshida H, Mori K, Kaufman RJ. (2002). IRE-1 mdeiated nonconventional mRNA splicing and S2P-mediated ATF6 cleave merge to regulate XPB1 in signaling the unfolded protein response. Genes Dev , 16: 452-466.

Leslie NR, and Downes CP. (2002). PTEN: the down side of PI-3 kinase signalling . Cell signal, 14: 285-295.

Letourneau P. (2009). Actin in axons: stable scaffolds and dynamic filaments. Results Probl Cell DifferL 48: 65-90.

Lewcock JW, Genoud N, Lettieri K, Pfaff SL. (2007). The ubiquitin ligase Phr1 regulates axon outgrowth through modulation of microtubule dynamics. Neuron, 56: 604-620.

Li C, Chalfie M .(1990). Organogenesis in C. elegans: positioning of neurons and muscles in the egg-laying system. Neuron, 4:681-695.

Li G, Zhou X, Zhao G, Schindelin H, Lennarz WJ. (2005). Multiple modes of interaction of the deglycosylation enzyme, mouse peptide N-glycanase, with the proteasome. Proc Natl Acad Sci USA, 102:15809-15814.

Li G, Zhao G, Zhou X, Schindelin H, Lennarz WJ. (2006). The AAA ATPase p97 links peptide N-glycanase to the endoplasmic reticulum-associated E3 ligase autocrine motility factor receptor. Proc Natl Acad Sci USA. 103:8348-8353.

Lickteig KM, Duerr JS, Frisby DL, Hall DH, Rand JB, Miller Dm, 3rd. (2001). Regulation of neurotransmitter vesicles by the homeodomain protein UNC-4 and its transcriptional corepressor UNC-37/groucho in Caenorhabditis elegans cholinergic motor neurons. J neurosci, 21: 2001-20014.

Lilley BN, Ploegh HL. (2005). Multiprotein complexes that link dislocation, ubiquitination, and extraction of misfolded proteins from the endoplasmic reticulum membrane. Proc Natl Acad Sci USA, 102: 14296-14301.

Liu BP, and Strittmatter SM. (2001). Sempahrin-mediated axonal guidance via Rho-related G proteins. Curr Opinion in Cell Bio, 13: 619-626.

Lorand L, and Graham RM. (2003). Transglutaminases: crosslinking enzymes with pleiotropic functions. Nat Rev Mol Cell Biol, 4: 140-156.

Lowerely LA, Van Vactor D.(2009). The trip of the tip: understanding the growth cone machinery. Nat Rev Mol Cell Biol, 20: 332-343.

Ma L, and Tessier-Lavigne M. (2007). Dual branch-promoting and branch-repelling actions of Slit/Robo signaling on peripheral and central branches of developing sensory axons. J Neurosci, 27: 6843-6851.

Madura K. (2004). Rad23 and Rpn10: perennia wallflowers jion the melee. Trends Biochem, 29: 637-640.

Maerz S, Funakoshi Y, Negishi Y, Suzuki T, Seiler S. (2010). The neurospora peptide:N-glycanase ortholog PNG1 is essential for cell polarity despite its lack of enzymatic activity. J Biol Chem, 285: 2326–2332.

Maerz S, Ziv C, Vogt N, Helmstaedt K, Cohen N, Gorovits R, Yarden O, Seiler S. (2008). The nuclear Dbf2-related kinase COT1 and the mitogen-activated protein kinases MAK1 and MAK2 genetically interact to regulate filamentous growth, hyphal fusion and sexual development in Neurospora crassa. Genetics, 179:1313-1325.

Mah AS, Jang J, Deshaies RJ (2001) Protein kinase Cdc15 activates the Dbf2-Mob1 kinase complex. Proc Natl Acad Sci U S A 98:7325-7330.

Manser E, Leung T, Salihuddin H, Zhao ZS, Lim L. (1994). A brain serine/threonine protein kinase activated by Cdc42 and Rac1. Nature 367:40-46.

Mann F, Peuckert C, Dehner F, Zhou R, Bolz J. (2002). Ephrins regulate teh formation of terminal axonal arbors during teh development of thalamocortical projections. Development, 129: 65-76.

Markus A, Zhong J, Snider WD. (2002). Raf and akt mediated distint apsects of sensory axon growth. Neuron, 35: 65-76.

Mastutani C, Araki M, Sugasawa K, Van der Spek PJ, Yamada A, Uchida A, Maekawa T, Bootsma D, Joejimkers JH, Hanaoka F. (1997). Identification and characterization of XPC-binding domain of hHR23. Mol Cell Biol , 17: 6915-6923.

Mazanka E, Alexander J, Yeh BJ, Charoenpong P, Lowery DM, Yaffe M, Weiss EL. (2008). The NDR/LATS family kinase Cbk1 directly controls transcriptional asymmetry. PLoS Biol, 6:e203.

McGovern M, Yu L, Kosinski M, Greenstein D, Savage-Dunn C. (2007). A role for sperm in regulation of egg-laying in the nematode C. elegans. BMC Dev Biol, 4:41.

Mehnert M, Sommer T, Jarosch E. (2010). ERAD ubiquitin ligases: multifunctional tools for protein quality control and waste disposal in the endoplasmic reticulum. Bioessays, 32: 905-913.

Mehta N, Loria PM, Hobert O. (2004). A genetic screen for neurite outgrowth mutants in Caenorhabditis elegans reveals a new function for the F-box ubiquitin ligase component LIN-23. Genetics, 166: 1253-1267.

Meier C, Anastasiadou S, Knolll B. (2011). Ephrin-A5 suppresses neurotrophin evoked neuronal motility, ERK activation, and gene expression. PLoS ONE , 6: E26089.

Menager C, Arimura N, Kukata Y, Kaibuchi K. (2004). PIP3 is invovlved in neuronal polarization and axon formation. J Neurochem, 89: 109-118.

Meusser B, Hirsch C, Jarosch E, Sommer T. (2005). ERAD: the long road to destruction. Nat Cell Biol 7:766-772.

Meyer Y, Buchanana BB, Vignols F, Reichheld JP. (2008). Thioredoxin and glutaredoxins as facilitators of protein folding. Biochim Biophys Acta, 1783: 641-650.

Min JH, and Pavletich NP. (2007). Recognition of DNA damage by the Rad4 nucleotide excision repair protein. Nature, 449: 570-575.

Mori K. (2000). Tripartite management of unfolded proteins in the endoplasmic reticulum. Cell , 101: 451-454.

Mori K, Ma w, Gething MJ, Sambrook J. (1993). A transmembrane protein with a cdc2+/CDC28-related kinase activity is required for signaling from the ER to the nucleus. Cell, 74: 349-355.

Mori K, Sant A, Kohno K, Normington K, Gething MJ, Sambrook JF. (1992). A 22 bp cis-acting element is necessary and sufficient for the induction of the yeast KAR2 (BiP) gene by unfolded protein response. EMBO J , 11: 2583-2593.

Murray AW. (2004). Recycling the cell cycle: cyclins revisited. Cell , 6: 221-234.

Murzin AG, Brenner SE, Hubbard T, Chothia C. (1995). SCOP: a structural classification of proteins database for the investigation of sequences and structures. J Mol Biol, 247: 536-540.

Myung J, Kim KB, Crews CM. (2001). The ubiquitin-proteasome pathway and proteasome inhibitors. Med Res Rev, 4: 245-273.

Myers TR, Greenwald I. (2005). Lin-35 Rb acts in the major hypodermis to oppose ras-mediated vulva induction in C. elegans. Dev Cell 8: 117-123.

Nalepa G, Rolfe M, Harper JW. (2006). Drug discovery in the ubiquitin-proteasome. Nat Rev Drug Discov , 5: 596-613.

Neukirchen D, Bradke F. (2011) Neuronal polarization and the cytoskeleton. Semin Cell & develop boil, 22: 825-833

Ng J, Nardin T, Harms M, Tzu J, Goldstein A, Sun Y et al. (2002). Rac GTPases control axon growth, guidance and branching. Nature , 416: 442-447.

Ng JM, Vermeulen W, Van der Horst GT, Bergink S, Sugasawa K, Vrieling H, Hoijmakers JH. (2003). A novel regualtion mechanism of DNA repair by damage-induced and RAD23-dependetn stabilization of xeroderma pigmentosum group C protein. Genes Dev , 17: 1630-1645.

Nikawa J I, Yamashita S. (1992). IRE1 encodes a putative protein kinase contaiing a membrance-spaning domain and is required for inosito phototrophy in Sacchromyces cerevisiae. Mol Micorbiol , 6: 1441-1446.

Nishiyama M, Hoshino A, Tsai L, Henley JR, Goshima Y, Tessier-Lavigne, M, Poo MM, Hong K. (2003). Cyclic AMP/GMP-dependent modulation of Ca2+ channels sets the polarity of nerve growth-cone turning. Nature, 424: 990-995.

Nobes CD, Hall A. (1995). Rho, rac, and cdc42 GTPases regualte te3h assembly of multimolecualr focal complexe assocaited with actin stress fibers, lamellipodia, and filopodia. Cell, 81: 53-62.

Ohnami S, Endo M, Hirai S, Uesaka N, Hatanaka Y, Yasmashita T. (2008). Role of RhoA in activity-dependent cortical axon branching. J Neurosci , 28: 9117-9121.

Okabe S, and Hirokawa N. (1991). Actin dynamics in growth cones. J Neurosci, 11: 1918-1929.

Okabe S, and Hirokawa N. (1990). Turnover of fluorescently labelled tubulin and actin in the axon. Nature 343, 479-82. Narure , 343: 479-482.

O'Donnell M, Chance RK, Bashaw GJ. (2009). Axon growth and guidance: receptor regulation and signal transduction. Annu Rev Neurosci, 32:383-412.

O'Leary DD, Terashima T. (1988). Cortical axons branch to multiple subcortical targets by

interstitial axon budding: implications for target recognition and "waiting periods". Neuron, 1:901-910.

O'Leary DD, Bicknese AR, De Carlos JA, Heffner CD, Koester SE, Kutka LJ, Terashima T. (1990). Target selection by cortical axons: alternative mechanisms to establish axonal connections in the developing brain. Cold Spring Harb symp Quant Biol, 55: 453-468.

O'Leary DD, McLaughlin t. (2005). Mechanisms of retinotopic map development: Ephs, ephrins, and spontaneous correlated retinal activity. Prog Brain Res, 147: 43-65.

Ortolan TG, Chen L,Tongankar P, Madura K. (2004). Rad23 stabilized Rad4 from degradation by the Ub/proteasome pathway. Nucleic Acids Res, 32: 6490-6500.

Ortolan TG, Togaonkar P, Lambertson D, Chen L, Madura K. (2000). The Rad23 DNA repair protein is a negative regulator of substrate-linked multi-ubiquitin chain assembly. Nature Cell Biol, 2: 601-608.

Ozaki S,and Snider WD. (1997). Initial trajectories of sensory axons toward laminar targets in the developing mouse spinal cord. J Comp Neuro, 380: 215–29.

Ozdinler Ph, and Erzurumlu RS. (2002). Slit2, a branching-arborization factor for sensory axons in the mammalian CNS. J Neurosci , 22: 4540-4549.

Park HK, Suh D, Hyun M, Koo HS, Ahn B. (2004). A DNA repair gene of Caenorhabditis elgeans: a homologof human XPF. DNA repair, 3: 1375-1383.

Park HK, Yook JS, Koo HS, Choi IS, Ahn B. (2002). Caenorhabditis elegans XPA homolog of human XPA. Mol Cells , 14:50-55.

Park H, Suzuki T, Lennarz WJ. (2001). Identification of proteins that interact with mammalian peptide:N-glycanase and implicate this hydrolase in the proteasome-dependent pathway for protein degradation. Proc Natl Acad Sci USA, 98:11163-11168.

Peckol EL, Zallen JA, Yarrow JC, Bargman CI. (1999). Sensory activity effects sensory axon development in C. elegans. Development, 126: 163-1073.

Pickart CM. (2004). Back to the future with ubiquitin. Cell , 116: 181-190.

Pickart CM. (2001). Mechanisms underlying ubiquitination. Annu Rev Biochem , 70: 503-533.

Pickart CM, Fushman D. (2004). Polyubiquitin chains: polymeric protein signals. Curr Opin Chem Biol, 8: 610-616.

Pilon M, Romisch K, Quach D, Schekman R. (1998). Mol Biol Cell, 9: 3455-3477.

Pilon M, Schekman R, Römisch K. (1997). Sec61p mediates export of a misfolded secretory protiens from the endoplasmic reticulum to the cytosol for degradation. EMBO J, 16: 4540-4548.

Plemper RK, Böhmler S, Bordallo J, Sommer T, Wolf DH. (1997). Mutant analysis links the translocon and BiP to retrograde protein transport for ER degradation. Nature, 388: 891-895.

Prakash S, and Prakash L. (2000). Nucleotide excision repair in yeast. Mutat Res, 451: 13-24.

Raasi S, and Pickart CM. (2003). Rad23 ubiquitin-assocaited domains (UBA) inhibit 26S proteasome-catalyzed proteolysis by sequestering lysine 48-linked polyubiquitin chains. J Biol Chem, 278: 8951-8959.

Raasi S, Varadan R, Fushman D, Pickart M. (2005). Diverse polyubiquitin interaction properties of ubiquitin-assocaited domains. Nat Struct Mol Biol, 358: 708-714.

Raftopoulou M, and Hall A. (2004). Cell migration: Rho GTPases lead the way. Dev Biol, 265: 23-32.

Read DE, and Gorman AM. (2009). Involvment of Akt in neurite outgrowth. Cell mol Life Sci, 66: 2975-2984.

Reber M, Burrla P, Lemke G. (2004). A relative signalling model ofr the formation of a topographic neural map. Nature, 431: 847-853.

Reichard LF. (2006). Neurotrophin-regulated signalling pathways. Philos Trans R Soc Lond B Biol Sci, 361:1545-64.

Ridley AJ. (2006) Rho GTPases and actin dynamics in membrane protrusion and vescle trafficing. Trends in Cell Biol, 26: 522-529.

Rivera-Bergman A, McDaniel LD, Schultz RA, Freidberg EC. (2007). A novel XPC pathogenic variant detected in archival material from a patient diagnosed with Xeroderma pigmentosum: a case report and reveiw of the genetic variants reported in xpc. DNA Repair, 6: 100-114.

Rock KL, York IA, Goldberg AL. (2004). Post-proteasomal antigen procesing for major histocompatibility complex class I presentation. Nat Immunol 5: 670-677.

Rogers EE, and Theibert AB. (2002). Functions of PI 3-kinase in development of the nervous system. Int J Dev Neurosci , 20: 187-197.

Sanchez Al, Matthews bJ, Meynard MM, Hu B, Javed S, Cohen Cory S. (2006). BDNF increase synapse density in dendrites of developing tectal neurons in vivo. Development, 7: 1059-1069.

Sarmiere PD, and Bamburg JR. (2003). Regulation of the Neuronal Actin Cytoskeleton by ADF/Cofilin. J Neurobiol, 58: 103: 117.

Schaefer AW, Kabir N, and Forscher P. (2002). Filopodia and actin arcs guide the assembly and transport of two populations of microtubules with unique dynamic parameters in neuronal growth cones. J Cell Biol, 158: 139-152.

Schaefer AW, Schoonderwoert VT, Ji L, Mederios N, Danuser G, Forscher P. (2008). Coordination of actin filaments and microtubule dynamics during neurite outgrowth. Dev Cell, 15: 146-162.

Schäfer A, Wolf DH. (2009). Sec61p is part of the endoplasmic reticulum-associated. EMBO J, 28: 2874-2884.

Schaheen B, Dang H, Fares H. (2009). Derlin-dependent accumulation of integral membrane proteins at cell surfaces. J Cell Sci, 13: 2228-2239.

Schafer AM, Hadwiger GD, Nonet ML. (2000). rpm-1, a conserved neuronal genes that regulates targeting and synaptogenesi in C.elegans. Neuron, 26: 345-356.

Schafer WR. (2006). Genetics of Egg-laying in worms. Annu Rev Genet, 40: 487-509.

Schmidt A, and Hall A. (2002). Guanine nucleotide exchange factors for Rho GTPases: turning on the switch. Genes Dev, 16: 1587-1609.

Schmidt H, and Rathjen F. (2012). Signalling mechanisms regulating axonal branching in vivo. Bioassays, 32: 977–985.

Schmidt H, Stonkute A, Ju¨ttner R, Scha¨ffer S, Buttgereit J, Feil R, Hofmann F. (2007). The receptor guanylyl cyclase Npr2 is essential for sensory axon bifurcation within the spinal cord. J Cell Bio , 179: 331-340.

Schmitz A, Maintz M, Kehle T, Herzog V. (1995). In vivo iodination of a misfolded proinsulin reveals co-localized signals for Bip binding and for degradation in the ER. EMBO J, 14: 1091-1098.

Schroder M, Kaufman RJ. (2006). Divergent roles of IRE1α and PERK in the unfolded. Curr Mol Med, 6: 5-36.

Shan L, Molberg O, Parrot I, Hausch F, Filiz F, Gray GM, Sollid L, Khosla C. (2002). Structural basis for gluten intolerance in celiac sprue. Science, 297: 2275–2279.

Sharma-Kishore R, White JG, Southgate E, Podbilewicz B. (1999). Formation of the vulva in Caenorhabditis elegans: a paradigm for organogenesis. Development, 126:691-699.

Shatz CJ. (2009). MHC class I: an unexpected role in neuronal plasticity. Neuron , 64: 40-45.

Shen K, Fetter RD, Bargmann CI. (2004). Synaptic specificity is generated by the synaptic guidepost protein SYG-2 and its receptor, SYG-1. Cell, 116:869-881.

Shen X, Zhang K, Kaufman RJ. (2004). The unfolded protein response-a stress signaling pathway of the endoplasmic reticulum. J Chem Neuro, 28: 79-92.

Shen X, Ellis RE, Lee K, Liu Cy, Yang K, Solomon A, Yoshida H, Marimoto R, Kumit DM, Mori K, Kaufman RJ. (2001). Complementary signaling pathways regulate the unfolded protein response and are required for C.elegans development. Cell, 107: 893-903.

Shen x, Zhang K, Kaufman RJ. (2004). The unfolded protein response: a stress signaling pathway of the endoplasmic reticulum. J Chem Neuroanat, 28: 89-92.Shilton JK. (2006). Molecular mechanism of axon guidance. Dev Biol, 292: 13- 24.

Schindler AJ, Sherwood DR. (2012). Morphogenesis of the Caenorhabditis elegans vulva. WIREs Dev Biol, doi:10.1002/wdev.87.

Song HJ, and Poo MM. (1999). Signal transduction underlying growth cone guidance by diffusible factors. Curr Opin Neurobiol, 9: 355-363.

Song HJ, Ming GL, He Z, Lehmann M, McKerracher L, Tessier-Lavigne M, Poo MM. (1998). Converstion of neuronal growth cone responses from repulsion to attraction by cyclic nucleotides. Sciecne, 281: 1515-1518.

Spitzweck B, Brankatschk M, Dickson BJ. (2010). Distinct protein domains and expression patterns confer divergent axon guidance functions for Drosophila Robo receptors. Cell, 140: 409-420.

Sasagawa Y, Yamanaka K, Ogura T. (2007). ER E3 ubiquitin ligase HRD-1 and its specific partner chaperone BiP play important roles in ERAD and developmental growth in Caenorhabditis elegans. Genes Cells, 12: 1063-1073.

Seiler S, Plamann M., (2003). The genetic basis of Cellular morphogenesis in the filamentous fungus Neurospora crassa. Mol Biol Cell, 14: 4352-4364

Selby M, Erickson A, Dong C, Cooper S, Parham P, Houghton M, Walker CM. (1999). Hepatitis C virus envelope glycoprotein E1 originates in the endoplasmic reticulum and requires cytoplasmic processing for presentation by Class I MHC molecules. J Immunl, 162: 669-676.

Spiro RG. (2004). Role of N-linked polymannose oligosaccharides in targeting glycoproteins for endoplasmic reticulum-associated degradation. Cell Mol Life Sci, 61; 1025-1041.

Staub O, Gautschi I, Ishikawa Y, Breitschopf K, Ciechanover A, Schild L, Rotin D. (1997).

Regulation of stability and function of the epithelial Na+ channel (ENaC) by ubiquitination. EMBO J , 16: 6325-6336.

Stein E, Tessier-Lavigne M. (2001). Hierarchial organization of guidance receptors: silencing of netrin attraction by slit through a Robo/DCC receptor complex. Science, 291: 1928-1938.

Sternberg PW, Horvitz HR. (1986). Pattern formation during vulval development in C. elegans. Cell, 44:761-772.

Struckhoff EC, and Lundquist EA. (2003). The actin-binding protein UNC-115 is an effector of Rac signaling during axon pathfinding in C. elegans. Development , 130: 693-704.

Sulston JE, Schierenberg E, White JG, Thomson JN. (1983). The embryoinc cell lineage of the nematode Caenorhabditis elegans. Dev Biol , 100: 64-119.

Sulston JE, Horvitz HR. (1977). Post-embryonic cell lineages of the nematode Canorhabditis elegans. Philos Trans R Soc London Ser B, 275:287-297

Suzuki T and Lennarz WJ. (2003). Hypothesis: a glycoprotein-degradation complex formed by protein–protein interaction involves cytoplasmic peptide:N-glycanase. Bioch Biophy Res Comm, 302: 1–5.

Suzuki T, Park H, Lennarz WJ. (2002). Cytoplasmic peptide:N-glycanase (PNGase) in eukaryotic cells: occurrence, primary structure, and potential functions. FASEB J, 16:635-641.

Suzuki T, Park H, Kwofie MA, Lennarz WJ. (2001b). Rad23 provides a link between the Png1 deglycosylating enzyme and the 26 S proteasome in yeast. J Biol Chem, 276:21601-21607.

Suzuki T, Park H, Kitajima K, Lennarz WJ. (1998). Peptides glycosylated in the endoplasmic reticulum of yeast are subsequently deglycosylated by a soluble peptide:N-glycanase activity. J Biol Chem , 273: 21526-21530.

Suzuki T, Park H, Till EA, Lennarz WJ. (2001a). The PUB domain: a putative proteinprotein. Biochem Biophys Res Commun , 287: 1083-1087.

Suzuki T, Seko A, Kitajima K, Inoue Y, Inoue S. (1994). Purification and enzymatic properties of peptide:N-glycanase from C3H mouse-derived L-929 fibroblast cells. Possible widespread occurrence of post-translational remodification of proteins by N-deglycosylation. J Biol Chem, 269:17611-17618.

Suzuki T, Kitajima K, Emori Y, Inoue Y, Inoue S. (1997). Site-specific de-N-glycosylation of diglycosylated ovalbumin in hen oviduct by endogenous peptide: N-glycanase as a quality control system for newly synthesized proteins. Proc Natl Acad Sci USA, 94:6244-6249.

Suzuki T, Park H, Hollingsworth NM, Sternglanz R, Lennarz WJ. (2000). PNG1, a yeast gene encoding a highly conserved peptide:N-glycanase. J Cell Biol, 149:1039-1052.

Suzuki T, Tanabe K, Hara I, Taniguchi N, Colavita A. (2007). Dual enzymatic properties of the cytoplasmic peptide: N-glycanase in C. elegans. Biochem Biophys Res Commun, 358:837-841.

Svitkina TM, and Borisy GG. (1999). Arp2/3 complex and actin depolymerizing factor/cofilin in dendritic organization and treadmilling of actin filament array in lamellopodia. J. Cell Biol, 145: 1009 -26.

Szlanka T, Haracska L, Kiss I, Deak P, Kurucz Z Ando, I, Viragh E, Udvardy, A. (2002). Deletion of proteasomal subunit S5a/Rpn10/p54 causes lethality, multiple mitotic defects and overexpression of proteasomal genes in Drosophila melanogaster. J Cell Sci , 116: 1023–1033.

Tabara H, Grishok A, Mello CC. (1998). RNAi in C.elegans: soaking in the genome sequence. Science, 282: 430-431.

Tamaskovic R, Bischsel SJ, Rogniaux H, Steger MR, Hemmings B. (2003). Mechanism of Ca2+-mediated regulation of NDR protein kinase through autophosphorylation and phosphorylation by an upstream kinase. J Biol Chem, 278: 6710-6718.

Tang F, Kalil K .(2005). Netrin-1 induces axon branching in developing cortical neurons by frequency-dependent calcium signaling pathways. J Neurosci, 25:6702-6715.

Tang F, Dent EW, Kalil K .(2003). Spontaneous calcium transients in developing cortical neurons regulate axon outgrowth. J Neurosci, 23:927-936.

Tessier-Lavigne M, and Goodman CS. (1996). The molecular biology of axon guidance. Sciecne, 274: 1123-1133.

Thrower JS, Hoffman L, Rechsteiner M, Pickart CM. (2000). Recognition of the polyubiquitin proteolytic signal. EMBO J, 19: 94-102.

Timmons L, and FIre A. (1998). Specific interference by ingested dsRNA. Nature, 395: 854.

Toyofuku T, Yoshida J, Sugimoto T, Zhang H, Kumanogoh A, Hori M, Kijutani H. (2005). FARP2 triggers signals fro Sema3A-mediated axonal repulsion. Nat Neurosci, 8: 1712-1719.

Turner LJ, Nicholls S, Hall A. (2004). The activity of the plexin-A1 receptor is regulated by Rac. J Biol Chem, 279: 33199-33205.

Urano F, Betolottie A, Ron D. (2000b). IRE1 and efferent signaling from the endoplsmic reticulum. J Cell Sci, 113: 3697-3702.

Urano F, Calfon M, Yoneda T, Un C, Kiraly M, Clark SG, Ron D. (2002). A survival pathway for Caenorphabditis elegans with a blocked unfolded protein response. J Cell Bil, 158: 639-646.

Urano F, Wang X, Betolottie A, Zhang Y, Chung P, Harding HP, Ron D. (2000a). Coupling f stress in the ER to activation of JNK protein kinases by transmembrne protein kinase IRE1. Science, 287: 664-666.

Van Leeuwen FW, et al. (1998). Frameshift mutants of B-amyloid precursor protein and ubiquitin-B in Alzheimer's and Down patients. Science, 279: 242-247.

Van Nocker S, Sadis S, Rubin MD, Glickman M, Fu H, Coux O, Wefes I, Finley D, Vierstra RD. (1996). The multiubiquitin-chain-binding protein Mcb1 is acomponent of the 26S proteasome in Saccharomyces cerevisiae and plays a nonessential, substrate-specific role in protein turnover. Mol Cell Biol, 16:6020–6028.

Verkhratsky A. (2005). Physiology and pathophysiology of the calcium store in the endoplasmic reticulum of neurons. Physiol Rev, 85: 201-279.

Vlamis-Gordikas A, and Holmgren A. (2002). Thioredoxin and glutaredoxin isoforms. Methods Enzymol, 347: 286-296.

Volker M, Mone MJ, Karmakar P, Van Hoffen A, Schul W, Vermeulen W, Hoijmakers JH, Van Driel R, Van Zeeland AA, Mullenders LH. (2001). Sequential assembly of the nucleotide excision repair factors in vivo. Mol Cell, 8: 213-224.

Waggoner LE, Zhou GT, Schafer RW, Schafer WR. (1998). Control of alternative behavioral states by serotonin in Caenorhabditis elegans. Neuron, 21: 203-214.

Wan HI, DiAntonio A, Fetter RD, Bergstrom K, Strauss R,Goodman CS. (2000). Highwire regulates synaptic growth in Drosophila. Neuron , 26: 313-329.

Wang GX, and Poo MM . (2005). Requirement of TRPC channels in netrin-1-induced chemotropic turning of nerve growth cones. Nature, 434: 898-904.

Wang H and Macagno ER. (1998). A detached branch stops being recognized as self by other branches of a neuron. J Neurobiol, 35: 53–64.

Wang KH, Brose K, Arnott D, Kidd T, Goodman CS, Henzel W, Tessier-Lavigne M. (1999). Biochemcial purification of a mammalian slit proteins as a positive reguator of sensory axon elongation and branching. Cell , 96: 771-784.

Watkins JF, Sung P, Prakash L, Prakash S. (1993). The Saccharomyces cervisiae DNA repair gne Rad23 encodes a nuclear protein containing a ubiquitin-like domain required for biological function. Mol Cell Biol, 13: 7757-7765.

Wen Y, Eng CH, Schmoranzer J, Cabrera-Poch N, Morris EJ, Chen M, Wallar BJ,Alberts AS, Gundersen, GG. (2004). EB1 and APC bind to mDia to stabilize microtubules downstream of Rho and promote cell migration. Nat Cell Biol, 6: 820 - 830.

White J, Southgate E, Thomson N, Brenner S. (1986). The structure of the Caenorhabdities elegans nervous system. Philos Trans R Soc London Ser B, 314: 1-340.

Wiertz EJ, Tortorella D, Bogyo M, Yu J, Mothes W, Jones TR, Rapoport TA, Ploegh HL. (1996). Sec61-mediated transfer of a membrane protein from the endoplasmic. Nature, 384: 432-438.

Wilcox AJ, Laney JD. (2009). A ubiquitin-selective AAA-ATPase mediates. Nature, 11: 1481-1486.

Wilkinson CR, Seeger M, Hartmann-Petersen R, Stone M, Wallace M, Semple C,. (2001). Proteins containing the UBA domain are able to bind to multiubiquitin. Nat Cell Biol, 3: 939-943.

Williamson T, Gordon-Weeks PR, Schachner M, Taylor J. (1996). Microtubule reorganization is obligatory for growth cone turning. Proc Natl Acad Sci USA , 93: 15221-15226.

Witmann T, Bokoch GM, Waterman-Storer C. (2003). Reglation of leading edge microtubule and actin downstream of Rac1. J Cell Biol, 5: 845-851.

Wong K, Ren XR, Huang YZ, Xie Y, Liu G, Saito H, Tang H, Wen L, Brady Kalnay SM, Mei L, Wu JY, Xiong W, Rao Y. (2001). Signal transduction in neuronal migration: roles of GTPase activating proteins and the small GTPase Cdc42 in the Slit-Robo pathway. Cell, 107: 209-221.

Weiss EL, Kurischko C, Zhang C, Shokat K, Drubin DG, Luca FC. (2002). The Saccharomyces cerevisiae Mob2p-Cbk1p kinase complex promotes polarized growth and acts with the mitotic exit network to facilitate daughter cell-specific localization of Ace2p transcription factor. J Cell Biol, 158:885-900.

Yamashita T, and Tohyama, M. (2003). The p75 receptor acts as a displacement factor that releases Rho from Rho-GDI. Nat Neurosci, 6: 461-467.

Yang L, and Bashaw GJ. (2006). Son of sevenless directly links the ROBO receptor to Rac activation to control axon repulsion at the midline. Neuron , 52: 595-607.

Yates PA, Roskies AL, McLaughlin T, O'Leary DD. (2001). Topographic-specific axon branching controlled by ephrin-As is the critical even in retinotectal map development. J Neurosci, 21: 8548-8563.

Ye Y, Meyer HH, Rapoport TA. (2001). The AAA ATPase Cdc48/p97 and its partners transport proteins from the ER into the cytosol. Nature, 414: 652-656.

Ye Y, Shibata Y, Yun C, Ron D, Rapoport TA. (2004). A membrane protein complex mediates retro-translocation from ER into the cytosol. Nature , 429: 841-847.

Yi JJ, and Ehler MD. (2007). Emerging Roles for ubiquitin and protein degradation in neuronal function. Pharmacological Revi, 59: 114-139.

Yoshida H, Matsui T, Hosokawa N, Kafuman RJ, Nagata K, Mori K. (2003). A time-dependent phase shift in the mammalian unfolded protein response. Dev Cell, 4: 265-271.

Yoshida H, Okada T, Haze K, Yanagi H, Yura T, Negishi M, Mori K. (2001). Endoplasmic reticulum stress -induced formation of trancription factor complex ERSF including NF-Y(CBF) and activating transcription factors 6alpha and 6beta that activates the mammalian unfolded protein response. Mol Cell Biol, 21: 1239-1248.

Yoshimura T, Arimura N, and Kalbuchi K. (2006). Signaling networks in neuronal polarization. J of Neurosci, 26: 10626-10630.

Yuan XB, Jin M, Xu X, Song YQ, Wu CP, Poo MM, Duan S. (2003). Signalling and crosstalk of Rho GTPases in mediating axon guidance . Nat Cell Biol, 5: 38-45.

Yu H, Kaung G, Kobayashi S, Kopito RR. (1997). Cytosolic degradation of T-cell receptor alpha chains by the proteasome. J Biol Chem. 272: 20800-20804.

Zallen JA, Peckol EL, Tobin DM, Bargmann CI. (2000). Neuronal cell shape and neurite initiation are regulated by the Ndr kinase SAX-1, a member of the Orb6/COT-1/warts serine/threonine kinase family. Mol Biol Cel, l 11:3177-3190.

Zallen JA, Kirch SA, Bargman CI. (1999). Genes requried for axon pathfinding and extension in the C. elegans nerve ring. Development, 126: 3679-3692.

Zhao G, Zhou X, Wang L, Li G, Kisker C, Lennarz W, Schindelin H. (2006). Strucutre of the mouse peptide N-Glycanase-HR23 complex suggest Co-evolution of the endoplasmic reticulum-associated degradation and DNA repair pathways. J Biol Chem , 281: 13751-13761.

Zhen M, Huang X, Bamber B, Jin Y. (2000). Regulation of presynaptic terminal organization by C.elegans RPM-1, a putative guanine nucleotide exchange with a RING-H2 finger domain. Neuron , 26: 331-343.

Zhou FQ, and Cohan CS. (2004a). How actin filaments and microtubules steer growth cones to their targets. J Neurobiol , 58: 84-91.

Zhou FQ, Zhou J, Dedhar S, Wu YH, and Snider WD. (2004b). NGF-induced axon growth is mediated by localized inactivation of GS-3 beta and functions of teh microtubule plus end binding proteins APC. Neuron , 42: 897-912.

Zhou Z, Thomas JH, Chen N, Sheps JA, Baillie DL. (2007). Comparative genomics and adaptive selection of the ATP-binding cassette gene family in Caenorhabditis species. Genetics, 175: 1407-1418.

Zhou X, Zhao G, Truglio JJ, Wang L, Li G, Lennarz WJ, d Schindelin H. (2006). Structural and biochemical studies of the C-terminal domain of mouse peptide-N-glycanase identify it as a mannose-binding module. Proc Natl Acad Sci USA, 103: 17214–17219.